The Radio Science Bulletin

ISSN 1024-4530

INTERNATIONAL
UNION OF
RADIO SCIENCE

UNION
RADIO-SCIENTIFIQUE
INTERNATIONALE

No 304
March 2003

Publié avec l'aide financière de l'ICSU
URSI, c/o Ghent University (INTEC)
St.-Pietersnieuwstraat 41, B-9000 Gent (Belgium)

Contents

Front cover: Figure 1 from "The optical image (left), polarimetric color-coded image (center), and interferometric coherence (right) over Oberpfaffenhofen (Germany)."(more on pp. 48-58)

For information, please contact :
The URSI Secretariat
c/o Ghent University (INTEC)
Sint-Pietersnieuwstraat 41, B-9000 Gent, Belgium
Tel.: (32) 9-264 33 20, Fax: (32) 9-264 42 88
E-mail: ursi@intec.rug.ac.be
http://www.ursi.org

Editorial

What's in this Issue

When a nonlinear crystal material is pumped by a sufficiently strong laser, spontaneous emission of photons can occur. This is a direct result of the quantum nature of light. Such emitted photons occur in coupled pairs, with a prescribed relationship for their directions of propagation. In fact, there is a collective wave-function of the photon pairs that mixes together the functions of the individual photons. This is referred to as an entangled state, and the electromagnetic fields associated with such photons are known as biphoton electromagnetic fields. Carlo Novero presents a very clear explanation of how such fields are produced: it can be easily understood even without a background in quantum mechanics. He then goes on to describe how such fields can be used in two very important applications. The first is a direct and very accurate measurement of photon detectors' quantum efficiencies, which can be determined with simple photon-counting measurements. The second is a very fundamental test of quantum mechanics. This is a very clearly written, easy-to-understand paper, which presents a fascinating introduction to the topic. It also includes some of the most recent results in the field. Sadly, Carlo Novero died after the paper was submitted, and before it could be published. It is a fitting memorial to Prof. Novero. I really appreciate Elio Bava's help in making it possible to publish this paper.

As electronic devices become more and more sensitive, their susceptibility to the direct and indirect effects of lightning becomes greater. Understanding, modeling, predicting, and protecting against such effects requires knowledge of the statistics and parameters of the currents and electromagnetic fields associated with and produced by lightning. Understanding and models of the coupling of such currents and fields into the electronics are also required. In his paper, based on his Commission E Tutorial Lecture given at the Maastricht General Assembly, Michel Ianoz provides an overview of the current state of knowledge about lightning. He identifies areas where additional information and measurements would be beneficial, and highlights a potential problem with some of the existing data. He also reviews the various models available for predicting the coupling of lightning effects into electronics, and surveys how and to what extent some of these models have been validated. The result is an excellent tutorial.

Code-division multiplexing has been widely used in RF telecommunications, having being part of spread-spectrum military communications for more than 50 years. It is currently the basis of one of the major approaches to advanced cellular communications: CDMA (code-division multiple access). The same techniques can be applied to optical, or photonic, communications. Hideyuki Sotobayashi describes how this is done in his paper, based on his Commission D Tutorial Lecture presented at the Maastricht General Assembly. He first reviews how optical code-division multiplexing (OCDM) is done. He then goes on to describe four major applications of OCDM in photonic networks used for transporting data. The result is a fascinating look at one of the technologies that will almost certainly play a central role in future high-speed data transmission.

Synthetic-aperture radar (SAR) has become a basic tool in the remote sensing of the Earth, and in the detection of surface and buried targets. When an object scatters an electromagnetic wave, important information about the object is contained in the way the wave's polarization changes due to the scattering. Methods have been developed to extract this information from polarimetric SAR data. Analogously, information about the object is also contained in the change in the coherence of the wave that results from scattering. Interferometric SAR data processing makes use of this information. Current and near-term future satellite-borne SAR systems will permit combining polarimetric and interferometric data processing. In their paper, based on the Commission F Tutorial Lecture given at the Maastricht General Assembly, Eric Pottier, Shane Cloude, and Wolfgang Boerner explain how such data are recorded and processed. They then give several examples of the types of remote-sensing information that can be obtained using such techniques. The amount and quality of quantitative information obtainable using these methods is impressive.

Does long-term exposure to electromagnetic radiation simulating radiation from a GSM cellular phone cause cancer in mice? One experiment suggested that such exposure caused an increase in observed cancers. A later experiment, designed to address questions raised about the first experiment, seemed to contradict the first experiment. It turns out that there are questions to be raised about both. For a fascinating look at some important results in this field – and, as importantly, some reminders about the value of proper experimental design and interpretation – read Jim Lin's "Radio-Frequency Radiation Safety and Health" column in this issue.

Thank You Robert Hunsucker

For the past eight years, Bob Hunsucker has been the Editor of *Radio Science*, the journal co-sponsored by URSI and published by the American Geophysical Union. He has done an outstanding job. With his leadership, the journal has maintained and improved its stature within the field, both in terms of acceptance as a desirable place to be published, and in terms of Impact Factor and cited half-life, as reported by *Journal Citation Reports*. During his tenure, the journal has moved to electronic submission and reviewing of manuscripts. He had made a significant contribution to radio science through his service as Editor, and he deserves URSI's thanks. He has agreed to remain an Associate Editor of the *Radio Science Bulletin* and a member of the URSI Standing Committee on Publications, so we will be able to continue to benefit from his experience and expertise.

Tarek Habashy has been appointed the new Editor of *Radio Science*. An announcement of this and a short biography appear in this issue, and we welcome Tarek to the URSI editorial family.

Your Help Needed!

The *Radio Science Bulletin* needs your help. If you would like to serve as an Associate Editor in charge of a book review column, please contact me. We're looking for someone who will actively solicit reviews of books of interest to our community. The duties of this position include obtaining books for review (no, you won't have to buy them!), finding qualified people to do the reviews, and providing the editorial and review functions for such reviews. It is hoped that this column will also include a listing and abstracts of PhD dissertations in radio science, so the Associate Editor would need to solicit and coordinate these, as well.

We need your papers! If you have a paper that is of interest to radio scientists in more than one of URSI's Commissions – and this includes papers reporting new results of broader interest, as well as tutorials and reviews – submit it to the *Radio Science Bulletin*. Our backlog is modest, we try to get papers reviewed and published promptly, we're flexible on length, we have no page charges, and we are one of the best ways to reach the radio science community. We are also indexed in INSPEC. If you are organizing a conference that includes papers appropriate for the *Bulletin*, please urge their authors to submit them, and/or let me know about them.

This issue of the *Bulletin* marks the start of its 65th year of publication. We're going to try to make this year of the *Bulletin* another year of outstanding value to the radio science community, by bringing you quality papers, columns, reports, and information you need and can use. To do this, we have to have quality input. I hope you'll help.

Erratum

We sincerely apologize for a mistake in the "List of URSI Officials", published in No 303 (December 2002) of the Radio Science Bulletin.

Due to an unfortunate error, Professor Shoogo Ueno's name was omitted on page 81 as Official Member in Japan for Commission K. We have already added his name and coordinates in the Web issue of the December RSB at http://www.ursi.org/RSBissues/RSBdec2002address.pdf.

Professor Shoogo Ueno
Department of Biomedical Engineering
Graduate School of Medicine
University of Tokyo
7-3-1 Hongo, Bunkyo-ku
Tokyo 113-0033 Japan
Tel: + 81 3 5841 3563
Fax: +81 3 5689 7215
E-mail: ueno@medes.m.u-tokyo.ac.jp

Biphoton Electromagnetic Fields and Their Applications

C. Novero

Abstract

This paper describes the parametric down-conversion (PDC) effect, and some of its applications. After a brief introduction on photon statistics of electromagnetic fields, the peculiar nature of PDC emission is examined, and it is shown to consist of a pair of conjugated photons. A brief review of nonlinear optical processes from which PDC originates is given, and then some applications are discussed. A metrological application to the measurement of the quantum efficiency of photodetectors is presented in detail. Later on, some experiments of fundamental physics that make use of PDC, namely, tests of quantum mechanics, are described. Recently achieved results in both applications are discussed, as well.

1. Introduction

There are probably few concepts in modern physics that are discussed as much as is the photon, especially in recent years. The term "photon" was introduced in 1926, by G. N. Lewis, to describe the *quantum of light*, a concept already present for years in physics, and mainly associated with celebrated papers by Albert Einstein [1]. Einstein was, in fact, possibly the true *inventor* of the photon, but all along its life, he had not had a very good feeling about it. In a letter to his close friend, Michele Besso, he remarkably pointed out his point of view on the matter: "...I feel that the real joke that the eternal inventor of enigmas has presented us with [one that] has absolutely not been understood as yet...." [2].

Despite the authority of Einstein, and despite the fact that, in the author's opinion, his assertion today still keeps all its validity intact, the photon became the object of widespread research. It was mainly statistical techniques that proved their usefulness in analyzing the properties of different sources of light. In a period from the 1960s to the 1980s, much work was performed on the statistical properties of *classical* and *quantum* sources of light, and the term "quantum" became more solid in the face of these results. The Poisson distribution inn laser light, and such properties as *photon bunching* in thermal light, and *antibunching* in atom fluorescence, were asserted [3].

It was along with this field of research that a quite new source of photons – that is, *parametric down conversion* in nonlinear crystals – made its appearance in the fall of 1960. Such sources were soon discovered to have quite distinctive statistical properties. The autocorrelation function of photons shows, in fact, a *super-Poissonian* feature, a distinctive property not known before. It soon appeared clear that photons were emitted in pairs, with a very strong correlation in the wavelengths and propagation directions of the twin photons. Since then, a great deal of work – which has been increasing with time – has been performed on this strange electromagnetic field. A number of possible applications of this new source have been discovered, in fact, and a great interest is now growing in the practical aspects of the field. All this is the subject of the forthcoming pages.

2. The Parametric Down-Conversion Effect

The widespread success of microwave technology, a cornerstone of modern telecommunications, probably could not have come to be without recourse, in some periods of history, to parametric processes. The parametric amplifier is, in fact, among the devices with the lowest noise figure. Its applications range from VHF frequencies up to microwaves. A very nice review of microwave parametric amplifiers can be found in the literature [4].

Parametric processes are based on the remarkable fact that some power can be transferred between two signals by properly modulating a reactance in an electric circuit. Manley and Rowe demonstrated that in order for the process to take place, a third signal should circulate, to assure energy and momentum conservation [5]. Historically, the signal from which power is extracted is called the *pump*, the signal to be amplified is the *signal*, and the third signal is usually called the *idler*, a term that reflects its general uselessness and necessity to be disposed of, in some way. In microwave technology, this is usually done by a proper dissipative termination. The reactance that is modulated is often a capacitive reactance, in the form of a varactor diode: its capacity, which is a parameter of the circuit, is modulated by the pump signal; hence the term, *parametric*, for the effect.

Carlo Novero was with the Istituto Elettrotecnico Nazionale Galileo Ferraris, Strada delle Cacce 91, 10135 Torino, Italy. Regrettably, he died April 30, 2002, after this paper was submitted (see "In Memoriam," Radio Science Bulletin, No. 302, September 2002, p. 71).

Special thanks are due to Prof. Elio Bava of the Dipartimento di Elettronica e Informazione, Politecnico di Milano, Italy, for his assistance in bringing this article to publication.

Parametric effects are quite general physical effects, not restricted to only electronic circuits. There are, in fact, parameters that can be modulated by an electromagnetic wave, and which do not necessarily take the form of a discrete component. This is the case, for example, of the electric polarization in dielectrics. An electromagnetic wave that propagates through a dielectric medium builds up an electric polarization inside the medium. The generic component *i* of the polarization is given by [6]

$$P_i = \varepsilon_0 \sum_{j=1}^{3} \chi_{ij}^{(1)} E_j + \sum_{j,k=1}^{3} \chi_{ijk}^{(1)} E_j E_k \,. \qquad (1)$$

Actually, polarization is an infinite series in the electric field, *E*, now restricted to second order for the cases of interest here. The term linear in *E* is the term usually considered in the standard theory of linear dielectrics. It is related to a macroscopic refraction index, *n*, by (in the simple case of an isotropic dielectric)

$$n = \sqrt{1 + 4\pi\chi_L^{(1)}} \,. \qquad (2)$$

There are dielectrics where the second-order electric susceptibility, $\chi^{(2)}$ – even if very low – is markedly different from zero. It was not until the invention of the laser and, consequently, the possibility of sending very large electric fields through dielectrics that the presence of $\chi^{(2)}$ terms was put into evidence. Historically, the generation of the second harmonic of light was the first experimental hint [7]. Soon after, it was followed by the discovery of optical frequency mixing and optical parametric amplification [8, 9]. The presence of a term of second order in *E* leads, in fact, to a variety of effects.

To explain how optical parametric amplification builds up, we start with the non-homogeneous Maxwell's equation for a perfectly transparent and nonmagnetic medium (zero conductivity, and $\mu = \mu_0$), with a source term due to nonlinear polarization:

$$\nabla^2 \vec{E} - \varepsilon \frac{\partial^2 \vec{E}}{\partial t^2} = \frac{\partial^2 \vec{P}}{\partial t^2} \,, \qquad (3)$$

with

$$P_i = \sum_{j,k=1}^{3} \chi_{ijk}^{(2)} E_j E_k \,. \qquad (4)$$

It is common practice to define

$$A_i = \sqrt{\frac{n_i}{\omega_i}} E_i \,, \qquad (5)$$

where n_i is the usual refraction index at frequency ω_i. After some lengthy calculations, one ends up with

$$A_1(z) = A_1(0)\cosh\frac{g_0}{2}z + iA_2^*\sinh\frac{g_0}{2}z \,, \qquad (6)$$

$$A_2^*(z) = A_2^*(0)\cosh\frac{g_0}{2}z - iA_1(0)\sinh\frac{g_0}{2}z \,,$$

where the field E_3 is taken as the *pump* field, of constant amplitude. *z* is the direction of propagation for the fields, and the very important term g_0 is given by

$$g_0 = \frac{2}{c} d_{eff} \sqrt{\frac{\omega_1\omega_2\omega_3}{n_1 n_2 n_3}} A_3 \,. \qquad (7)$$

The speed of light is *c*, A_3 is the pump amplitude, and, finally, d_{eff} is a term containing the second-order susceptibility, χ, in a rather complicated way. The term g_0 is the *parametric gain*. It depends on the pump power through A_3, and on nonlinear contributions to the electric polarization in the medium through d_{eff}.

Equations (6) tell us the very important fact that if $A_1(0)$ and $A_2(0)$ are zero, then also $A_1(z)$ and $A_2(z)$ are always zero, for all values of *z*. In other words, the parametric amplifier is a true linear amplifier: without an input signal there is no output. Up to now, in fact, the treatment of parametric effects has been fully a classical treatment. Things change when one turns to a quantum treatment of parametric amplification in the realm of the second quantization of the electromagnetic field. From a theoretical point of view, early in the 1960s it was foreseen that there was a very different situation in the quantum realm, and the experimental confirmation came soon after [10, 11]. In the quantum description of the parametric amplifier, one derives a set of equations for the signal and idler-field operators, $\hat{N}_1(t)$ and $\hat{N}_2(t)$, which are basically the number of signal and idler photons. These equations are very similar to Equations (6), but for a great difference [12]:

$$\hat{N}_1(t) = \frac{\hat{N}_1(0)}{2g_0}\sinh(2g_0t) \cdot$$
$$+\left[\hat{N}_1(0) + \frac{1}{2}\left(1 - \hat{M}\right)\right]\cosh(2g_0t) - \frac{1}{2}\left(1 - \hat{M}\right) \qquad (8)$$

$$\hat{N}_2(t) = \frac{\hat{N}_2(0)}{2g_0}\sinh(2g_0t) \cdot$$
$$. + \left[\hat{N}_2(0) + \frac{1}{2}\left(1 + \hat{M}\right)\right]\cosh(2g_0t) - \frac{1}{2}\left(1 + \hat{M}\right)$$

Here, the operator $\hat{M} = \hat{N}_1 - \hat{N}_2$ is demonstrated to be a constant of the motion, and this demands that the signal and idler photons be created in pairs. But the great novelty is in the presence of the constant term, 1, which gives a contribution to $\hat{N}_1(t)$ and $\hat{N}_2(t)$, even in the case $\hat{N}_1(0) = 0$ and $\hat{N}_2(0) = 0$. This is the spontaneous parametric down-conversion emission.

The term 1 in the equations comes directly from the commutation relations for field operators in quantum electrodynamics, and makes the big difference from the classical case. Now, in fact, the signal and idler fields are different from zero at the output of the dielectric, even if they are strictly zero at the input. An emission of light is foreseen from a nonlinear dielectric pumped by a strong laser field, and this is actually what happens. The constant term, 1, is very often considered to be one input photon that is always present in the signal and idler modes due to vacuum fluctuations. In the second quantization, in fact, the vacuum, defined as the state of minimal energy, can have photons of all wavelengths for very short times, thanks to the uncertainty relation between time and energy. Therefore, on the average, a photon at the right wavelength and with the correct propagation direction can always find itself at the input of the dielectric and, in this situation, the quantum parametric amplifier is much the same as its classical counterpart. This description, which can sound a bit naive, leads, in fact, to the correct numerical predictions, and is quite sufficient for our scope.

Yet, an important detail is intrinsic in this description, namely, that there is no restriction to the wavelengths of the photons of spontaneous emission. As an immediate consequence of this, the quantum parametric amplifier is expected to work at the same time at a very large number of frequencies, actually over a continuous spectrum. Some restrictions, however, are present. First of all, energy is to be conserved in the process, so that idler (ω_i), signal (ω_s), and pump (ω_p) modes should satisfy

$$\omega_i + \omega_s = \omega_p \,. \tag{9}$$

Moreover, the three photons, treated as particles, should conserve total linear momentum:

$$\vec{k}_i + \vec{k}_s = \vec{k}_p \,. \tag{10}$$

On the face of this, we can guess the form of the spontaneous emission from the quantum parametric amplifier. Idler and signal photons should be simultaneously present, due to energy conservation, and their direction of propagation should match the vector relation of Equation (10). This relation requires that the three vectors be in the plane of the pump, but puts no restriction on the angle of this plane in space. For a given wavelength for signal and idler photons, the angles of vectors $\vec{k}_i$ and $\vec{k}_s$ with respect to $\vec{k}_p$ are fixed, but the two vectors can rotate everywhere around the pump vector. Therefore, the spontaneous emission from a quantum parametric amplifier is expected to be a mixing of conical surfaces, nested one into the other, corresponding to different colors, and with their axes coincident with the pump axis. This is what actually happens. The situation is illustrated in Figure 1, which presents a sketch of the spontaneous emission as seen on a translucent screen in front of a dielectric with the pump laser blocked by an absorbing medium. Figure 2 is an actual picture taken in author's lab.

A very instantaneous picture of parametric emission should appear quite different, however, with only two photons in some directions and colors. We expect, in fact, that photons should be emitted at random directions and wavelengths, because of the random fluctuation of the vacuum, but with the constraint of being always in coupled

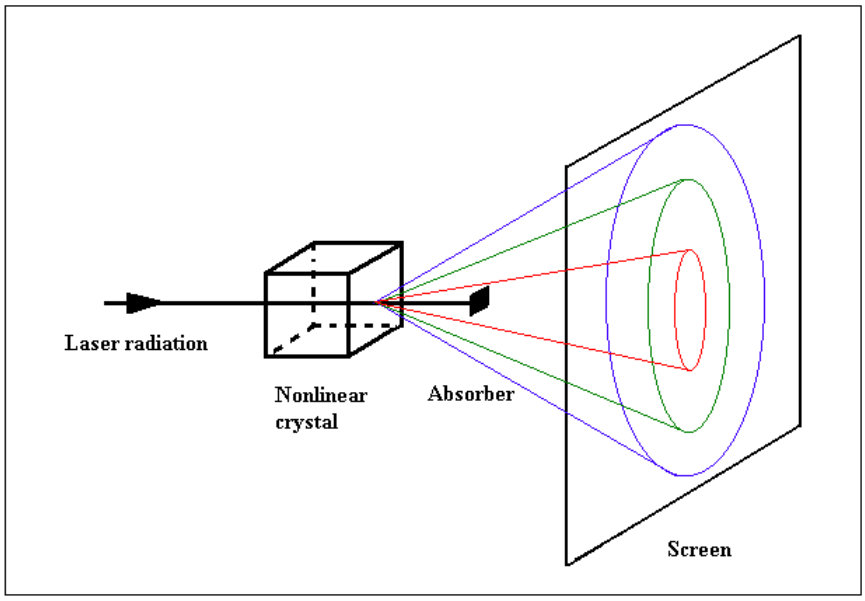

Figure 1. The parametric down-conversion effect. A strong laser beam, termed the "pump," is sent through a transparent crystal with second-order nonlinearities in the electric field, and is then stopped by an absorber. A broadband emission of light originates from the crystal, in the form of conical surfaces of different colors nested one upon the other.

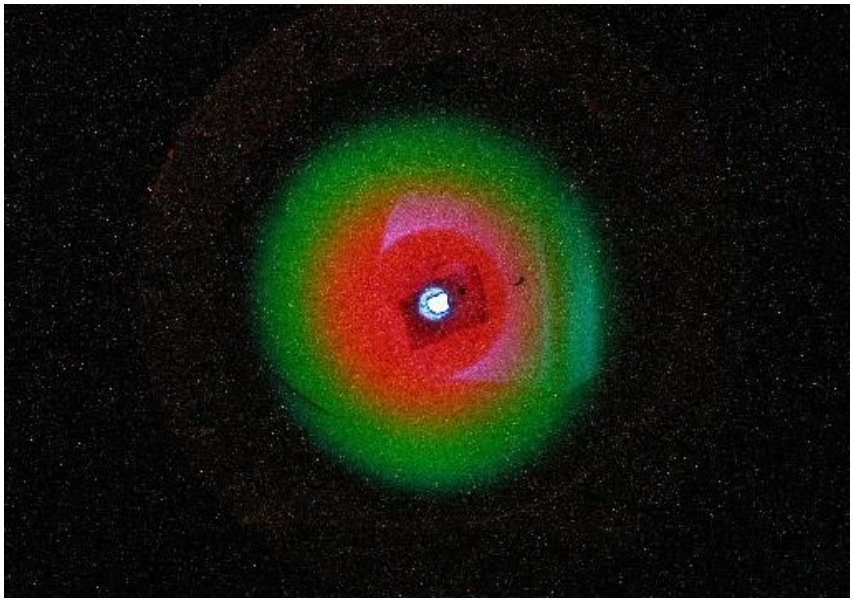

Figure 2. A picture of spontaneous parametric down-conversion emission from a crystal of Lithium Iodate, pumped by ultraviolet light. The blue spot at the center is a remnant of the pump laser.

pairs, and with the respective directions of propagation satisfying the relation of Equation (10). The term *biphoton electromagnetic field* for spontaneous emission from a quantum parametric amplifier is now clear. Since its experimental discovery in the 1970s, the effect has been given different names: parametric noise, parametric scattering, parametric fluorescence, and so on. However, the term *parametric down conversion* (PDC) is possibly the most used in the recent literature. Its very non-classical nature reflects itself not only in photons being emitted in pairs (a major interest for metrological applications, as will be discussed later). In fact, there is a deep quantum nature hidden in the effect, which becomes more evident when considering its description in terms of the quantum wave-function. A full quantum treatment of PDC has been worked out by L. Mandel [12], and results in a wave-function of the form

$$\Psi(t) = \int d\omega_1 d\omega_2 F(\omega_1, \omega_2) \Phi_s(\omega_1, t) \Phi_i(\omega_2, t), \quad (11)$$

where F is a rather complicated function of ω_1 and ω_2, and the Φ are the individual wave-functions of the signal (s) and idler (i) photons. We see from the expression that wave-functions Φ_s and Φ_i are deeply nested together and can by no means be divided apart, because of the F factor in the integral. In one sense, there is a collective wave-function of the photon pairs that mixes together the functions of the individual photons. Such a state, which is peculiar to the quantum realm and has no counterpart in the classical world, is called an *entangled* state. The role of entangled states in fundamental physics is enormous, and is growing with time. It will be discussed in the next section, concerned with applications.

Something should be mentioned at this point concerning the magnitude of the PDC effect and the polarization of photons. The nonlinear dielectrics that show large second-order susceptibilities are generally inorganic crystals with transparency in the visible trough the infrared. Quartz is notably one of them, and it was, in fact, with quartz that people performed the first successful experiment of second-harmonic generation. Birefringence is a mandatory feature of crystals to be used in nonlinear optics, because it is necessary for phase-matching performance. Phase matching is achieved in birefringent crystals due to the fact that there are two waves, an ordinary wave and an extraordinary wave, which can have different propagation velocities and can thereby keep a fixed phase relationship between them. Both uniassic and byassic crystals are used in nonlinear optics, and two basic schemes are employed for phase matching, the so-called Type I and Type II schemes. In Type I, which is used in all applications discussed in the next section, the pump laser enters the crystal as an extraordinary wave, and PDC photons are emitted as ordinary waves. The pump and PDC are therefore orthogonally polarized.

A last word concerns the magnitude of the PDC effect. The nonlinearities at work in the aforementioned crystals, even if greater than in conventional dielectrics, are, anyway, very small. Second-order effective susceptibilities are usually of the order of a few picometers/volt [13, 14], so for a pump power of some hundreds of milliwatts, the spontaneous PDC emission is nine to ten orders of magnitude less. Even if nicely visible to the naked eye, it falls quite naturally in the domain of photon counting.

3. Applications

Two main applications of biphoton fields are now discussed: one in the realm of optical metrology, and the second concerning fundamental physics. Even if apparently very different, they are actually closely related, as both are concerned with precision measurements.

3.1 Quantum Efficiency Measurements

Historically, this is the first application of biphoton fields in the realm of accurate measurements. The method was probably suggested for the first time by Burhnam and Weinberg [11], and soon after was deeply investigated by the Russian school [15]. The basis for it is very simple, indeed. If we consider the experimental setup of Figure 3, we see a couple of single-photon detectors counting photons along two correlated directions and wavelengths, and some electronics for measuring events in coincidence between the two channels. We define the quantum efficiencies, η_1 and η_2, of Detector 1 and Detector 2, as the ratios between the number of events recorded by the detectors over the number of incoming photons. The number of events recorded on the two channels (in a time interval τ) is therefore

$$N_1 = \eta_1 \Phi_1, \tag{12}$$

$$N_2 = \eta_2 \Phi_2,$$

with Φ_2 and Φ_2 being the fluxes of photons in the two channels. On the other hand, the joint probability of events in coincidence between the channels is

$$N_c = \eta_1 \eta_2 \Phi_c, \tag{13}$$

where Φ_c is now the flux of photons in coincidence. From the features of PDC, however, the following relevant relation holds:

$$\Phi_1 = \Phi_2 = \Phi_c . \tag{14}$$

As an immediate consequence, we obtain

$$\eta_1 = \frac{N_c}{N_2}, \quad \eta_2 = \frac{N_c}{N_1} \tag{15}$$

This very important result means that a direct measurement of the detectors' quantum efficiencies is possible by measuring three numbers: the number of events from each detector and the number of coincidences between the two channels. Such a result is even more important in that the actual photon fluxes are of no concern, and, moreover, there is no need for a known and calibrated reference source. This last question is especially relevant as there is a lack of references at the very low powers connected with photon counting. Radiometric standards – such as, for example, cryogenic radiometers – work, in fact, at the microwatt level. In order to scale down to the picowatt (or even femtowatt) levels concerned with photon counting, one should make use of neutral-density filters that, in turn, need to be calibrated against a known radiometric source. Moreover, the 50-60 dB of attenuation required is hard to manage, as the danger of stray light is always present. Last but not least, measurements are not restricted to particular wavelengths, as any possible couple of correlated photons in the whole PDC spectrum can work. It is, in principle, possible to make a measurement of quantum efficiency versus wavelength over the entire spectrum of PDC.

The interest among the radiometric community in the new technique rose very fast. A large number of experiments devoted to the measurement of quantum efficiency with metrological criteria were soon performed [16-18]. The very crude sketch of Figure 3 is, of course, not an operational method, as a number of things should be managed. First of all, it is very difficult, if not impossible, to have $\Phi_1 = \Phi_2$ exactly. This calls, in fact, for a perfect identity of the two channels, which, in turn, calls for a perfect identity in the solid angles subtended by the two detectors and for quite identical overall optical losses. However, if one is not interested in simultaneously measuring η_1 and η_2, things can be considerably relaxed. It is common practice to treat the two channels in quite different ways. On one channel, usually called the trigger, one does not care about the efficiency of photon collection (the solid angle, optical losses, and so on), nor about the quantum efficiency of the

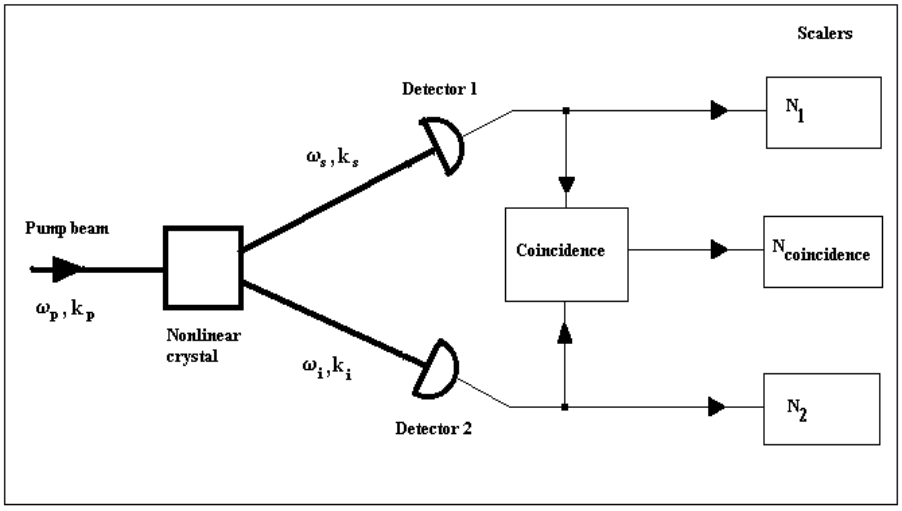

Figure 3. The principle of quantum-efficiency measurement. Detectors 1 and 2 are single-photon detectors, mainly silicon avalanche photodiodes operated in the Geiger mode. The number of events in a time interval, τ, detected by each detector, and the number of events in coincidence between the two detectors, are counted by three scalers. From the basic properties of PDC light, the quantum efficiency of the detectors is given directly by the quantity $\eta_{12} = N_{coincidence} / N_{2,1}$.

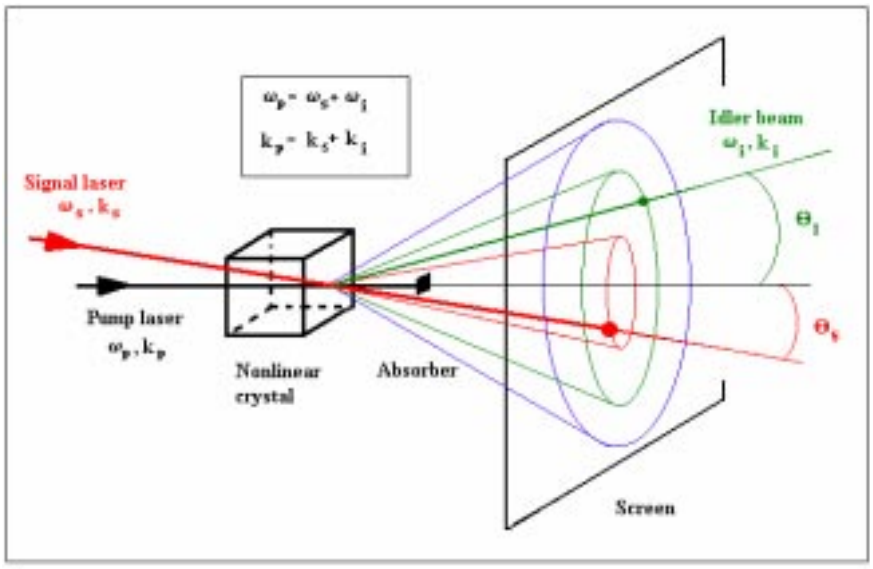

Figure 4. An optical parametric amplifier. A beam from a near-infrared diode laser is injected into the nonlinear crystal at an angle, θ_s , which satisfies the phase-matching relations (in the box). An idler signal at the frequency $\omega_i = \omega_p - \omega_s$ is emitted at the angle θ_i given by phase-matching. Two bright spots – a large spot from the signal laser (red in the figure), and a smaller spot from the idler beam (green) – are clearly visible on the screen.

detector itself. On the second channel, the only thing to insure is to collect *all* the photons correlated with those of the trigger. This is a considerably relaxed requirement, as the solid angle of the trigger can be reduced at will, by means of pinholes or diaphragms, until the photon flux is still sufficiently higher than detector's dark noise. This, in turn, makes it easy to have a collection solid angle that surely matches the solid angle of the trigger on the second channel. The device under test (DUT) is therefore calibrated against the trigger's events, no matter what their number is, and the device under test can, in principle, catch many more photons than necessary, without any problem. Attention should be paid only to not have so large a flux on the device under test so as to spoil its dead time: that is, the time required for the detector to recover its operation after an event has been detected, and during which time it is blind.

A second relevant experimental question is how to pick up a pair of correlated directions and wavelengths in the whole PDC emission. This is perhaps an even worse problem than the previous one. The standard way of managing it is by means of narrow interference filters at the proper wavelengths. By carefully scanning the two coronas, corresponding to the wavelengths of interest, coincidences between the channels are found. This procedure is sometimes time consuming, but, luckily enough, there is a different way out of the problem.

Parametric down conversion is, first of all, a parametric process. As we saw before, the classical counterpart of PDC is the parametric amplifier, which calls for three fields at work. The optical version of the parametric amplifier works as well, much in the same way as the microwave version. By properly injecting an external laser field into the nonlinear crystal, an idler signal appears at the wavelength and propagation angle that satisfy phase-matching relations. The experimental setup takes the form shown in Figure 4. A near-infrared laser beam at the wavelength ω_s – usually, from a semiconductor laser – is sent into the crystal so that it spatially overlaps the pump beam, at the wavelength ω_p , in the crystal's center. The phase-matching relation for energy, Equation (9), requires that $\omega_i + \omega_s = \omega_p$, so that a beam, usually called the idler beam, at the wavelength ω_i , is emitted by the crystal. The frequency of the idler beam is fixed by virtue of energy conservation, but its direction of propagation is also fixed. Each wavelength in the PDC spontaneous-emission spectrum is, in fact, correlated to an angle such that the phase-matching relation for momentum, Equation (10), is satisfied. The laser and the idler beams therefore identify the loci of a couple of correlated photons in spontaneous emission. The idler power, even if very low, results regardless in a beam that can easily be followed for some meters downstream of the crystal. Two detectors can therefore be aligned on the two beams. When the diode laser is switched off, coincidences between the detectors readily appear: only slightly minor adjustments are required to peak the coincidence signal. To give an idea of the numbers at work, with a pump power of 300 mW at 351 nm, and a diode-laser power of 50 mW at 789 nm, an idler signal of a of few nanowatts at 633 nm is emitted. Such a beam can easily be followed along a distance of a couple of meters or more [19].

A practical operational setup for quantum-efficiency measurements therefore takes the form shown in Figure 5 [20]. By exchanging a few optical components (mainly, pinholes and irises), the roles of trigger and device under test can be interchanged, and calibration at two different wavelengths is easily performed. Due to the large number of pumping wavelengths and diode-laser emission ranges, a rather large number of correlated wavelengths can be covered, so that calibration over a large spectral interval appears to be feasible. A list of spectral intervals, with existing semiconductor lasers in combination with Argon-ion laser pumps, was reported in the literature [21].

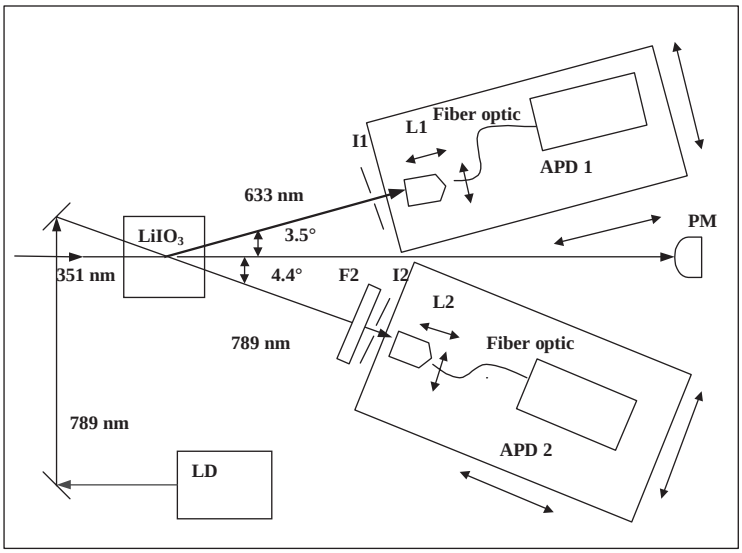

Figure 5. The practical experimental setup for the quantum-efficiency measurements reported in the text. APD1 and APD2 are avalanche photodiode detectors provided with coupling to fiber optics. L1 and L2 are the collimators for the coupling of the PDC light to the fibers. PM is a meter for the monitoring of ultraviolet power stability. The angles given in the figure are related to the actual wavelengths at which the measurements were performed.

A few words are due regarding the description of the electronics. It is a quite standard setup of the kind commonly employed in nuclear physics. The output signals from the detectors are TTL-like pulses, which are routed to a couple of scalers, for counting signal and trigger events, and to the start and stop inputs of a time-to-amplitude converter (TAC). The output from the time-to-amplitude converter is a pulse with an amplitude that is proportional to the delay between a start pulse and a stop pulse. Downstream from the time-to-amplitude converter, there is a single-channel analyzer (SCA), which filters the pulses in a given amplitude window, thereby selecting events in a corresponding delay interval. The output from the single-channel analyzer is directed to a third scaler, for the counting of coincidence events. Eventually, the output from the time-to-amplitude converter is directed to a multi-channel analyzer (MCA), for visualizing the coincidence peak on a screen. The whole electronic setup is described in Figure 6, whereas Figure 7 shows a typical coincidence peak as it is seen on the multi-channel analyzer scope.

With the setup of Figure 4, the author and coworkers calibrated a couple of avalanche single-photon detectors at the aforementioned 789 nm and 633 nm wavelengths, with an ultraviolet pump wavelength of 351 nm from an Argon-ion laser. The detectors were solid-state silicon avalanche photodiodes, operated in the Geiger mode, of the so-called active-quenching type. This means that the avalanche process was stopped by an appropriate current pulse from the

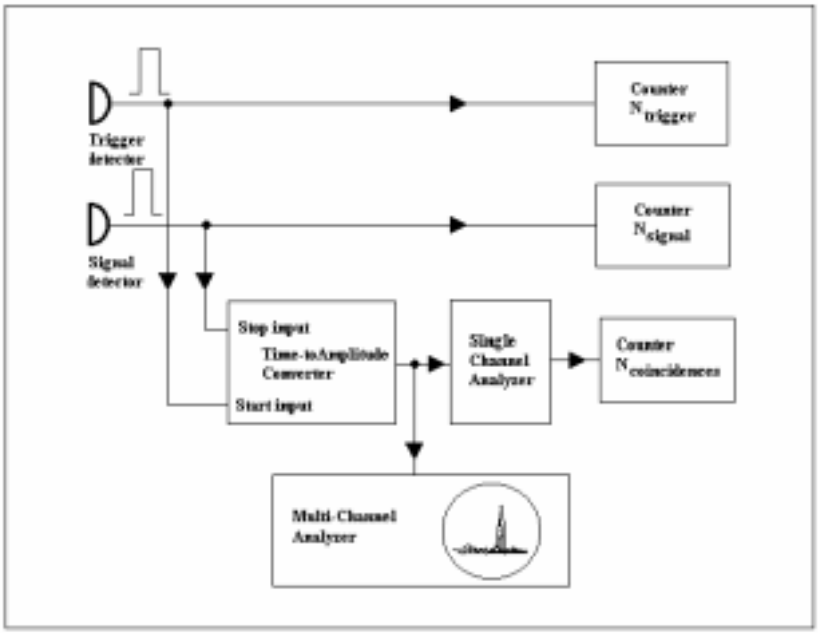

Figure 6. The setup of the electronics for quantum-efficiency measurements. Coincidences are measured via a time-to-amplitude converter (TAC), which provides an output pulse with amplitude proportional to the delay between the start and stop pulses. A single-channel analyzer (SCA) sets the "coincidence window," which is the time interval over which "true" coincidences are detected, as opposed to random coincidences of uncorrelated events on the start and stop channels. The output from the TAC is sent to a multi-channel analyzer (MCA) for visualizing the coincidence peak on a screen.

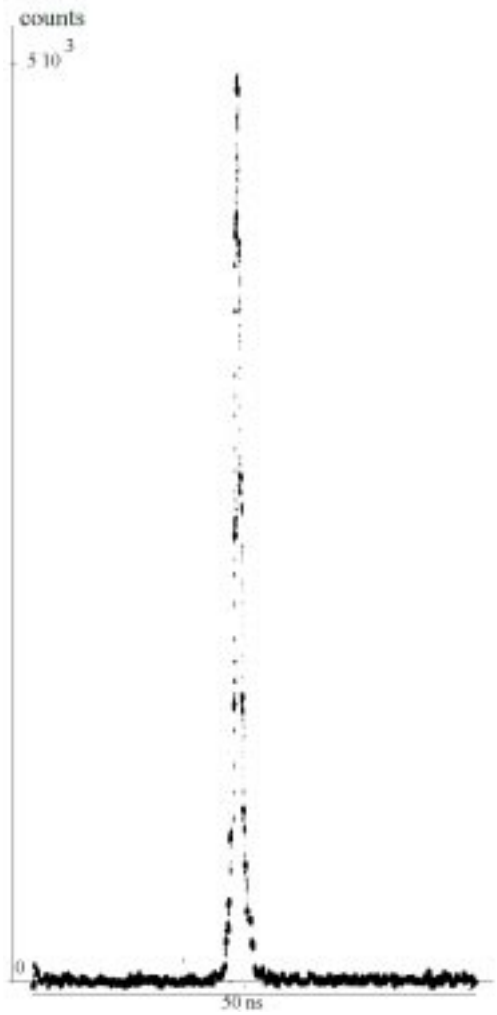

Figure 7. An actual record of coincidence events between idler and signal photons, as seen on the multi-channel analyzer in the setup of Figure 6. The number of coincidence counts is on the y scale, and the delay between the start and stop input signals is on the x scale. A straight enhanced peak, corresponding to "true" coincidences, emerges from the background of spurious coincidences of uncorrelated events, the noise floor in the figure. The electric delays in the setup are chosen so that the coincidence peak is moved away from zero delay, a point where the electronics does not work properly.

electronics, rather than relying on the time constants of the passive supply circuitry. The detectors were provided with coupling to multimode fibers of 100 μm diameter, and rather standard optics were used for coupling the PDC photons to the fiber. The results of calibration were found to be in quite good agreement with the data from the manufacturer [21]: we measured efficiencies at 633 nm to be $(38.0 \pm 0.5)\%$ and $(37.9 \pm 0.9)\%$, and at 789 nm to be $(32.3 \pm 0.7)\%$ and $(33.9 \pm 1.2)\%$, respectively, for the two detectors. Later on, the agreement with a more-conventional measurement technique was also found to be good, as discussed below.

The uncertainties quoted deserve some comment. They were calculated along the theory reported in the literature [22], and were simply the random standard deviation of measurements, and not actually an accuracy figure. The latter should be evaluated anyway for assessment of the technique, and this job is currently under way in different laboratories [23]. The hard task is to measure losses in the optical paths. If, on the one hand, the propagation of photons from the crystal to detectors in plain air is easily modeled, on the other hand, the main losses are internal to the crystal. For a couple of photons, it may happen, in fact, that one is absorbed by the crystal and the companion is left to propagate unaffected. As a consequence of this, a coincidence is lost, and this spoils the final result. The electronics itself should be carefully evaluated, as the dead times of both the detectors and the time-to-amplitude converter – that is, the times for which the electronics do not work – may result in serious losses of counts.

Despite the fact that a final figure of accuracy is still lacking, people's opinion is that the correlated-photons technique can be pushed to the 10^{-3} accuracy level, limited mainly by inaccuracy in the evaluation of crystal losses [24]. A direct comparison of results against standard techniques, based on neutral-density filters and a laser source at 633 nm, showed a good agreement at the 10^{-2} accuracy level [25].

3.2 Tests of Quantum Mechanics

A second application, quite different from the former application, concerns tests of fundamental physics. Since its birth, quantum mechanics has raised questions that are still waiting for definitive answers. Actually, it is the existence of quite peculiar electromagnetic fields, such as the ones we are dealing with, that leads to such questions. This was already recognized as early as 1935, in a celebrated paper by Einstein, Podolsky, and Rosen [26]. In that work, the authors considered the outcome of polarization measurements on a couple of particles (fermions) in a singlet state, that is, a state where the spin of the whole system is zero. Even when the flight of the two particles is well apart the total spin is conserved: whatever the actual spin is of the one particle, that of the other particle should be the opposite. It is not difficult to imagine that strange things could happen in this situation, such as, for example, forecasting the outcome of a measurement on one of the two particles without actually performing it, simply from measurements performed on the second particle. So, it is possible to know a priori and simultaneously the value of non-commuting quantities, a fact forbidden in principle in quantum mechanics. From these considerations, the authors of the 1935 paper concluded that quantum mechanics is incomplete, and the ensemble of their considerations has been known since then as the EPR paradox.

A possible way out of the paradox – originally proposed by the authors themselves, and, later on, the object of a huge amount of research work – calls for the existence of a set of variables that, in principle, completely determine the state of a physical system in quantum mechanics, but that are in

some sense *hidden*, so that in computing predictions on the system integration should be over the state of these variables [27]. The *hidden-variable theories* [HVT] acquired large popularity after the works by Bohm et al., but it was not until 1964 that the question of discriminating between standard quantum mechanics [SQM] and hidden-variables theories entered the realm of experimental physics. In that year, J. Bell – at the time, at the European Center for Nuclear Physics (CERN), in Geneva – wrote a fundamental paper, in which he demonstrated, with arguments from set theory, that some physical quantities, accessible to experiment, should take different values in standard quantum mechanics and in hidden-variable theories [28].

What is basically of interest is the quantity derived from the joint probability of detection of a given physical state for a couple of particles in a singlet state. To understand Bell's results, it is better to rely on a slight modification of them due to J. F. Clauser and M. A. Horne. If we denote by $P_{12}(\theta_1,\theta_2)$ the joint probability for detection of both particles 1 and 2 when the physical quantities θ_1, θ_2, θ_1', and θ_2' are measured (in the overwhelming majority of cases, these are angles of polarizers), the quantity

$$R=\frac{P_{12}(\theta_1,\theta_2)-P_{12}(\theta_1,\theta_2')+P_{12}(\theta_1',\theta_2)+P_{12}(\theta_1',\theta_2')}{P_{12}(\theta_1',-)+P_{12}(-,\theta_2)} \tag{16}$$

is predicted to be always smaller than zero in hidden-variable theories, whereas for a proper choice of parameters, it can be greater than zero if standard quantum mechanics holds. Here, $P_{12}(\theta_1',-)$ and $P_{12}(-,\theta_2)$ denote the joint-detection probabilities with one of the two polarizers removed. It can be easily demonstrated that a choice of parameters of

$$\theta_1=0\,,\quad \theta_2=3\pi/8\,,\quad \theta_1'=-\pi/4\,,\quad \theta_2'=\pi/8\,, \tag{17}$$

leads to a value $R\approx 1.207$ in standard quantum mechanics. This fundamental result opened the door to a huge amount of experimental work [29-31].

A typical experimental setup for polarization coincidence measurement is depicted in Figure 8. All of these kinds of experiments call for a source of couples of particles in an entangled state. There is no restriction on the particles to be used, so that experiments have been performed both with fermions and bosons. The latter, in the overwhelming majority of cases, have been done with photons. Downstream from the source, two polarizers analyze the particles, which are then detected by a couple of detectors. Quite standard electronics, of the type described in the previous section, completes the setup for measuring rates on the single channels, as well as coincidences.

In 1982, A. Aspect and coworkers performed a cornerstone experiment with correlated photons that gave justice to standard quantum mechanics. The source of photons was the radiative cascade of $^{40}\mathrm{Ca}\,4\mathrm{p}^{21}\mathrm{S}_0\rightarrow 4\mathrm{s}\,4\mathrm{p}^1\mathrm{P}_1\rightarrow 4\mathrm{s}^{21}\mathrm{S}_0$, in which two photons (anti-) correlated in polarization and direction, are emitted. This experiment remained unrivaled for many years, despite some intrinsic limitations. One of these limitations is concerned with the poor angular correlation of the two photons. The atom recoil can, in fact, take a fraction of the total momentum in a probabilistic way, and this reflects itself directly in an incomplete correlation between the photon pair [32].

Late in the 1980s, people started looking for a better source of correlated photons, and the answer was quite naturally found in parametric down conversion. For PDC, there is no mechanism that could destroy the correlation between linear momentum and wavelength of the photon pair. A number of new experiments was performed in the 1990s, with photons from both Type I and Type II PDC, and all results were in accord with quantum mechanics [33-34]. The situation seems to be assessed, therefore, with no more space left for hidden-variable theories, but things are actually a bit different.

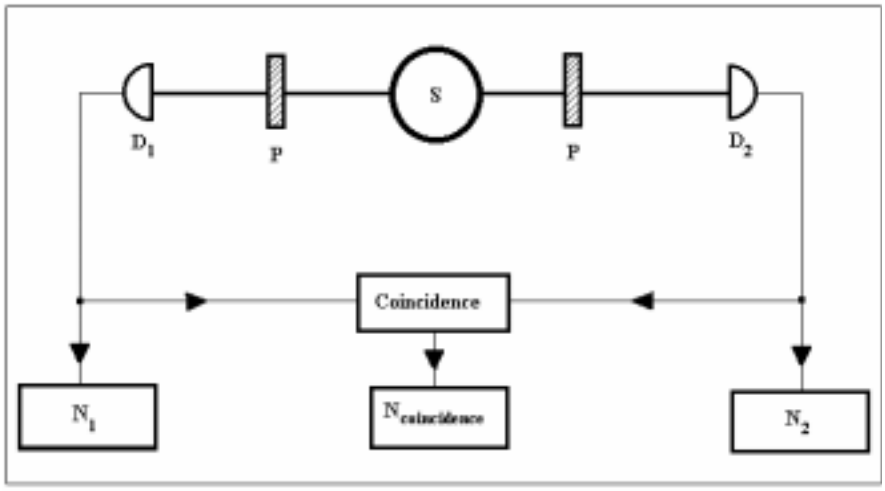

Figure 8. The basic setup for polarization-correlation measurements. S is a source of polarization-correlated photons, D1 and D2 are single-photon detectors, P identifies the two polarizers, and a standard electronic chain – with a coincidence system and three scalers, N1, N2, and Ncoincidence – is necessary for counting the events on each channel. The heavy lines in the figure refer to photon trajectories, whereas the lighter lines are the electric-signal paths.

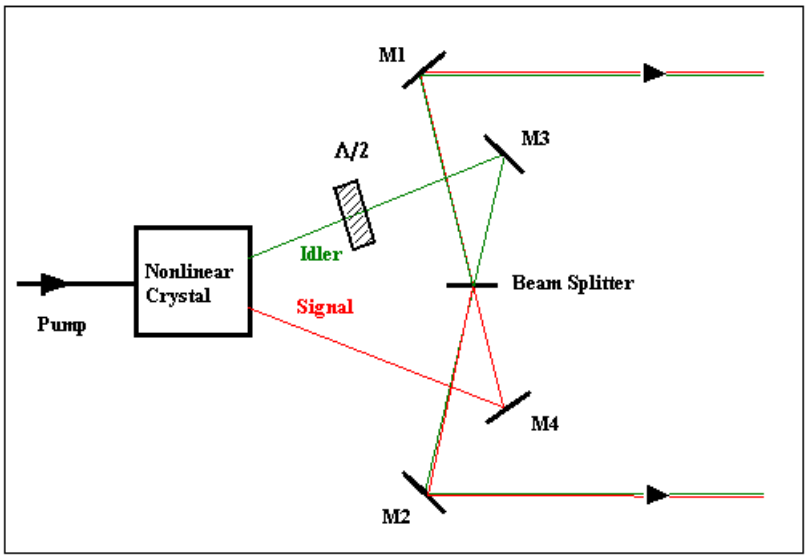

Figure 9. A standard way of building a polarization-entangled photon state from Type I PDC. M1 to M4 are totally reflecting mirrors, and $\Lambda/2$ is a 90° retardation plate, which rotates the polarization of the idler beam. The beam splitter superimposes two different polarizations, and builds up a polarization-entangled state.

A new question emerges in critical reviews of existing experimental data [35]. All experiments – in fact, even the most recent ones – suffer from a low overall efficiency. This means that only a fraction of the total pairs of particles emitted by the source is collected. This is mainly due to the poor quantum efficiency of single-photon detectors, which is at most around 80%, but losses in optical components, especially polarizers, play a role. Now, for each experiment, it is possible to construct an ad hoc hidden-variable theory that is in agreement with the data. It is basically the necessity to assume the so-called "*fair sample*" condition that limits the experiment. In fact, we should suppose that the set of particles that we detect are a good representation of the whole ensemble. From a purely theoretical point of view, however, one should face the possibility of some hidden variable changing the detected states with respect to the whole ensemble. This problem was the object of lots of papers in the literature.

It is not only the poor detection efficiency of photodetectors that is in question, but also the preparation of the states on which measurements are performed. With the exception of a few experiments performed directly with time-energy entanglement of PDC [36], the majority of experiments involve polarization measurements, as explained before. To build a state entangled in polarization there are essentially two methods. One involves Type II PDC, and has its problems, which we do not discuss in this paper. The second way is represented in Figure 9, and consists of superimposing the idler and signal beams on a beam splitter, after properly rotating the polarization of one of the two. The output from the beam splitter can be written in the form

$$|\Psi\rangle = \frac{|HV\rangle + |VH\rangle}{\sqrt{2}}, \qquad (18)$$

where H denotes horizontal polarization and V denotes vertical polarization. It appears immediately from Figure 9 that at least half of the incoming population is lost in this way, due to the beam splitter.

A different experimental scheme, which overcomes the problem, was proposed as early as 1990 in the literature [37], and recently realized [38]. It consists of superimposing the spontaneous emission from two crystals in cascade, pumped by the same laser, and with polarizations rotated by 90° of one with respect to the other. The experimental setup takes the form of Figure 10, and it was given the name ENOS (entangled nonlinear optical setup). After the first crystal pump laser is displaced »1 mm by a quartz plate (P) for compensating birefringence displacement, the PDC emission is then focused by a system of biconvex lenses, which work as an optical condenser, onto the second crystal. A retardation plate, $\Lambda/2$, rotates the pump polarization before it enters the second crystal, and the crystal itself is rotated 90° with respect to the first crystal. In this way, the two emissions from the crystals are orthogonally polarized. If one is able to superimpose them exactly, the output is a photon state entangled in polarization.

The difficulties in the alignment of such a system were already pointed out in the 1990 proposal. Once again, the trick of parametric amplification is of help, here. As in the case of quantum-efficiency measurements, an infrared diode laser can be injected into the crystals at the proper angle. By rotating its polarization midway between the two crystals, idler signals from both crystals are excited. By careful adjustment of the crystals' positions, it is possible to superimpose the two beams, and to so have a fine superposition of both idlers and signals from the two parametric down-conversions, as requested for a Bell inequalities test. An entangled state results as a consequence of the indistinguishability in the generation of PDC photons in the two crystals. A major feature of ENOS is the possibility

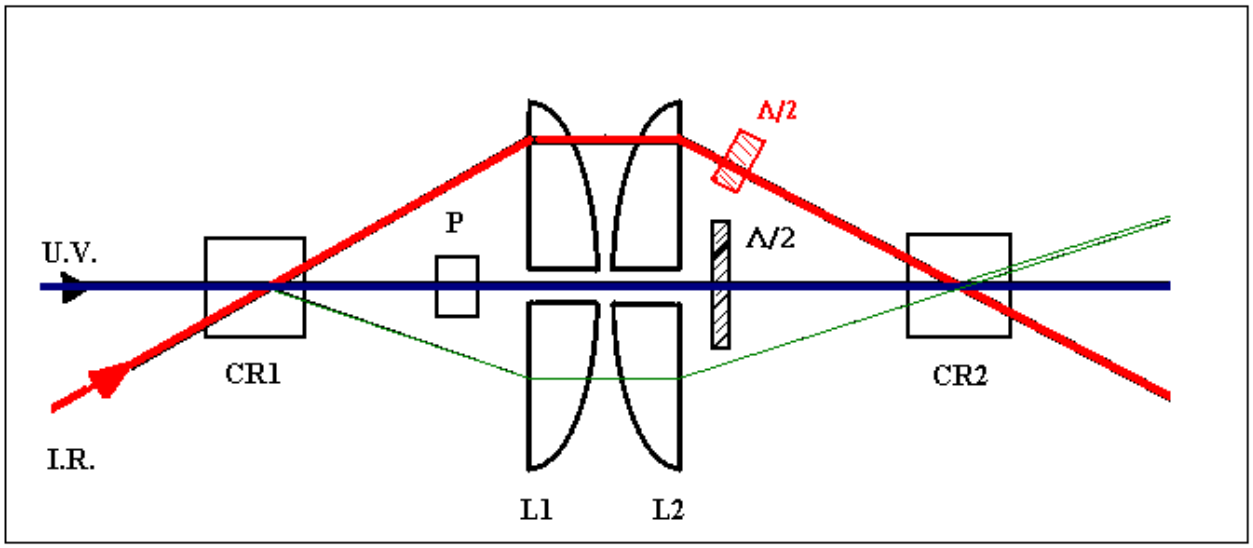

Figure 10. The "entangled nonlinear optical setup" (ENOS). The spontaneous PDC emissions from two crystals, CR1 and CR2, are superimposed. Quartz plate P compensates for the displacement of the pump beam after crystal CR1 due to birefringence; lenses L1 and L2 operate as an optical condenser, and focus emission from CR1 into CR2. The retardation plate, $\Lambda/2$, rotates the polarization of the pump 90°, and crystal CR2 is also rotated 90° with respect to CR1. The infrared laser beam (I.R.), which is the determinant for system alignment, is indicated, together with its retardation plate for polarization rotation and the corresponding idler emissions shown by the thinner lines (green in the color version of the figure).

of changing the power of the pump laser in between the crystals, and to thereby have different photon fluxes from the two PDCs. The wavefunction of the final state can be cast in the form

$$|\Psi\rangle = \frac{|HH\rangle + f\,|VV\rangle}{\sqrt{1+f^2}}, \qquad (19)$$

with the parameter *f* being tunable from zero to unity. The deep interest in such an experimental degree of freedom relies in the fact that it has recently been pointed out that, for non-maximally-entangled states, an overall quantum efficiency of 67% is sufficient for a loophole-free test of Bell inequalities [39].

A first experiment has been performed with ENOS. Its quantum efficiency was still low, as we used fiber-coupled detectors, but the first results were encouraging. They were in quite good agreement with standard quantum mechanics. The Bell inequality resulted:

$$R = 1.082 \pm 0.031,$$

to be compared against the theoretical value of 1.16, corresponding to the experimental case $f = 0.4$. Future experiments with better detectors could possibly result in a further step toward a definitive test of hidden-variable theories.

4. Conclusions

This very rapid and, undoubtedly, very simple presentation of biphoton fields couldn't be closed without at least a minor glance at some other applications, not treated in the paper. Not surprisingly, they are in the realm of communications, a matter where electromagnetic fields traditionally find their place.

A first application, which is directly linked to the EPR paradox and Bell inequalities, concerns making communications secret. So-called "*quantum cryptography*" was born at the beginning of the 1980s, mainly from the work of Bennet and Brassard [40]. Their celebrated algorithm has since become widely known. Without entering too much into the subject, the main feature of quantum cryptography is the fact that by performing measurements on an entangled state of two photons, the entanglement itself can be destroyed. In other terms, a spy who steals information from a communication channel can be readily discovered by performing, for example, a measurement of Bell inequalities. If the receiver at the end of a quantum information channel finds results different from what is theoretically expected, he immediately knows that someone is stealing information, and the channel is no longer secure. He can therefore reject information received so far, and try another communication [41].

A second application is even more "exotic," if possible. The subject of "*quantum teleportation*" has become a very "hot" field of research in recent years. It is, again, the

entanglement itself that makes it possible to reconstruct a quantum state at a distance. Experiments have already proved the validity of the idea, even if there are still limitations, mainly due to technical questions, and not in principle [42].

Despite the fact that biphoton fields have aged more than thirty years, it looks like they are very young. With the development of powerful technical apparatus and experimental techniques, it is not unlikely that in forthcoming years, a great number of surprises will come from the matter.

5. References

1. G. N. Lewis, *Nature*, **118**, 1926, pp. 874-875.

2. A. Pais, *"Subtle is the Lord:" The Science and the Life of Albert Einstein*, Oxford, Oxford University Press, 1982, pp. 411.

3. L. Mandel, *Physica Scripta*, **T12**, 1986, pp. 34-42.

4. B. L. Walsh, *International Science and Technology*, No. 17, 1963, p. 75.

5. J. M. Manley and H. E. Rowe, *Proc. IRE*, **47**, 1959, p. 2115.

6. A. Yariv and P. Yeh, *Optical Waves in Crystals*, New York, J. Wiley & Sons, 1984.

7. P. A. Franken, A. E. Hill, C. W. Peters, and G. Weinreich, *Phys. Rev. Lett.*, **7**, 1961, p. 118.

8. C. C. Wang and G. W. Racette, *Appl. Phys. Lett.*, **6**, 1965, p. 169.

9. J. A. Giordmaine and R. D. Miller, *Phys. Rev. Lett.*, **14**, 1965, p. 973.

10. D. N. Klyshko, *Sov. Phys. JETP*, **28**, 1969, p. 522.

11. D. C. Burnham and D. L. Weinberg, *Phys. Rev. Lett.*, **25**, 2, 1970, p. 84.

12. L. Mandel and E. Wolf, *Optical Coherence and Quantum Optics*, New York, Cambridge University Press, 1995, pp. 1074-1093.

13. V. G. Dimitriev, G. G. Gurzadyan, and D. N. Nikogosyan, *Handbook of Nonlinear Optical Crystals*, Berlin, Springer, 1997.

14. G. Borsa, S. Castelletto, A. Godone, and M. L. Rastello, *Optical Review*, **4**, 4, 1997.

15. D. N. Klyshko, *Photons and Nonlinear Optics*, New York, Gordon and Breach, 1988.

16. J.G. Rarity, K. D. Ridley, and P. R. Tapster, *Appl. Opt.*, **26**, 1987, p. 4616.

17. V. M. Ginzburg, N. G. Keratishvili, Ye. L. Korzhenevich, G. V. Lunev, A. N. Penin, *Metrologia*, **29**, 1992, p. 95.

18. S. Castelletto, A. Godone, C. Novero, and M. L. Rastello, *Metrologia*, **32**, 1995/1996.

19. G. Brida, S. Castelletto, C. Novero, M. L. Rastello, *Metrologia*, **35**, 4, 1998, p. 247.

20. G. Brida, S. Castelletto, C. Novero, M. L. Rastello, *Metrologia*, **35**, 4, 1998, p. 397.

21. G. Brida, S. Castelletto, C. Novero, and M. L. Rastello, *J. Opt. Soc. Am. B*, **16**, 1999, p. 1623.

22. P. G. Kwiat, A. M. Steinberg, R. Y. Chiao, P. H. Eberhard, and M. D. Petroff, *Appl. Opt.*, **33**, 10, 1994, p. 1844.

23. G. Brida, S. Castelletto, I. P. Degiovanni, M. Genovese, C. Novero, and M. L. Rastello, *Metrologia*, **37**, 2000, p. 629.

24. A. Migdall, *IEEE Transactions on Instrumentation and Measurements*, **50**, 2, 2001.

25. G. Brida, S. Castelletto, I. P. Degiovanni, C. Novero, and M. L. Rastello, *Metrologia*, **37**, 2000, p. 625.

26. A. Einstein, B. Podolsky, and N. Rosen, *Phys. Rev.*, **47**, 1935, p. 777.

27. D. Bohm, *Phys. Rev.*, **85**, 1952, p. 166, p. 180.

28. J. S. Bell, *Physics*, **1**, 1964, p. 195.

29. S. J. Freedman and J. F. Clauser, *Phys. Rev. Lett.*, **28**, 1972, p. 938.

30. F. M. Pipkin in D. R. Bates and B. Bederson (ed.), *Advances in Atomic and Molecular Physics*, New York, Academic Press, 1978.

31. J. F. Clauser, *Phys. Rev. Lett.*, **36**, 1976, p. 1123.

32. A. Aspect, P. Grangier, and G. Rogier, *Phys. Rev. Lett.*, **47**, 7, 1981, p. 460.

33. Y. H. Shih, C. O. Alley, *Phys. Rev. Lett.*, **61**, 26, 1988, p. 2921.

34. Y. H. Shih, A. V. Sergienko, *Physics Lett. A*, **186**, 1994, p. 29.

35. E. Santos, *Phys. Rev. Lett.*, **66**, 1991, p. 1388.

36. J. D. Franson, *Phys. Rev. Lett.*, **62**, 19, 1989, p. 2205.

37. L. Hardy, *Phys. Lett. A*, **161**, 1992, p. 326.

38. G. Brida, M. Genovese, C. Novero and E. Predazzi, *Phys. Lett. A*, **268**, 2000, p. 12.

39. P. H. Eberhard, *Phys. Rev. A*, **47**, 1996, p. R747.

40. C. H. Bennett and G. Brassard, *Proceedings of the IEEE International Conference on Computers, Systems and Signal Processing*, Bangalore, India, New York, IEEE, 1984, p. 175.

41. A. K. Ekert, *Phys. Rev. Lett.*, **67**, 1992, p. 661.

42. D. Boumeester, J.-W. Pan, K. Mattle, M. Eibl, H. Weinfurter, and A. Zeilinger, *Nature*, **390**, 1997, p. 575.

Lightning Electromagnetic Effects: Do We Know Everything ?

Michel Ianoz

Abstract

In the last twenty years, the widespread use of sensitive electronic devices has increased the interest in transients, in particular those caused by lightning (direct and/or indirect). This tutorial presents the latest developments in modeling the electromagnetic (indirect) effects of lightning. The progress in field-to-transmission-line coupling calculations for networks permits the analysis of more complicated structures subject to a lightning electromagnetic field. In parallel, it has been observed that the lightning current parameters obtained from measurements of real lightning strokes are polluted by the measurement arrangement, and that data decontamination is needed. Approximations using low-frequency coupling expressions that neglect the propagation in the case of complicated circuits with small dimensions will also be discussed. Such approaches can give approximate solutions and orders of magnitude, helpful for correct EMC design for very complex configurations such as control and protection circuits in power-network substations, for instance.

1. Introduction

In the last 15-20 years, the widespread use of sensitive electronic devices in data transmission networks, in power-system equipment (circuit breakers, disconnects, control and protection circuits), and in household appliances has increased the interest in transients. From this point of view, transients caused by lightning (direct and/or indirect) can be one of the major causes of malfunction, or even destruction, of electrical equipment. In particular, lightning-induced voltages – which can cause micro-interruptions of the power supply, or disruption in the telecommunication or data-transmission networks during thunderstorms – have been seriously reconsidered, due to the increasing demand by customers for good quality in the power supply, and for reliability in the transmission of information. The opening of the telecommunication market, followed now by that of electrical power, is only accelerating this trend.

There is no clear evidence in the power-system literature of the relationship between the number of outages during thunderstorms and lightning-flash density in the proximity of the place of failure. However, a case reported in Sweden – in which, during a heavy thunderstorm, one high voltage and several distribution transformers exploded, leaving 11,000 people without electricity for 24 hours – is symptomatic of the impending danger of lightning, in particular since it occurred in a highly developed country [1]. This case has also shown that the interruption of information and of the electrical supply in modern society can have severe consequences. A lightning stroke in the proximity of a big hotel in the town of Lausanne (Switzerland) induced a voltage in the satellite antenna and destroyed the TV sets in the building. Recently (July 11, 2002), direct lightning strokes to trees during heavy thunderstorms have caused accidents in Germany; another stroke to an ammunition storage facility, near the town of Samara (Russia), triggered a big explosion. Some more data on over-voltages, measured on aerial lines and on telecommunication equipment, will be presented later.

The more frequent use of lightning detection systems [2], which give, in principle, the possibility of correlating lightning strokes at ground level with failures, can in the future provide better statistics relating these two kind of events, and this is expected to support the introduction of more adequate protection measures.

The interaction between lightning and installations can be:

- Direct, if a lightning stroke directly hits a line connected to the installation or the equipment;
- Indirect, if the strike is at a certain distance and the currents are induced by the electromagnetic field generated by the lightning discharge.

In recent years, significant progress has been achieved in modeling the lightning discharge in the return-stroke channel, the field-to-transmission-line coupling, and also, to some extent, non-linear protection elements. This progress provides the possibility of estimating, on the one hand, the level of over-voltages caused by direct lightning strokes on lines or grounding wires, or induced by nearby-lightning electromagnetic fields, and, on the other hand, the efficiency of different protection concepts, using numerical calculations.

Michel Ianoz is with the
Swiss Federal Institute of Technology of Lausanne,
LRE - DE, CH - 1015 Lausanne, Switzerland;
Tel: (+4121) 693 26 64;
Fax: (+4121) 693 46 62;
E-mail: michel.ianoz@epfl.ch

[Editor's Note: This invited paper was the Commission E Tutorial Lecture, presented at the XXVII General Assembly of URSI in Maastricht, The Netherlands, August 17-24, 2002.]

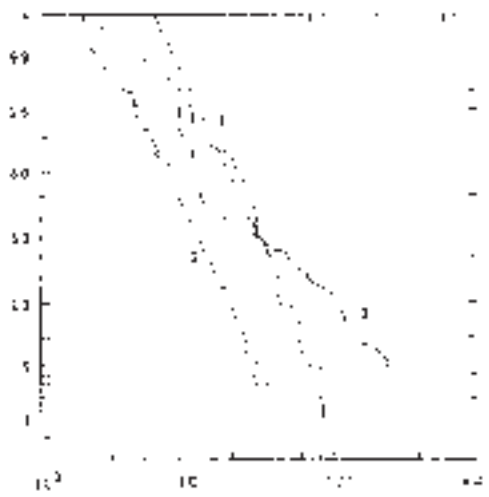

Figure 1. The peak current distribution for (1) negative first stroke, (2) negative subsequent strokes, and positive strokes, from Berger et al. [3]. The straight dashed lines represent log-normal distributions fit to experimental data (reproduced from [4]).

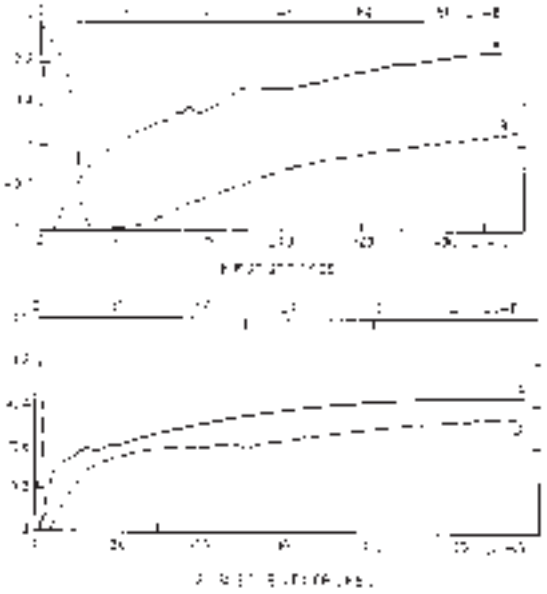

Figure 2. The average negative return-stroke current wave shapes, normalized to unity peak amplitude (reproduced from [4]).

Can we now say that we now have at our disposal all of the elements needed to design adequate protection, or is lightning still such an arbitrary phenomenon that we can hardly expect to know much about it? The aim of this tutorial is to present the latest developments in modeling lightning electromagnetic effects, and to discuss this question.

2. Statistics of Lightning Currents

As the primary cause of lightning electromagnetic effects is the lightning current, an overview of the existing statistics of measured natural lightning currents, based on data obtained by Berger et al. [3], is presented in Figure 1. Figure 2 presents the average wave shapes for negative first and subsequent strokes, based on the same data, at two different time scales. These data were measured during the 1950s and 1960s, with measurement instruments that did not have the same performance as those in use today. However, this remains the most complete set of data for natural lightning, and no better statistics have been produced. More recent natural lightning current measurements have been performed in Canada [5, 6], Germany [7, 8], Italy [9, 10], Russia [11], and South Africa [12]. These measurements, as well as field measurements, only indicate that smaller risetimes should be expected, in particular for subsequent return strokes.

3. Measured Lightning-Induced Voltages

Measurements of voltages induced by natural or triggered lightning strokes have been performed at different sites and using different methods. We show here a few typical experimental values, which demonstrate that over-voltages that are dangerous for electrical equipment are induced by nearby lightning strokes.

Figure 3 shows the voltage induced by a stroke on an unenergized aerial line in Mexico [13]. The line was 2.8 km long and 10 m high, which is typical for a distribution line in the particular case of 13 kV nominal voltage. The site was situated in the southwest of Mexico and is a region with a high keraunic level, about 100 thunderstorms/year.

Concerning telecommunication networks, other experimental evidence of dangerous lightning electromagnetic effects was obtained in a measurement campaign that was performed by the Centre National d'Etudes des Télécommunications in France [14]. Over-voltages due to lightning strokes were measured during a period of two years at nine sites with different keraunic levels, and in various environments (industrial, rural, residential), in France, as shown in Figure 4. A total number of 16,000 short events (lightning pulses on the telecommunication line, lightning and/or switching pulses on the mains) were recorded at the nine sites during the measurement period.

Figure 3. An oscillogram of the voltage induced at one end of an unenergized line in Mexico by a nearby lightning stroke (adapted from [13]).

Figure 4. The geographical location of the selected sites: •: control, monitoring and processing site; o: measurement sites

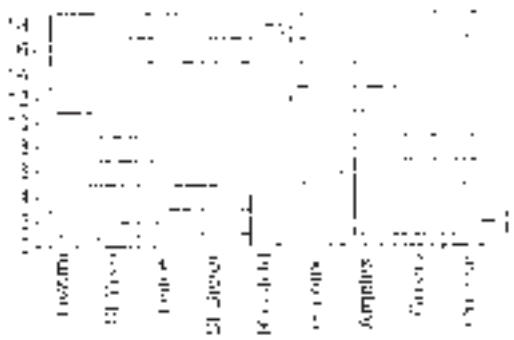

Figure 5. The number of common-mode voltages on the telecommunication line larger than 1.5 kV

From these events (as seen in Figure 5), 27 exceeded a peak value of 1.5 kV, which represents a dangerous value for any kind of telecommunication equipment, with a maximum value of 3.5 kV.

4. Modeling the Effects of Indirect Lightning Strokes

To analyze the effects of indirect lightning strokes on transmission lines or various kinds of circuits, it is necessary to go through the following steps:

1. The development of lightning return-stroke models, which means the modeling of the spatial-temporal distribution of the current in the lightning channel;
2. The calculation of the electromagnetic field radiated by such a current distribution, including propagation effects on soil with finite conductivity;
3. The evaluation of the voltages resulting from the coupling between the electromagnetic field and the line conductors.

A schematic view of the coupling of the field onto a multiconductor line due to a lightning discharge is shown in Figure 6. This modeling procedure has been successfully developed and validated by comparison with experimental data [15-18].

Figure 6. A schematic representation of the lightning electromagnetic field coupling to a multiconductor line.

4.1 Lightning Return-Stroke Current Models

Many return-stroke models have been developed during the last 30 years. As proposed by Rakov [19], they can be classified as a function of their sophistication in describing the physical process that takes place in the lightning discharge:

1. **Physical models**, involving the solution of the gas-dynamic equations of the plasma forming the lightning discharge. These models concentrate mainly on the radial evolution of a short segment of the lightning channel and its associated shock wave. The problems that are difficult to solve in these types of models are the initial conditions, such as the initial radius, the initial channel temperature, and pressure. A subcategory of these models can be considered to be those proposed and discussed in the works of Baker, Baum, and Gardner [20, 21], and of Strawe [22], in which the physics of the discharge is used to solve a transient phenomenon on a transmission line, and where the concept of an electromagnetic shock is introduced.
2. **Thin-wire antenna models**, which consider the discharge to be a thin-wire antenna radiating in the space, and using antenna-theory equations to calculate the field. A few such models have been introduced recently [23, 24], but the problem is the choice of the channel equivalent resistance.
3. **Distributed circuit models**, which consider the discharge to be a circuit with distributed parameters R, L, C, and G, in which a transient process takes place [25, 26].
4. **Models that specify the spatial-temporal distribution of the channel current** based on the current at the channel base, since it is only the channel-base current that can be measured directly and for which experimental data are available [27]. In these models, the return-stroke current can be simply related to the specified channel-base current. These have been conceived to describe the field *change* due to the return-stroke phase, the *total* return-stroke field being the sum of the return-stroke field change plus the final value of the field

produced by the preceding leader phase [17]. These models are also called "engineering models" due to their simplicity, which permits relating the return-stroke current to a channel-base current known from measurements in a straightforward way [19].

This last category is the category most used for practical calculations, as these models permit quite good estimation of the electromagnetic field produced by the lightning discharge, which is the second step in modeling the indirect effects of the lightning strokes.

The most popular of these models are probably the Transmission-Line (TL) model [28], the Traveling Current Source (TCS) model [29], the Modified TL (MTL) model [30-32], and the Diendorfer-Uman (DU) and Diendorfer-Uman Modified (MDU) models [33, 34]. All of these models have been analyzed in detail in [18], and it was concluded that for most engineering coupling calculations, any one of the models is adequate. They all produce fields that are reasonable approximations to available measured fields from natural lightning, and are within a factor of two or so of each other. This conclusion is also supported by the results published in [35], where the above-mentioned models were compared on the basis of simultaneously measured channel-base currents, return-stroke speeds, and electric fields at about 5 km from triggered lightning in Florida.

4.2 Data Contamination due to Lightning Current Measurement on Elevated Structures

Berger has measured the lightning current hitting a relatively low tower (70 m height), situated in the Alps. However, the measurements in recent years in general have been performed on high structures, such as telecommunication towers, often hit by lightning. These include the Ostankino tower, in Moscow; the Preissenberg tower, in Germany; and the CN tower, in Toronto. In 1998, Guerrieri, Nucci, Rachidi, and Rubinstein [36] observed that the statistics of channel-base lightning currents based on measurements on high towers may contain errors, due to the reflection of the current at the tower bottom. Differences in the shape and peak current values in recordings performed at different heights of the Ostankino tower were put into evidence nearly 20 years ago, in 1977, by Gorin and Shkilev [11, 37]. However, their papers, published in Russian, remained unknown to the world lightning community for a long time. Gorin and Shkilev emphasized the mismatch among the impedance of the lightning channel (from 600 Ω to 2.5 kΩ); the characteristic impedance of the tower, of about 300 Ω; and the grounding resistance, which has a low-frequency value of 0.2 Ω. These mismatches give reflections, and the whole structure behaves like a distributed circuit [38]. Figure 7, adapted by Rakov [38] from Gorin and Shkilev [11], shows the different currents at different heights.

Different authors have tried to estimate the reflection coefficients at the tops and bottoms of towers [7, 39, 40]. In

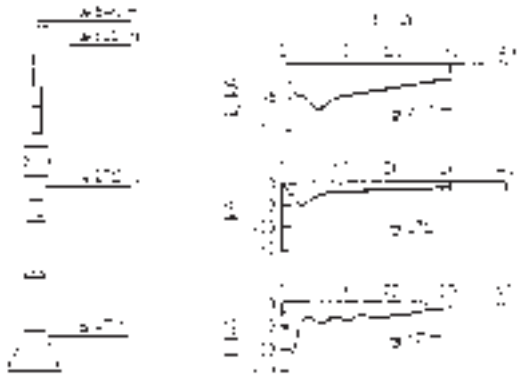

Figure 7. Return-stroke current waveforms of upward negative lightning, recorded near the top (at 533 m), in the middle (at 272 m), and near the bottom (at 47 m) of the 540 m high Ostankino TV tower in Moscow (from [38], where it was adapted from [11]).

[38], Rakov presented an exhaustive discussion of the influence of tall towers on the current, the current's derivative, and the radiated electric and magnetic fields. Recently, Bermudez et al. [41] derived closed-form formulas in the frequency domain for the calculation of the lightning current at any height of the tower. They proposed a method for deriving expressions for the reflection coefficients as a function of the frequency at the bottom of a tower from two currents measured at different heights. They also showed that at the top of the tower, a reflection coefficient as a function of frequency cannot be determined. Only an approximate, frequency-independent expression can be found. This concentration of effort to find methods for decontaminating the lightning currents measured on tall structures in recent years should permit obtaining reliable values for the channel-base current, and continuing use of the "engineering models" for indirect lightning-effect calculations.

4.3 Electromagnetic Field Propagation Over the Ground

Equations for the electromagnetic fields can be obtained by regarding the lightning channel as an antenna over a perfectly conducting plane, and by solving Maxwell's equations in terms of retarded scalar and vector potentials [42]. The lightning current distribution as a function of height and time, needed for these expressions, is given by the return-stroke models previously mentioned.

1. Short distances. For distances not exceeding a few kilometers, the perfect ground conductivity assumption is a reasonable approximation for the vertical component of the electric field and for the azimuthal component of the magnetic field [43-45], and closed-form formulas can be used. The horizontal component of the electric field, on the other hand, is appreciably affected by a finite ground conductivity. Methods for the calculation of the horizontal field using the exact Sommerfeld integrals are inefficient from the point of view of computer time. An analysis of the errors introduced by the use of the Norton [46] approximations of

the Sommerfeld integrals, for various distances and at different frequencies, was performed in [44]. This demonstrated that in the frequency range typical for lightning and at distances needed to calculate nearby lightning electromagnetic effects (up to 5 km), this approach permits obtaining a reasonable approximation, within the limits of a few percent.

2. Large distances (wave-tilt formula). The wave-tilt formula expresses the ratio of the Fourier transform of the horizontal electric field, $\underline{E}_r(j\omega)$, to that of the vertical field, $\underline{E}_z(j\omega)$ [47]. This allows calculating the horizontal component of the electric field over a soil of finite conductivity from the knowledge of the vertical component of the same field:

$$W(j\omega) = \frac{\underline{E}_r(j\omega)}{\underline{E}_z(j\omega)} = \frac{1}{\sqrt{\varepsilon_{rg} + (\sigma_g / j\omega\varepsilon_0)}}, \quad (1)$$

where σ_g and ε_{rg} are the ground conductivity and relative permittivity, respectively. This approach is valid for radiated fields having a grazing angle of incidence with respect to the ground [47]. The use of this function for the case of lightning is therefore reasonable only for far observation points; its application for close distances may describe only the first microseconds of the horizontal field [15]. Thomson et al. [48], who simultaneously measured the vertical and horizontal electric fields from natural lightning at distances from 7 to 43 km, confirmed the applicability of the wave-tilt function for these distance ranges.

3. Intermediate distances. The analytical Cooray-Rubinstein expression, proposed in [49] and [50], uses the horizontal field at the height of interest, calculated by assuming a perfectly conducting ground, and the magnetic field component at ground level, calculated by way of the surface impedance of the ground:

$$\underline{E}_r(r, z, j\omega) =$$

$$\underline{E}_{rp}(r, z, j\omega) - \underline{H}_{\phi p}(r, 0, j\omega) \frac{c\mu_0}{\sqrt{\varepsilon_{rg} + \sigma_g / j\omega\varepsilon_0}}. \quad (2)$$

As shown in [51], this expression gives results that reproduce well the field shape as a function of time for all distances from the lightning channel, and represents a good compromise between precision and computing time. However, further tests are needed to better define its validity limits.

4.4 Field-to-Transmission-Line Coupling Models

The development of field-to-transmission-line coupling models was first performed in the 1970s, to calculate EMP effects on transmission lines (see, for instance, [52]).

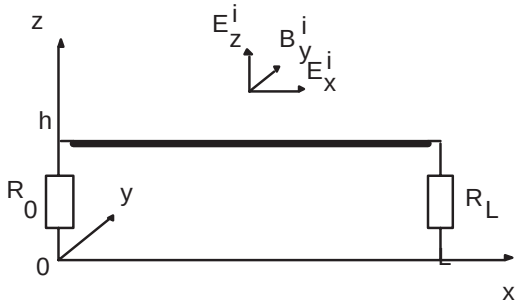

Figure 8. The geometry used for the calculation of over-voltages induced on a transmission line by an incident electromagnetic field.

It has been recently shown [53, 54] that among the various coupling models that are commonly adopted in the power literature to describe the coupling between lightning return-stroke fields and overhead lines, only the model by Agrawal et al. [55], and its equivalent formulations [56-58], are to be considered rigorous within the limits of the Transmission Line approximation. As a reminder, the Agrawal model is expressed by the following equations (see Figure 8 for the parameter definitions):

$$\frac{\partial u^s(x,t)}{\partial x} + R\,i(x,t) + L'\frac{\partial i(x,t)}{\partial t} = E^i_x(x,h,t), \quad (3)$$

$$\frac{\partial i(x,t)}{\partial x} + G'u^s(x,t) + C'\frac{\partial u^s(x,t)}{\partial t} = 0, \quad (4)$$

where $E^i_x(x,h,t)$ is the horizontal component of the incident electric field along the x axis, and $i(x,t)$ is the current induced along the line. The Agrawal model is written in terms of the *scattered* voltage, $u^s(x,t)$. The total voltage, $u(x,t)$, is given by the sum of the scattered voltage, $u^s(x,t)$, and the so-called *incident* voltage (the total field is given by the sum of the incident field, E_i, B_i, namely the field radiated by the channel plus the ground-reflected field, and the scattered field):

$$u^i = -\int_0^h E^i_z(x,z,t)\,dz \approx -E^i_z(x,0,t)\,h, \quad (5)$$

namely,

$$u(x,t) = u^s(x,t) + u^i(x,t). \quad (6)$$

The boundary conditions are

$$u^s(0,t) = -R_0\,i(0,t) - u^i(0,t), \quad (7)$$

$$u^s(L,t) = R_L\,i(L,t) - u^i(L,t). \quad (8)$$

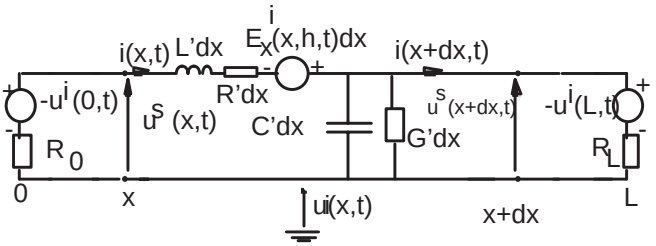

Figure 9. The equivalent "coupling" circuit describing the electromagnetic coupling between an incident electromagnetic field and a transmission line.

The equivalent coupling circuit, described by Equations (3)-(8), is shown in Figure 9.

From a conceptual point of view, the difference between the above-introduced model for a single line and a multiconductor line model is just quantitative: the unique voltage and current propagating on the line and the respective field components are replaced by vectors, and the unique line parameters (resistance, inductance, and capacitance) are replaced by matrices of self and mutual inductances and partial capacitances between the lines and between the conductors and the ground. Further details concerning the derivation of the equations for a single line and their form for multiconductor lines, known as the BLT equation and its solution, can be found, for instance, in reference [59].

Different codes using these models for plane-wave (HEMP) coupling have been developed in the frequency and time domains. Specific codes applied to lightning electromagnetic effects include one from the University of Florida [60]; *LCC* (Lightning Coupling Calculation), developed by F. M. Tesche [59]; one at the Centre National d'Etudes des Télécommunications in France [44]; one at the University of Uppsala in Sweden [61]; one at the Central Research Institute of Electric Power Industry, Tokyo [62]; and one from the Tokyo and Shizuoka Universities [63], in Japan. The previously discussed return-stroke and coupling models have been translated into the computer program *LIOV* (Lightning-Induced Over-Voltages [16]), developed in parallel at the University Bologna and at the Swiss Federal Institute of Technology, Lausanne, in the framework of an international research collaboration (see http://www.ing.unibo.it/die/liov/).

4.5 Interaction Effects due to Multiconductor Lines

When several parallel conductors are present, a reduction effect due to the interaction between them can be observed. This problem has been widely discussed in the power-network literature, due to its implications related to the protection of distribution lines against lightning (see, for instance, [62, 64-67]. The simulation model described above has allowed analysis of this effect, and has permitted clarification of some controversial results obtained by different authors.

A two-line configuration that has been used in other studies on the subject [66] has been analyzed in [67]. In the first (vertical) configuration, the three conductors were disposed along the same vertical axis at different heights above the ground. In the second (horizontal) configuration, the conductors were located at the same height above the ground. For both configurations, the presence of one or two ground wires was considered. For the two considered configurations, there was a shielding effect due to the presence of the other conductors. Table 1 gives the ratio between the peak voltages on each conductor and those calculated considering a single conductor situated at the same height. The calculated values reported in Table 1 show that the presence of other conductors has a reducing effect of 10-25% on the peak value of the induced voltages. For the vertical line configuration, the highest reduction occurred for the lowest conductor, while for the horizontally-configured line, the highest reduction occurred for the middle conductor. Reference [68] discussed these results, explaining why some controversial results have been obtained by different authors.

Voltage Ratio	Vertical Configuration	Horizontal Configuration
$V_1/V(h_1)$	0.75	0.85
$V_2/V(h_2)$	0.79	0.81
$V_3/V(h_3)$	0.89	0.85

Table 1. The ratio between the peak values of the induced voltages on a line conductor, V_i, and those corresponding to a single-conductor line of the same height $V(h_i)$.

The presence of ground wires decreases the induced voltages by about 20% for a three-phase line with one grounding wire in a vertical configuration, and up to 40% for two grounding wires for a horizontal configuration, due to a shielding effect. As a rule, power-distribution networks and telecommunication lines for which the lightning-induced voltages represent a danger cannot be built with a grounding wire, due to economic considerations. However, this effect can be used to demonstrate that by adding a conductor grounded at the two extremities, in parallel to any line connected to sensitive circuits, represents a cheap way for obtaining a shielding effect. The presence of a metallic

cable duct, grounded at both ends [69], also has a reducing effect.

An interesting single-wire representation of a multiconductor line, illuminated by lightning electromagnetic fields, was proposed in [68]. This approach gave the possibility of simplifying the calculations. It has also permitted comparison of the rigorous computation using the field-to-transmission-line coupling modeling with a simplified formula proposed by Rusck in [41], which gives the protective ratio of a shielding wire over a multiconductor line:

$$PR_i = 1 - \frac{h_s}{h_i} \frac{cL_{is}}{cL_{ss} + R_e}, \qquad (9)$$

where h_i and h_s are the heights of the conductor, i, and the shielding wire, respectively; L_{ss} is the self-inductance of the shielding wire; L_{is} is the mutual inductance between conductor i and the shielding wire; R_e is the earthing resistance of the shielding wire at both of its extremities; and c is the velocity of light. The comparison showed [68] that the Rusck formula gives results within a few percent of precision with respect to a rigorous calculation, and can therefore successfully be used for shielding-effect estimations. Note, however, that this expression is valid under the assumption that the ground wire is at earth potential. This means that the formula can be used only for lines with a short spacing between two consecutive groundings [70].

4.6 Extension to Networks with Several Branches

The field-to-transmission-line coupling equations can be applied not only to straight parallel lines, but also to tree-shaped networks with several branches. Different approaches in this sense have been presented in the literature [71-74]. In order to solve such configurations, different Field-to-Transmission-Line coupling codes have been interfaced with the Electromagnetic Transient Program (*EMTP*) [75, 76]. The link between *LIOV* and *EMTP*, achieved in collaboration between the University of Bologna and the Swiss Federal Institute of Technology of Lausanne, is based upon the following principle: Distribution lines are considered to be formed by a number of line segments, similar to those represented in Figure 8. The various line segments are interconnected by means of shunt impedances or nonlinear devices (surge arresters) to form a typical distribution line. The idea is to leave the task of solving the transmission-line coupling equations to the *LIOV* program for each of the line segments, and the task of solving the boundary conditions to the *EMTP* corresponding to the various interconnections.

Figure 10 shows an example of an overhead distribution line, including the presence of a power transformer and two surge arresters (see [77] for further details, including the modeling of the various power components). The over-voltages induced by a typical subsequent return stroke (with

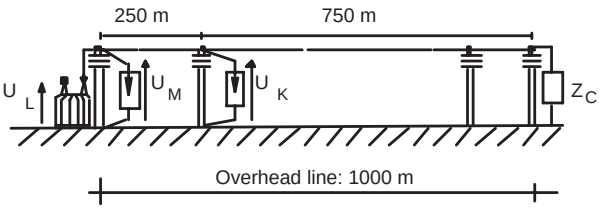

Figure 10. A distribution line illuminated by a return-stroke lightning electromagnetic field.

the peak value of the channel-base current equal to 50 kA and a maximum time derivative of 43 kA/μs) at three points on the line, calculated using the *LIOV – EMTP* link, are shown in Figure 11. The stroke location is equidistant from the line's termination, and 50 m from the line's center. Using the above-mentioned approach, it is possible to simulate and analyze the effect of protection elements installed at the entrance of a substation.

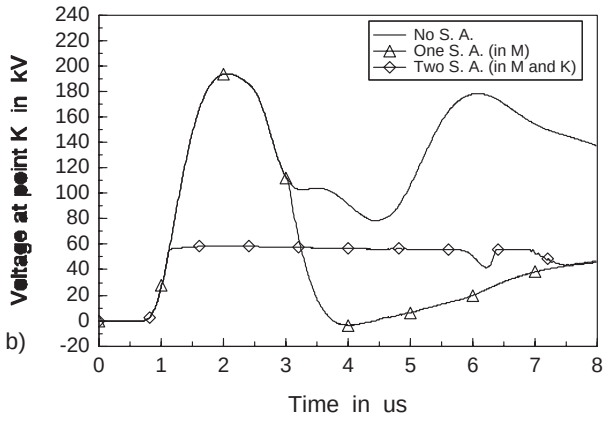

Figure 11. The over-voltage calculated at three points (L, M, and K) of the overhead distribution line shown in Figure 10, ignoring the presence of the surge arrester located at point K (adapted from [78]).

This first analysis has shown that if the protection device (a surge arrester) is efficient with respect to the relevant equipment, other points along the line can still remain at high potential, creating a danger of flashover across the insulator chains and, in consequence, micro-interruptions (e.g. [78]). The link between a coupling code and *EMTP* allows a more accurate estimation of lightning-induced voltages on realistic distribution lines, since now all the models of power-system components contained in the *EMTP* library are promptly available. Other *EMTP*-linked coupling codes have been proposed by other authors [79-81].

Concerning shielded cables, a classic approach, already developed in the 1980s, has been a computation in the frequency domain using analytical expressions or measured values for the transfer impedance [82, 83, 59]. A new mixed frequency-time-domain model, which uses a link to *EMTP*, has been developed and validated by comparison with measurements under an EMP simulator [84]. This last

feature makes the application of the second model to complex networks with several branches possible.

5. Validation of the Field-to-Transmission-Line Coupling Models

The validation of the electromagnetic field coupling to lines or circuits concerns different models, such as those for straight parallel lines, tree-shaped networks or circuits, nonlinear protection elements, and shielded cables. Independently of the source type and of the kind of situation to be simulated, the mathematical modeling of the coupling process is similar, which means that if the model is validated, the conclusions will reasonably apply to different kinds of sources, circuits, or protection elements. As explained in the previous section, the coupling modeling has been achieved using the Agrawal model, based on the Transmission-Line Approximation (TL Approximation). A first way to validate the method is to compare the results given by the TL Approximation and by the scattering theory, which can be considered to be an "exact" method [85]. A new method of calculation based on an iterative process, which corrects the TL Approximation, has been proposed [86]. Using this approach, it was shown that after one or two iterations, the extended Agrawal model can give very accurate results with respect to the "exact" approach, based on the scattering theory.

Another validation method is comparison with measurements. This has been done using either EMP simulations or triggered and natural lightning electromagnetic fields.

5.1 Validation Using EMP Simulators

The comparison between theory and experiment using EMP simulators can be considered to be satisfactory for a perfectly conducting ground [28, 50], and quite reasonable for soil with finite conductivity [44]. The case of a perfect conducting ground was simulated using the bounded-wave EMP simulator of the Swiss Federal Institute of Technology of Lausanne, in which the field is a very uniform plane wave in a defined working volume [87]. A tree-shaped circuit was installed inside the working volume of the simulator, as shown in Figure 12 [74]. Figure 13 shows the comparison between a calculation performed using the Agrawal coupling model and the measurement of the current induced on one end of the branched circuit illuminated in the SEMIRAMIS simulator. The excitation field in the working volume of the simulator had a risetime of about 10 ns, a decay time of about 250 ns, and a peak value of the vertical electric field component of 50 kV/m. As seen in Figure 13, the agreement between calculation and measurement was satisfactory [74].

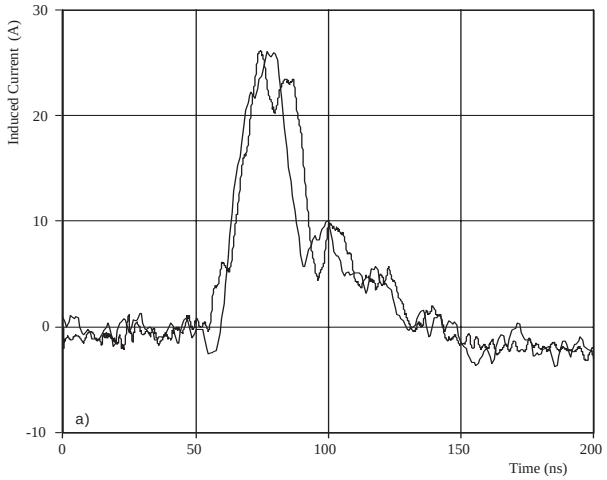

Figure 13. A comparison between a calculation with the Agrawal model and a measurement in the SEMIRAMIS EMP simulator for the EM field coupling on a network (reproduced from [74]).

For performing the comparison for soil with finite conductivity, a model of a three-phase line, with and without a grounding conductor, was built. The induced current measurements were made on a 30 m long, 3 m high overhead test line, mounted on plastic material supports, and open circuited at both ends. A grounding wire, short-circuited at both ends, was also fixed at a height of 50 cm above the wire. The test line was then installed under a half-loop hybrid radiated-wave EMP simulator of the Centre d'Etudes de Gramat (France), which has a half-loop diameter of 150 m and is 30 m high (Figure 14). This simulator produced a horizontally-polarized field along the 30 m of the line [67]. We show here an example of a comparison that refers to the current induced at the extremity of the grounding wire (Figure 15) [67]. It can be seen that while the wave shapes of the two curves are in good agreement, there is a disagreement of about 23% in the peak values. This differ-

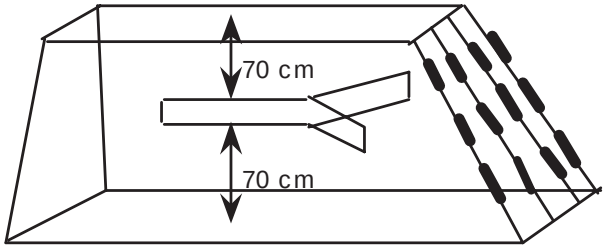

Figure 12. A tree-shaped structure in the SEMIRAMIS EMP simulator (reproduced from [74]).

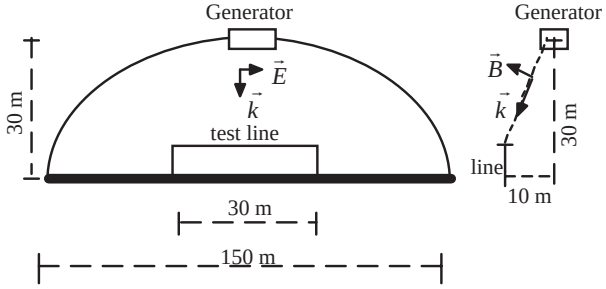

Figure 14. The relative position of the three-phase test line under the EMP simulator (reproduced from [67]).

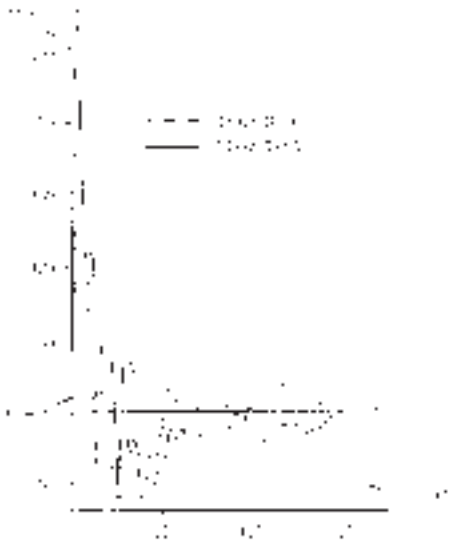

Figure 15. An example of a comparison between calculation and measurement of the current induced at one extremity of the grounding wire (adapted from [67]).

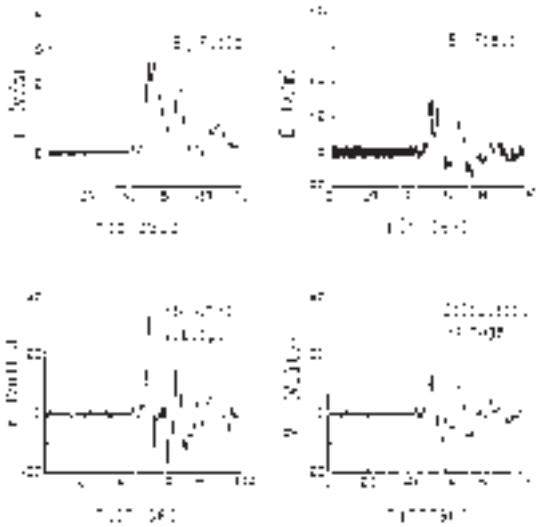

Figure 16. A comparison between the voltages induced by a natural lightning stroke, measured and calculated from the measured vertical electric-field component (reproduced from [88]).

ence can be explained by considering that the calculation was performed assuming a uniform incident field intensity of 25 kV/m, while in reality the field was decreasing at the extremities of the line. On the other hand, incorrect simulation of the earthing of the grounding wire at the two ends, and an error in the value of the ground conductivity, are two error sources that are difficult to avoid.

5.2 Validation Using Natural and Triggered Lightning

In testing the coupling models, the use of lightning fields is complicated by the intrinsic difficulty in performing a controlled experiment. A comparison using natural lightning was performed using the measured value of the vertical electric field component near the extremity of a transmission line. The horizontal component of the electric field was calculated from the vertical component with the wave-tilt formula (see Section 4.3), after which the coupling equations were solved to find the voltage induced at the two ends of the line. This calculated value was compared with the measured induced voltage. One example of this comparison is shown in Figure 16 [88].

Triggered lightning – which gives the possibility of simultaneously measuring the channel-base lightning current, the electric or magnetic field at different distances, and the voltage or current induced on a line situated in the proximity of the stroke – represents a powerful method for validating the whole modeling process of lightning electromagnetic effects. Triggered lightning facilities have been created in several countries [89-91]. The principle of triggering lightning strokes by launching small rockets to which a wire is attached in thunderstorm clouds is shown in Figure 17. An example of a triggered lightning facility is that of the University of Florida at Camp Blanding (Figure 18) [91].

A comparison between the voltage induced at the two ends of an aerial line situated 20 m from the launching pad of the rockets, and calculations performed with the recorded lightning current, is shown in Figures 19 and 20 [92]. It can be seen that while the shapes of the measured and calculated curves are similar, in order to obtain the same peak value for the west-end voltages, the lightning current had to be adjusted, but this resulted in a difference of a factor of two for the peak values at the east end.

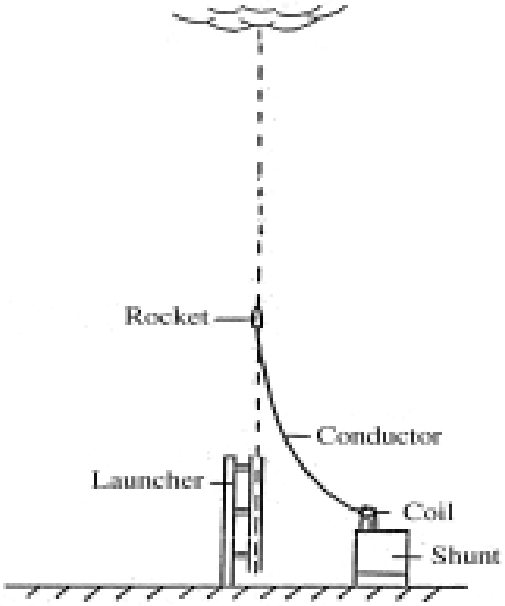

Figure 17. The principle of triggered lightning.

Figure 18. The Camp Blanding triggered-lightning facility (reproduced from [91]).

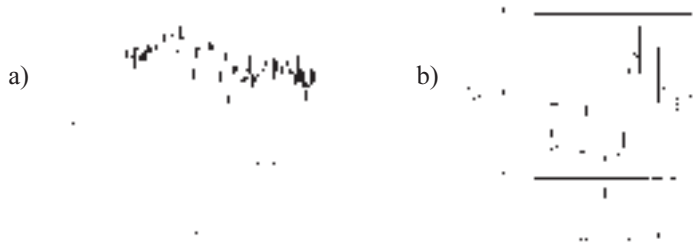

Figure 19. A comparison between a measurement (a) and a calculation (b) of the voltage at the east end of the line (adapted from [92]).

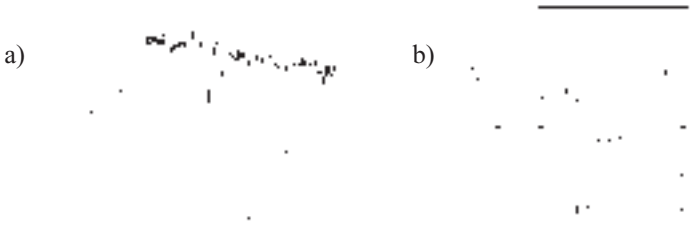

Figure 20. A comparison between a measurement (a) and a calculation (b) of the voltage at the west end of the line (adapted from [92]).

From the various results obtained from validations using different methods, it can be concluded that to the extent that the environment is well controlled, as in a bounded-wave simulator, the coupling calculations give very close results compared to measurements. When the environment is not under control, as for the radiated-wave simulator or for lightning, parameters such as uncertainties about the ground-conductivity value, and the presence of trees and other objects in the vicinity of the line that can give reflections of the field, result in errors in the calculation.

The validation of the line or circuit model terminated by nonlinear protection elements concerns not only the field-to-transmission-line coupling, but also the models of gas-discharge tubes, metallic varistors, and protective diodes. Rough models of such elements using the current-voltage characteristic have been developed, and first validations have been performed [71, 93] or are in progress in different research centers. Further work is needed in which the *EMTP* models for nonlinear protection elements and the link between coupling codes and *EMTP* (see Section 3) must be used.

6. The Electromagnetic Effect of the Leader

The very slowly varying electric or magnetic fields due to the stepped-leader process was discussed by Uman and McLain in 1970 [94], and then theoretically calculated by Uman in 1987 [4] (see Figure 21). However, only after the introduction of the technique of triggered lightning could a significant effect of these fields be measured on lines situated at very small distances from the lightning channel. In [95], calculations using the return-stroke field only were compared to measurements of voltages induced by a lightning stroke at about 20 m from an experimental line (Figure 22). This conclusion valid for the case presented in Figure 23, but has to be confirmed by more comparisons between calculations and measurements performed for various positions of lightning strokes striking at very short distances from overhead lines. A comparison of the results reported in [96] and those reproduced in Figure 23, taken from reference [95], shows that the overall agreement between calculated and measured induced voltages is appreciably improved by taking into account the leader effect.

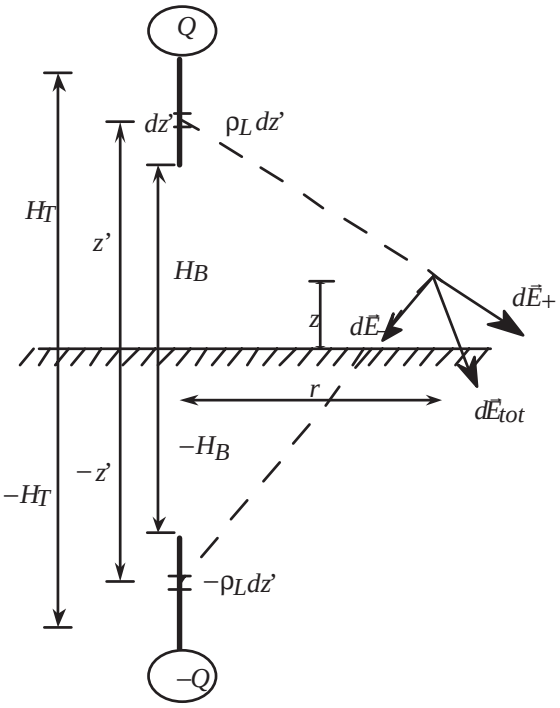

Figure 21. The leader model for close electric field calculation (reproduced from [4]).

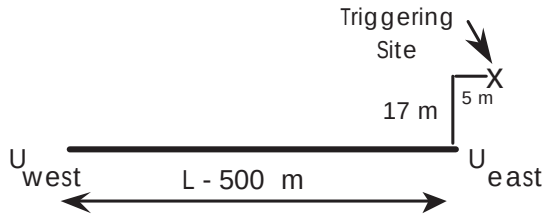

Figure 22. A schematic layout of the NASA Kennedy Space Center 1986 experiment (reproduced from [95]).

Figure 23. A comparison between the calculation and measurement of induced voltage on an overhead line by a nearby triggered lightning (reproduced from [95]).

7. Quasi-Static Simplified Estimation of Indirect Lightning Effects

In many cases, the configuration of the circuits submitted to indirect lightning effects is so complicated, and the number of conductors is so high, that use of the coupling models for tree-shaped networks, described in the previous sections, becomes prohibitive. Typical examples are the control and protection circuits in aerial or underground substations of power and distribution networks. The difficulty of applying these models does not come only from the complex configuration of the circuits, with multiple branches and changes of directions in different planes (the circuit is often not contained in a single plane, but is three-dimensionally shaped), but also from the parameters that must be known and used in the numerical calculation. Typically, these parameters are self and mutual inductances or partial capacitances between the wires of a cable bundle, or between the wires and the ground or the sheath. These parameters usually should be measured, because the complex configuration does not permit a calculation with reasonable precision [97].

A compromise solution is to use approximate calculations, based on simplified assumptions, such as ignoring the circuits other than the source of the disturbance and the victim, neglecting propagation, and using low-frequency approximations. In this case, simple expressions developed under the hypothesis of inductive or capacitive coupling can be used. The condition for neglecting propagation is that the circuits should have dimensions that are small or comparable to the minimum wavelength of the lightning electromagnetic field, i.e., $d \le \lambda_{min}$ (where $\lambda_{min} \approx 30$ - 60 m, corresponding to $f_{max} \approx 5$ -10 MHz), also called electrically small circuits. In this case, a quasistatic approach can be used. Such an approach permits a relatively simple estimation of maximum lightning-induced current values. As the line is very short, the influence on the coupling process of soil with finite conductivity can be neglected [51], and the ground can be taken to be a perfect

Figure 24. A comparison between measurements and calculations using a low-frequency quasistatic approximation for the coupling between a lightning magnetic field and an electrically small circuit (reproduced from [98]).

conductor. The line and its earthing can be modeled as a resistance of the line, R, in series with the grounding resistance, R_S , and an inductance, L, of the aerial part of the line. Figure 24 presents a comparison between measurements and calculations using the above simplified approach for the current induced by a triggered lightning at 70 m, from a line 8 m long and 1.8 m in height [98]. Note that if losses in the circuit are neglected ($R = 0$), the agreement with the measurements is worse. The resistance value of 1 W corresponds to the value for an average frequency of 1 MHz.

8. Electromagnetic Effects of Direct Strokes on Complex Structures

The danger of direct strokes to HV power transmission lines was already analyzed 30 or 40 years ago, and efficient protection measures were introduced. If these measures are correctly applied, when an HV line is submitted to a direct stroke or to a lightning current due to a backflash from the ground wire, the circuit breakers open the line, and close it again when the transient phenomenon comes to an end. However, direct strokes can also have secondary electromagnetic effects, inducing voltages and currents in circuits that are in the vicinity of a structure stricken by lightning.

8.1 Lightning Stroke on Buildings

The danger of damage due to a direct lightning stroke on a house is not completely eliminated, even with a correct protection installation. In 1996, a strong thunderstorm in the Leman lake region in Switzerland destroyed all the TV sets in a residential building of the town of Montreux. One possible scenario was that the huge lightning current flowing in the metallic structure of the building induced a high voltage in the low-voltage distribution network supplying the TV sets. Another possibility was that part of the lightning current returned through the grounding network into the apparatus installed in the building.

In order to avoid the penetration of lightning current in house installations, IEC Lightning Protection Standard 1312–1 [99] prescribes that 50% of the current of a stroke on a house must be evacuated to the ground by the grounding system. A comparison with measurements performed with triggered lightning at the Camp Blanding facility in Florida [100] showed that the percentage of current going to the ground strongly depends on the grounding impedance, which means that many building earthing systems do not comply with the IEC standard.

8.2 GSM Antennas Installed on Power-Line Towers

Another danger of destruction due to direct lightning strikes comes from a new application that has been introduced in recent years, the installation of GSM antennas for mobile phones on HV power-line towers. The electronics of these antennas is supplied by a low-voltage connection installed along the HV tower structure. The flashback of the lightning current from a phase conductor to the ground wire or to the tower structure results in a phase-to-ground short circuit. Fractions of this current can flow by induction or through the grounding system into the low-voltage cable supplying the GSM system. A simulation with a reduced current, simulating the flashover of an insulator due to a direct lightning stroke, followed by a short-circuit phase-to-ground, on a tower with a GSM antenna has been performed (Figure 25) [101]. The simulation with a 100 A injected current gave voltages of the order of 5 V between the neutral and the ground in the low-voltage circuits. Since 20 kA short-circuit currents can circulate in the line for a phase-to-ground fault due to a lightning stroke, this would mean a dangerous voltage of 1 kV between the neutral and the ground.

9. What we Still Don't Know

As discussed, a concept for the modeling of lightning electromagnetic effects on lines and circuits has been developed and tested, with good results for various configurations. The modeling procedure developed requires the knowledge of several parameters and the use of other models, such as the lightning current spatial-temporal distribution, the field coupling to complex circuits and structures, and the behavior of nonlinear protection elements. Some of these models are not known with enough precision.

Figure 25. Voltages induced by a lightning stroke in the supply circuit of a GSM antenna mounted on a HV tower: A comparison between calculation and measurements (reproduced from [101]).

Among the items needed to improve the modeling of lightning indirect effects, the following can be considered as requiring a better knowledge:

1. The lightning current at the channel base, which permits the use of the engineering lightning current models. As discussed, this current has been measured in different conditions. However, the oldest measurements of Berger [3], which contain the highest amount of data, have not been performed with the instrumentation available today and can contain errors, in particular in the current-derivative value. Recent real scale lightning-current measurements with rapid oscilloscopes have all been done using high telecommunication towers so that the data are contaminated by the reflections to ground, as discussed in Section 4.2. The decontamination process should be performed in the next few years.
2. The ground conductivity is a parameter that cannot be known with precision along a line as soon as the line is longer than a few hundred meters. The soil is, on the one hand, part of the medium in which the electromagnetic field propagates and, on the other hand, the return conductor of the current induced in overhead lines. As shown in reference [51], the ground conductivity plays a crucial role in electromagnetic wave propagation over the ground. Studies performed in the last few years have permitted development of new approaches for calculating the ground impedance [102]. However, even for the best expression of the impedance, the physical value of the soil conductivity must be known. Concerning the coupling mechanism for lines not longer than about 2 km at $f = 1\,\text{MHz}$ (1.5 km for $\sigma = 0.001$ S/m, 4.5 km for $\sigma = 0.01$ S/m), the conductivity of the soil is not important, but its influence increases for longer lines. This parameter depends not only on the meteorological conditions, but is also a function of metallic structures buried in the ground (metallic water and gas pipes, power-distribution cables), and these structures can change, or are not known with precision. This means that the ground conductivity can be known only with a certain degree of approximation
3. The models for nonlinear circuits that exist in codes like *EMTP* should be improved. This concerns both transformer behavior at HF and over-voltage protection elements.

It should be noted that a numerical simulation using *EMTP* of a direct lightning strike on an aerial transmission line, equipped with various transformers and protection elements, at Camp Blanding gave good agreement with the measured arrester discharge currents at different poles [103]. However, a simulation for the same overhead line from Camp Blanding for voltages induced by a nearby lightning strike, using the link between *LIOV* and *EMTP*, gave a very approximate agreement with the measurements [104]. This emphasizes the necessity for continuing the studies of lightning electromagnetic effects on complex structures.

10. Conclusions

In the last few years, remarkable progress has been made in the modeling of return-stroke lightning currents, electromagnetic field propagation over a ground with finite conductivity, and field-to-transmission-line coupling. New models have also been developed for power and telecommunication lines protection devices, including the typical nonlinear phenomena involved. This permits today the estimation with reasonable accuracy of the effects of indirect lightning on overhead lines. Recent developments also allow the linking of lightning-induced voltage-calculation codes with *EMTP*, providing the possibility to estimate lightning effects on more complex networks or circuits. Several problems that remain unsolved and require more studies, or that can never be known with enough precision, have been emphasized in this tutorial. New applications – for instance, the use of HV towers as a support for GSM antennas – create new problems and new challenges for the EMC engineer.

11. Acknowledgements

The author would like to acknowledge many years of friendly collaboration and fruitful discussions with Dr. F. M. Tesche on field propagation and coupling problems. He also considers that the completion of this tutorial would not have been possible without the 15 years of collaboration with Dr. F. Rachidi, from the Swiss Federal Institute of Technology of Lausanne. The author would also like to emphasize many years of close collaboration on this subject with Prof. C. Mazzetti, from the University of Rome, and with Prof. C. A. Nucci, from the University of Bologna. Many helpful discussions and interaction with Dr. W. Radasky, form Metatech Corp., Prof. M. A. Uman and Prof. V. Rakov, both from the University of Florida, Dr. M. Rubinstein, from the High Specialized School of Engineering of West Switzerland, and Dr. C. Baum, from Philips Lab, as well as many years of fruitful collaboration on coupling problems with the NEMP Labor from Spiez (Switzerland) and Electricité de France, should also be acknowledged.

12. References

1. S. Lundquist, "Effects on the Society of an Intense Lightning Storm," *Proc. 21st Int. Conf. on Lightning Prot. (ICLP)*, Berlin, 22-25 September 1992, Paper 8.01.

2. M. Rubinstein, E. Montandon, and M. Ianoz, "Analysis of Multi-Station Cloud Lightning Electric Field Pulses Recorded with the Swiss LPATS Network," *Proc. of 22nd Int. Conf. on Lightning protection (ICLP)*, Budapest, September 19-23 1994, R1c-07.

3. K. Berger, R. B. Anderson, and H. Kroninger, "Parameters of Lightning Flashes," *Electra*, No. 41, 1975, pp. 23-37.

4. M. A. Uman, "The Lightning Discharge," New York, Academic Press, 1987.

5. W. Janischewskyj, A. M. Hussein, W. A. Chisholm, J. S. Chang, Z. Kawasaki, and P. Idzurevych, "Comprehensive Measurement of Lightning Strokes to the CN Tower in Toronto," *Proc. 9th Int. Conf. on Atmospheric Electricity, Vol. III*, St. Petersburg, Russia, 1992.

6. W. Janischewskyj, A. M. Hussein, P. Dzurevych, V. Shostak, and W. A. Chisholm, "Characterization of the Current Wavefront Parameters of Lightning Strokes to the CN Tower in Toronto," *8th Int. Symp. on High Voltage Engineering*, Yokohama, Japan, 1994, paper No. 70 a.

7. O. Beierl, "Front Shape Parameters of Negative Subsequent Strokes Measured at the Peissenberg Tower," 21st International Conference on Lightning Protection, Berlin, 1992.

8. O. Beierl, "Lightning Current Measurements at the Peissenberg Tower," 7th ISH, Dresden, 1991, ref. 81.02.

9. E. Garbagnati and G. B. Lo Piparo, "Nuova Stazione Automatica per il Rilievo delle Caratteristiche dei Fulmini," *L'Energia Elettrica*, No. 6, 1973 (in Italian).

10. E. Garbagnati, G. B. Lo Piparo, and F. Marinoni, "Parameters of Lightning Currents. Interpretation of Results Obtained in Italy," 15th Int. Conf. on Lightning Protection, Sgedez, 1980.

11. B. N. Gorin and A. V. Shkilev, "Measurements of Lightning Currents at Ostankino Tower," *Elektricestvo,* No. 8, 1984, pp. 64-65 (in Russian).

12. H. Geldenhuys, A. J. Eriksson, and G. Bourn, "Fifteen Years Data of Lightning Current Measurements on a 60 Meter Mast," 19 ICLP, Graz, 1988, ref. 1.7.

13. F. de la Rosa, R. Valdiviva, H. Perez, and J. Losa, "Discussion about the Induction Effects of Lightning in an Experimental Power Distribution Line in Mexico," *IEEE Trans. on PWDR*, **3**, 3, July, 1988, pp. 1080-1089.

14. B. Djebari, L. Guérin, and M. Gléonec, "Conducted EM Disturbances on the Telecommunication Terminal Equipment Ports," *Proc. Int. Symp. EMC'94 Roma*, September 13-16, 1994, paper B-5.

15. M. J. Master and M. A. Uman, "Lightning Induced Voltages on Power Lines. Theory," *IEEE Transactions on Power, Apparatus and Systems*, **PAS-103**, 9, September 1984.

16. C. A. Nucci, F. Rachidi, M. Ianoz, and C. Mazzetti, "Lightning-Induced Overvoltages on Overhead Lines," *IEEE Transactions on Electromagnetic Compatibility*, **EMC-35**, 1, February 1993, pp. 75-86.

17. C. A. Nucci, "Lightning-Induced Voltages on Overhead Power Lines. Part I: Return-Stroke Current Models with Specified Channel-Base Current for the Evaluation of the Return-Stroke Electromagnetic Fields," *Electra*, No. 161, August, 1995.

18. C. A. Nucci, "Lightning-Induced Voltages on Overhead Power Lines. Part II: Coupling Models for the Evaluation of the Induced Voltages," *Electra*, No. 162, October, 1995.

19. V.A. Rakov, "Lightning Electromagnetic Fields: Modeling and Measurements," *Proc. 12th Int. Zurich Symp. on EMC*, February 18-20, 1997, paper 11C1.

20. C. E. Baum and L. Baker, "Analytic Return-Stroke Transmission-Line Model," in R. L. Gardner (ed.), *Lightning Electromagnetics*, New York, Hemisphere Publishing Corporation, 1990.

21. C. E. Baum, R. L. Gardner, "An Introduction to Leader Tip Modeling," in R. L. Gardner (ed.), *Lightning Electromagnetics*, New York, Hemisphere Publishing Corporation, 1990.

22. D. F. Strawe, "Nonlinear Modeling of Lightning Return-Stroke," Proc. FAA/Florida Inst. Tech., Workshop Grounding Lightning Technology, Florida, March, 1979.

23. A. S. Podgorski and J. A. Landt, "Three Dimensional Time Domain Modeling of Lightning," *IEEE Transactions on Power Delivery*, **PWRD-2**, 1987, pp. 931-938.

24. R. Moini, B. Kordi, V. A. Rakov, and M. A. Uman, "An Antenna Theory Model for the Lightning Return Stroke," *Proc. 12th Int. Zurich Symp. on EMC*, February 18-20, 1997, paper 28F1.

25. P. F. Little, "Transmission Line Representation of a Lightning return Stroke," *J. Phys. D: Appl. Phys*., **11**, 1978, pp. 1893-1910.

26. M. A. da F. Mattos and C. Christopoulos, "A Nonlinear Transmission Line Model of the Lightning Return Stroke," *IEEE Transactions on EMC*, **EMC-30**, 1988, pp. 401-406.

27. C. A. Nucci, G. Diendorfer, M. A. Uman, F. Rachidi, M. Ianoz and C. Mazzetti, "Lightning Return Stroke Current Models with Specified Channel-Base Current: A Review and Comparison," *Journal of Geophysical Research*, **95**, November 1990, pp. 20395-20408.

28. M. A. Uman and D. K. McLain, "Magnetic Field of Lightning Return Stroke," *Journal of Geophysical Research*, **74**, 1969.

29. F. Heidler, "Traveling Current Source Model for LEMP Calculation," *Proc. 6th Symposium and Technical Exhibition on Electromagnetic Compatibility*, Zurich, March 5-7, 1985.

30. C. A. Nucci, C. Mazzetti, F. Rachidi and M. Ianoz, "On Lightning Return Stroke Models for LEMP Calculations," *Proceedings 19th Int. Conf. on Lightning protection*, Graz, April 1988.

31. C. A. Nucci and F. Rachidi,"Experimental Validation of a Modification to the Transmission Line Model for LEMP Calculations," *Proc. 8th International Symposium and Technical Exhibition on Electromagnetic Compatibility*, Zürich, 1989.

32. V. A. Rakov and A. A. Dulzon, "A Modified Transmission Line Model for Lightning Return Stroke Field Calculations," *Proc. 9th International Symposium and Technical Exhibition on Electromagnetic Compatibility*, Zürich, 1991.

33. G. Diendorfer and M. A. Uman, "An Improved Return Stroke Model with Specified Channel-Base Current," *J. of Geoph. Res.*, **95**, D9, August 20, 1990, pp. 13621-13644.

34. R. Thotappilil, D. K. McLain, M. A. Uman and G. Diendorfer, "Extension of the Diendorfer-Uman Lightning Return Stroke Model to the Case of a Variable Upward Return Stroke Speed and a Variable Downward Discharge Current Speed," *J. Geoph. Res.*, **96**, D9, September 20, 1991, pp. 17143-17150.

35. R. Thotappilil and M. A. Uman, "Comparison of Lightning Return-stroke Models," *J. of Geoph. Res.*, **98**, D12, December 20, 1993, pp. 22903-22914.

36. S. Guerrieri, C. A. Nucci, F. Rachidi, and M. Rubinstein, "On the Influence of Elevated Strike Objects on Directly Measured and Indirectly Estimated Lightning Currents," *IEEE Transactions on Power Delivery*, **13**, 1998, pp. 1543-55.

37.B. N. Gorin, V. I. Levitov, and A. V. Shkilev, "Lightning Strikes to the Ostankino Tower," *Elektricestvo*, No. 8, 1977, pp. 19-23 (in Russian).

38.V. A. Rakov, "Transient Response of a Tall Object to Lightning," *IEEE Transactions on EMC*, **EMC-40**, 4, November 2001, pp. 654-661.

39.W. Janishewskyj, V. Shostak, J. Barratt, A. M. Husein, R. Rusan, and J. S. Chang, "Collection and Use of Lightning Return Stroke Parameters Taking into Account Characteristics of the Struck Object," *Proc. 23th Int. Conf. On Lightning Protection*, Florence, 1996, pp. 16-23.

40.F. Fuchs, "On the Transient Behavior of the Telecommunication Tower at the Mountain Hoher Preisenberg," *Proc. 24th Int. Conf. On Lightning Protection*, Birmingham, 1998, pp. 36-41.

41.J. L. Bermudez, M. Rubinstein, F. Rachidi, and M. Paolone, "A Method to Find the Reflection Coefficients at the Top and Bottom of Elevated Strike Objects from Measured Lightning Currents," *Proc. 14th Int. Zurich Symp. on EMC*, February 20-22, 2001, paper 63J8.

42.M. J. Master and M. A. Uman, "Transient Electric and Magnetic Fields Associated with Establishing a Finite Electrostatic Dipole," *Am. Jour. of Physics*, No. 51, 1983, pp. 118-126.

43.B. Djébari, J. Hamelin, C. Leteinturier, and J. Fontaine, "Comparison Between Experimental Measurements of the Electromagnetic Field Emitted by Lightning and Different Theoretical Models. Influence of the Upward Velocity of the Return Stroke," *Proc. 4th Int. Symp. on Electromagnetic Compatibility*, Zurich, 1981.

44.A. Zeddam and P. Degauque, "Current and Voltage Induced on a Telecommunication Cable by a Lightning Stroke," in R. L. Gardner (ed.), *Lightning Electromagnetics*, New York, Hemisphere Publishing Corp., 1990, pp. 377-400.

45.M. Rubinstein, M. A. Uman, E. M. Thompson, and P. Medelius, "Voltages Induced on a Test Distribution Line by Artificially Initiated Lightning at Close Range: Measurement and Theory," *Proc. 20th Int. Conf. Lightning Prot. (ICLP)*, Interlaken, 24-28 September 1990, paper 4.12.

46.K. A. Norton, "The Propagation of Radio Waves over the Surface of the Earth and in the Upper Atmosphere," *Proceedings of the Institute of Radio Engineers*, **25**, 9, September 1937, pp. 1203-1236.

47.J. Zenneck, *Wireless Telegraphy* (English translation by A. E. Seelig), New York, McGraw Hill, 1915.

48.E. M. Thomson, P. J. Medelius, M. Rubinstein, M. A. Uman, J. Johnson, and J. W. Stone, "Horizontal Electric Fields from Lightning Return Strokes," *Journal of Geophysical Research*, **93**, 1988, pp. 2429-2441.

49.V. Cooray, "Horizontal Fields Generated by Return Strokes," *Radio Science*, **27**, 4, July-August 1992, pp. 529-537.

50.M. Rubinstein, "An Approximate Formula for the Calculation of the Horizontal Electric Field from Lightning at Close, Intermediate, and Long Range," *IEEE Transactions on Electromagnetic Compatibility*, **EMC-37**, 3, August 1995, pp. 531-535.

51.F. Rachidi, C. A. Nucci, M. Ianoz, and C. Mazzetti, "Influence of a Lossy Ground on Lightning-Induced Voltages on Overhead Lines" *IEEE Transactions on Electromagnetic Compatibility*, **EMC-38**, 3, August 1996, pp. 250-264.

52.M. Ianoz, C. A. Nucci, and F. M. Tesche, "Transmission Line Theory for Field-to-Transmission Line Coupling Calculations," *Electromagnetics*, **8**, 2-4, 1988, pp. 171-211.

53.C. A. Nucci, F. Rachidi, M. Ianoz, and C. Mazzetti, "Comparison of Two Coupling Models for Lightning-Induced Overvoltage Calculations," *IEEE Transactions on Power Delivery*, **10**, 1, January 1995, pp. 330-339.

54.V. Cooray, "Calculating Lightning-Induced Overvoltages in Power Lines: A Comparison of Two Coupling Models," *IEEE Transactions on Electromagnetic Compatibility*, **EMC-36**, 3, August 1994, pp. 179-182.

55.A. K. Agrawal, H. J. Price, and S. H. Gurbaxani, "Transient Response of a Multi-Conductor Transmission Line Excited by a Nonuniform Electromagnetic Field," *IEEE Transactions on Electromagnetic Compatibility*, **EMC-22**, 2, May 1980, pp. 119-129.

56.R. S. Taylor, C. W. Satterwhite, and C. W. Harrison, "The Response of a Terminated Two-Wire Transmission Line Excited by a Nonuniform Electromagnetic Field," *IEEE Transactions on Antennas and Propagation*, **AP-13**, 1965.

57.F. Rachidi, "Formulation of the Field-to-Transmission Line Coupling Equations in Terms of Magnetic Excitation Fields," *IEEE Transactions on Electromagnetic Compatibility*, **EMC-35**, 3, August 1993.

58.C. A. Nucci and F. Rachidi, "On the Contribution of the Electromagnetic Field Components in Field-to-Transmission Lines Interaction," *IEEE Transactions on Electromagnetic Compatibility*, November, 1995.

59.F. M. Tesche, M. Ianoz, and T. Karlsson, *EMC Analysis Methods and Computational Models*, New York, J. Wiley & Sons, 1996 (code available on the Web at http://www.tesche.com).

60.G. Diendorfer, "Induced Voltage on an Overhead Line to nearby Lightning," *IEEE Transactions on EMC*, **EMC-32**, 4, November 1990, pp. 292-299.

61.V. F. Hermosillo and V. Cooray, "Calculation of Fault Rates of Overhead Power Distribution Lines due to Lightning-Induced Voltages Including the Effect of Ground Conductivity," *IEEE Transactions on EMC*, **EMC-37**, 3, August 1995, pp. 392-399.

62.S. Yokoyama, "Calculation of Lightning-Induced Voltages on Overhead Multiconductor Systems," *IEEE Trans. on Power App. Syst.*, **PAS-103**, 1, January 1984, pp. 100-108.

63.M. Ishi, K. Michishita, Y. Hongo, and S. Oguma, "Lightning-Induced Voltage on an Overhead Wire Dependent on Ground Conductivity," *IEEE Transactions on Power Delivery*, **9**, 1, January 1994, pp 109-118.

64.S. Rusck, "Induced Lightning Overvoltages on Power Transmission Lines with Special Reference to the Overvoltage Protection of Low Voltage Networks," *Transactions of the Royal Institute of Technology*, No.

65.E. Cinieri and A. Fumi, "Effetto Della Presenza di Più Conduttori e di Funi di Guardia Sulle Sovratensioni Atmosferiche Indotte Nelle Linee Elettriche," *L'Energia Elettrica*, No. 11-12, 1979, pp. 595-601.

66. P. Chowdhuri, "Lightning-Induced Voltages on Multiconductor Overhead Lines," *IEEE Transactions on Power Delivery*, **5**, 2, April 1990, pp. 658-667.

67. M. Ianoz, F. Rachidi, C. Mazzetti, and C.A. Nucci, "Response of Multiconductor Power Lines to Indirect Close Lightning Strokes," *Proc. Power System EMC CIGRE Symp.*, Lausanne, Oct. 18-20, 1993, paper 200-07.

68. F. Rachidi, C. A. Nucii, M. Ianoz, and C. Mazzetti, "Response of Multiconductor Lines to nearby Lightning Return Stroke Electromagnetic Fields," *Proc. IEEE/PES Trans. & Distrib. Conf.*, Los Angeles, September 15-20, 1996.

69. D. Maciel, "Etude et Modélisation des Risques Électromagnétiques Supportés par des Câbles de Transmission d'Information Contenus dans des Chemeins Métalliques Installés sur des Sites Industriels," PhD Thesis No. 1093, Lille University, 1993.

70. A. Borghetti, C. A. Nucci, M. Paolone, and F. Rachidi, "Characterization of the Response of an Overhead Line to Lightning Electromagnetic Fields," *25th International Conference on Lightning Protection, ICLP'2000*, Rhodos, Greece, September 2000.

71. F. M. Tesche and T. K. Liu, "Application of Multiconductor Transmission Line Network Analysis to Internal Interaction Problems," *Electromagnetics*, No. 6, 1986, pp. 1-20.

72. M. D'Amore and M. S. Sarto, "Time Response of a Network Containing Field-Excited Multiconductor Lossy Lines with Non-Linear Loads," *Proc. 1993 IEEE EMC Symposium*, Dallas, TX, August 9-13, 1993.

73. K. Keroum, F. Paladian, J. Fontaine and O. Daguillon, "Etude Topologique de Systèmes Constitués de Lignes Multifilaires Interconnectées par des Réseaux Linéaires Soumis à une Impulsion Électromagnétique," *Actes 7ème Colloque International sur la CEM*, Toulouse , March 2-4, 1994, BI, pp. 241-246.

74. S. Guerrieri, M. Ianoz, F. Rachidi, P. Zweiacker, and C.A. Nucci, "A Time-Domain Approach to Evaluate Induced Currents and Voltages on Tree-Shaped Electrical Networks by External Electromagnetic Fields," *Proc. 11th Int. Zurich Symp. EMC*, March 7-9, 1995, paper 82M5.

75. C. A. Nucci, V. Bardazzi, R. Iorio, A. Mansoldo, and A. Porrino, "A Code for the Calculation of Lightning-Induced Overvoltages and its Interface with the Electromagnetic Transient Program," *Proc. 22nd International Conference on Lightning Protection*, Budapest, 19-23 September, 1994.

76. D. Orzan, Ph. Baraton, M. Ianoz, F. Rachidi, "Comparaison, Entre Deux Approches pour Traiter le Couplage Entre un Champ Électromagnétique et Desréseaux de Lignes," *Proc. 8ème Symp. Int. en Langue Française sur la Compatibilité Electromagnétique*, Lille, 3-5 September 1996.

77. A. Borghetti, R. Iorio, C. A. Nucci, and P. Pelacchi, "Effect of the Presence of Distribution Transformers on the Voltages Induced by Nearby Lightning on Overhead Distribution Lines," *Proc. Int. Conf. on Power systems transients*, 3-7 September, Lisbon, 1995.

78. R. Iorio, C. A. Nucci, A. Porino, and F. Rachidi, "Lightning Induced Voltages on Distribution Lines: Impact on Distribution Transformers," *Proc. Symp. CIGRE EMC in Power Networks*, Lausanne, 18-20 October, 1993, paper 300-09.

79. A. Xémard, Ph. Baraton, and F. Boutet, "Modelling External Electromagnetic Field," *Proc. Int. Conf. on Power Systems Transients*, Lisbon, September 3-7, 1995.

80. T. Henriksen, "Calculation of Lightning Overvoltages Using EMTP," *Proc. Int. Conf. on Power Systems Transients*, Lisbon, September 3-7, 1995.

81. M. D'Amore and M. S. Sarto, "An EMTP-Compatible Procedure for the Evaluation of Electromagnetic Induced Effects on Power Networks," *Proc. Int. Conf. on Power Systems Transients*, Lisbon, September 3-7, 1995.

82. E. Vance, *Coupling to Shielded Cables*, New York, J. Wiley, 1978.

83. M. Aguet, M. Ianovici, and C. C. Lin, "Transient Electromagnetic Field Coupling to Long Shielded Cables," *IEEE Transactions on EMC*, **EMC-22**, 4, 1980, pp. 276-282.

84. D. Orzan, M. Ianoz, and B. Nicoara, "Response of Shielded Cables to an External Electromagnetic Field Excitation. Modeling and Experimental Validation," *Proc. 13th Int. Zurich Symp. EMC*, February 16-18, 1999, paper 36G3.

85. F. M. Tesche, "Comparison of the Transmission Line and Scattering Models for Computing the NEMP Response of Overhead Cables," *IEEE Transactions on EMC*, **EMC-34**, 2, May 1992, pp. 93-99.

86. S. Tkatchenko, F. Rachidi, and M. Ianoz, "Electromagnetic Field Coupling to a Line of Finite Length: Theory and Fast Iterative Solutions in Frequency and Time Domains," *IEEE Transactions on EMC*, **EMC-37**, 4, November 1995.

87. F. Arreghini, M. Ianoz, P. Zweiacker, and D. V. Giri, A. Tehori, "SEMIRAMIS: An Asymmetrical Bounded Wave EMP Simulator with a Good Confinement Inside the Transmission Line," *Proc. 10th Int. Zurich Symp. on EMC*, March 9-11, 1993, paper 109P5.

88. M. Rubinstein, A. Y. Tzeng, M. A. Uman, P. J. Medelius, and E. M. Thompson, "An Experimental Test of a Theory of Lightning-Induced Voltages on an Overhead Wire," *IEEE Transactions on EMC*, **EMC-31**, 4, November 1989, pp. 376-383.

89. C. Gary, A. Cimador, R. Fieux, C. Gary, B. Hutzler, A. Eybert-Berard, P. Hubert, A. Meesters, P. Perroud, J. Hamelin, and J. M. Person, "Research on Artificially Triggered Lightning in France," *IEEE Transactions on Power Application Systems*, **PAS-97**, 1978, pp. 725-33.

90. K. Hori, in *Memoirs of the Faculty of Engineering Nagoya University*, **34**, 1982, Nagoya, Japan, pp. 77-112.

91. M. A. Uman, V. A. Rakov, K. J. Rambo, T. W. Vaught, M. I. Fernandez, R. Bernstein, and C. Golden, "Triggered Lightning Facility for Studying Lightning Effects on Power Systems," 23rd Int. Conf. on Lightning Protection, Florence, 1996.

92. M. Rubinstein, M. A. Uman, P-J. Medelius, and E. M. Thompson, "Measurements of the Voltage Induced on an Overhead Power Line 20 m from Triggered Lightning," *IEEE Transactions on EMC*, **EMC-36**, 2, May 1994.

93. Ph. Baraton, A. Zeddam, O. Fafif, and B. Jecko, "Détermination de la Tension Parasite Transitoire Induite aux Extrémités d'un Câble Coaxial par une IEM – Analyse de la Protection par un Circuit Non-Linéaire," *Actes 5ème Colloque Int. sur la*

Compatibilité Electromagnétique, Evian, 12-14 September 1989, contribution EI-3.

94.M. A. Uman and D. K. McLain, "Radiation Field and Current of the Lightning Stepped Leader," *J. Geoph. Res.*, **75**, 6, February 20, 1970.

95.F. Rachidi, M. Rubinstein, C. A. Nucci, and S. Guerrieri, "Influence of the Leader Electric Field Change on Voltages Induced by very Close Lightning on Overhead Lines," *Proc. 22nd Int. Conf. Light. Prot.*, Budapest, September 19-23, 1994, paper R3b-10.

96.M. Rubinstein, M. A. Uman, P. J. Medelius, and E. M. Thosmson, "Measurements of the Voltage Induced on an Overhead Power Line 20 m from Triggered Lightning," *IEEE Transactions on Electromagnetic Compatibility*, **EMC-36**, 2, May 1994, pp. 134-140.

97.P. Wallet, "Approche Topologique Appliquée à la Caractérisation des Paramètres Physiques Localisés ou Répartis qui Influences les Couplages Électromagnétiques dans des Réseaux de Lignes Blindées," PhD Thesis, Université des Sciences et Technologies de Lille, November 1995.

98.F. Rachidi, M. Rubinstein, P. Zweiacker, M. Ianoz, B. Braendli, and A. Kaelin, "Indirect Lightning Effects on Short Overhead Lines," *Proc. Int. Symp. on EMC, EMC'98 Roma*, September 14-18, 1998.

99.IEC Std. 1312-1, 1995, Protection Against Lightning Electromagnetic Impulse, Part I: General Principles.

100.V. A. Rakov, M. A. Uman, M. I. Fernandez, C. T. Mata, K. J. Rambo, M. V. Stapleton, and R. R. Sutil, "Direct Lightning Strikes to the Lightning Protective System of a Residential Building: Triggered Lightning Experiments," *IEEE Transactions on Power Delivery*, **17**, 2, April 2002, pp. 575-586.

101.J. B. M. van Waes, A. P. J. van Deursen, P. C. T. van der Laan, M. J. M. van Riet, E. Proovost, and J. F. G. Cobben, "Risks due to Lightning Strikes on High Voltage Towers with LV Applications," 25th Int. Conf. On Lightning Protection, ICLP 2000, Rhodes, Greece, 18-22 September 2000, Paper 9.16.

102.M. D'Amore and S. Sarto, "A New Formulation of Lossy Ground Return Parameters for Transient Analysis of Multiconductor Dissipative Lines," IEEE/PES Winter Meeting 1996, paper 96 WM 074-5 PWRD.

103.C. T. Mata, M. I. Fernandez, V. A. Rakov, and M. A. Uman, "EMTP Modeling of a Triggered-Lightning Strike to the Phase Conductor of an Overhead Distribution Line," paper PE-044PRD (o5-200); accepted for publication in the *IEEE Transactions on Power Delivery*, 2000.

104.D. Orzan, "Couplage Externe et Interne Entre un Champ Électromagnétique et un Réseau de Lignes Multifilaires," Thèse No. 1768 (1998), Ecole Polytechnique Fédérale de Lausanne.

UTC Time Step

On n'introduira pas de seconde intercalaire à la fin de juin 2003.
La différence entre UTI et le Temps Atomique International TAI est :
du 1er janvier 1999, 0h UTC, jusqu'à nouvel avis : UTC - TAI = -32 s
Des secondes intercalaires peuvent être introduites à la fin des mois de décembre ou de juin, selon l'évolution de UT1-TAI. Le Bulletin C est diffusé deux fois par an, soit pour annoncer un saut de seconde, soit pour confirmer qu'il n'y aura pas de saut de seconde à la prochaine date possible.

No positive leap second will be introduced at the end of June 2003.
The difference between UTC and the International Atomic Time TAI is :
from 1999 January 1, 0 h UTC, until further notice : UTC - TAI = -32 s
Leap seconds can be introduced in UTC at the end of the months of December and June, depending on the evolution of UT1-TAI. Bulletin C is mailed every six months, either to announce a time step in UTC, or to confirm that there is no time step at the next possible date.

Daniel GAMBIS
Director, Earth Orientation Center of IERS
Fax: +33 1-40 512291
E-mail: iers@obspm.fr

Ultra-Fast Photonic Networks Based on Optical Code-Division Multiplexing

H. Sotobayashi

Abstract

Ultra-fast photonic networks based on optical code-division multiplexing (OCDM) are reviewed. The demonstrated applications of OCDM are as follows: 1) high spectral efficiency transport system (1.6 bit/s/Hz, 6.4 Tbit/s QPSK-OCDM/WDM transmission experiment), 2) photonic access node (10 Gbit/s packet-selective photonic label-based add/drop multiplexing), 3) optical path networks (transparent virtual optical code/wavelength path network with optical code and wavelength-convertible nodes), 4) photonic routing (optical-code-correlation-based ultra-fast photonic routing).

1. Introduction

The roots of optical code-division multiple access are found in spread-spectrum communication techniques. Spread spectrum was developed in the mid-1950s, mainly as a novel form of transmission, overcoming the grid restrictions in radio bandwidth allocation [1-3]. It is based on the idea of spreading the spectrum of the narrowband message over a much wider frequency spectrum by means of digital codes [4, 5]. Due to the spreading, the transmitted signal arrives at the receiver as a noise-like signal. Furthermore, message recovery is impossible unless the original code is known. The received signal is correlated by the authorized receiver with a local code, which is a replica of the transmission code. Despreading and signal recovery in the presence of interference from other users can be accomplished. As a result, spread spectrum found application in military communications, as a mechanism of transmitting signals in a very noisy environment with very high security. Furthermore, with the emergence of satellite and mobile communications, spread spectrum was considered for the basis of a new multiple-access technique, named CDMA [code division multiple access] [6].

In photonic transport systems, optical time-division multiplexing and wavelength-division multiplexing are two primary techniques for multiplexing data onto a single transmission fiber. Optical code-division multiplexing (OCDM) is an alternative technique. The first work in optical CDMA was carried out in the late 1970s, in the area of fiber delay lines for signal processing [7]. Since then, many research groups around the world have been active in research on optical CDMA.

In OCDM systems, each channel is optically encoded with a specific code. Only the intended user with the correct code can recover the encoded information. A proper choice of optical codes allows signals from all connected network nodes to be carried without interference between signals. Therefore, simultaneous multiple access can be achieved, without complex network protocols. As a result, multiple users can share the same transmission bandwidth.

OCDMA systems are generally classified into incoherent and coherent regimes, depending on the degree of coherence of the signal source. Coherent OCDM adopts a carrier-phase-shifted optical sequence [8]; on the other hand, incoherent OCDM uses intensity-modulated code sequences [9]. In the coherent case, a pulse sequence of phase-shifted bipolar optical chips represents a binary code. Incoherent OCDM uses a unipolar code, in which an on/off keying modulation format is adopted. The most significant advantage of the coherent scheme is the higher signal-to-interference-noise ratio. This is directly attributed to the

Hideyuki Sotobayashi is with the Research Laboratory of Electronics, Massachusetts Institute of Technology,
77 Massachusetts Avenue, room 36-323,
Cambridge, MA 02139, USA;
Tel: +1 (617) 253-8949; Fax: +1 (617) 253-9611;
E-mail: hideyuki@mit.edu.
He is also with the Communications Research Laboratory, Independent Administrative Institution
4-2-1, Nukui-Kita, Koganei,
Tokyo 184-8795, Japan;
Tel: +81 42-327-5320; Fax: +81 42-327-7035;
E-mail: soba@crl.go.jp

[Editor's note: This invited paper is the Commission D Tutorial Lecture, presented at the XXVII General Assembly of URSI in Maastricht, The Netherlands, 17-24 August, 2002.]

superior orthogonality between the codes, which, in turn, yields higher processing gains. Most of the work in the 1980s dealt with incoherent optical codes, but this revealed limited system performance. With the advent of optical device technology, the difficulties of optical phase encoding have been overcome in recent years. Hereafter, the focus will be on the coherent approach.

As for the design of the optical code set, each CDMA code must have an autocorrelation peak that is as large as possible. Also, it is desirable that each CDMA code can be easily distinguished from every other CDMA code in the set. For asynchronous CDMA, each CDMA code must be distinguished from a shifted version of itself.

There are two encoding schemes: encoding in the frequency domain, and in the time domain. Encoding in the frequency domain is an analogy of the spread-spectrum technique [10]. In time-domain encoding, some time-resolved chip pulses are generated within one bit timeframe [11]. The phase of each chip pulse represents an optical code sequence. Matched filtering in the optical domain is a class of dispreading. In general, matched filtering is a detection technique that maximizes the signal-to-noise ratio. The impulse response of the matched filter on the decoder side is the complex conjugate of the optical encoder. The output of the decoder is expressed by the convolution of the matched filter. If the optical codes between the encoder and decoder match, the decoded time-despread signal reconstructs the original short pulse. On he other hand, unmatched codes remain randomly spread over one bit timeframe of *T* after the decoding.

In coherent OCDM systems, interference noise is the most severe problem. The processing gain is expressed as the ratio of one bit time duration to the gate time window. Time-gating should be introduced to achieve the strict sense of the processing gain. The time-gating opens to extract the autocorrelation peak. This operation is equivalent to narrowband filtering in wireless CDMA. Placing the optical time gate before the photo detector has a substantial advantage, because the requirement for the detector bandwidth is significantly relaxed compared to the bit rate.

The characteristics of OCDM systems, in contrast to wireless CDMA, are summarized in the following and as shown in Figure 1. OCDM inherits unique features from the wireless counterpart: accommodation of a number of channels on a single carrier frequency, tell-and-go access capability, freedom from network-wide timing synchronization, soft capacity on demand, and security [12]. Therefore, the applications range from point-to-point transmission [13, 14], multiple access [15, 16], optical-path network [17, 18], secure optical communications, and label-switching routing [19, 20].

References [21] and [22] demonstrate one of the OCDM systems in the frequency domain. The basic idea is to realize parallel modulation in the frequency domain, to reshape a short pulse into a low-intensity pseudo-noise burst. The optical encoder consists of a suitably configured grating and lens apparatus. The first grating spatially decompresses the spectral component of the incident ultra-short light pulse. A phase mask is inserted at the focal point of the lens, where the optical spectral components experience maximum separation. The phase mask imposes specific phase shifts among the different spectral components of the initial short pulse, and therefore serves to encode its spectrum. The encoded spectral components are reassembled by the second lens and the second grating. The shape of the encoded pulse resembles a pseudo-noise signal. At the receiver, the intended signal is recovered by a spectral correlation process. The matched optical encoder is the complex conjugate of the encoder, and the original short pulse is restored. When the encoding and decoding phase mask do not match, the output pulse remains a low-intensity pseudo-noise burst. A 30 MHz-repetition-rate, 275 fs pulse was encoded using 63-chip BPSK [binary phase-shift keying] codes. After 10 km of transmission, the proof of the concept was experimentally demonstrated.

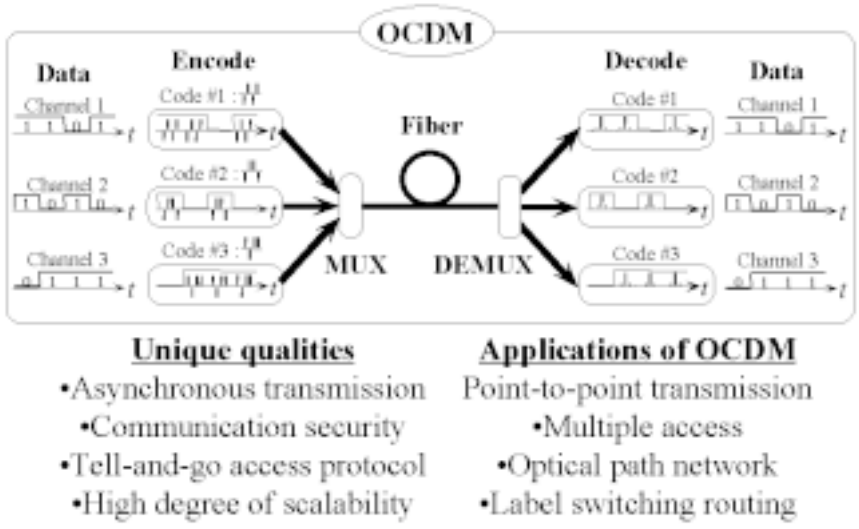

Figure 1. Optical code-division multiplexing.

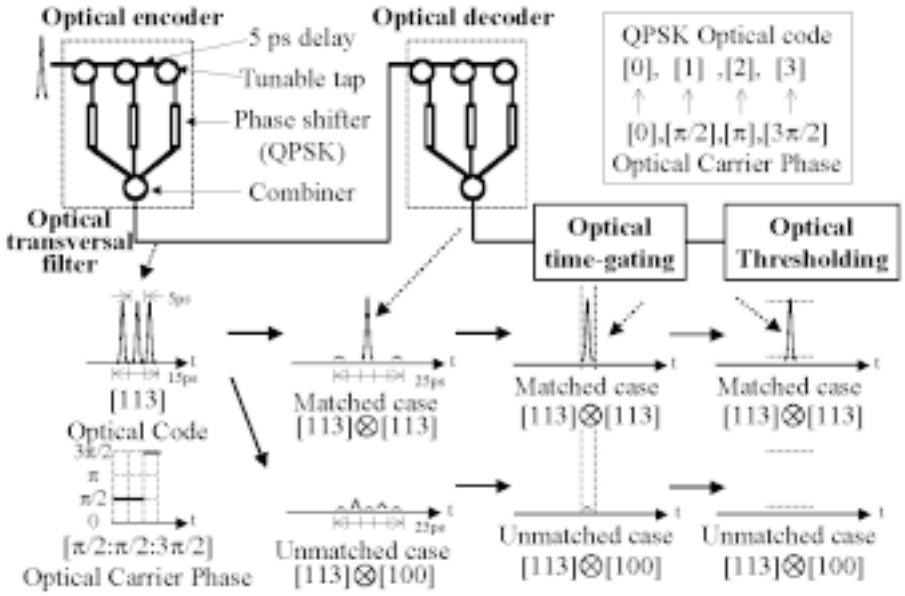

Figure 2. The principle of operation of QPSK code-OCDM with optical time gating and optical hard thresholding.

A group at NTT used the same spreading-despreading basis. A waveguide grating array with phase shifters was used as optical encoders/decoders [23, 24]. The input pulses were spectrally decomposed to their frequency components in an AWG (arrayed wavelength grating). Each phase was binary shifted by an encoding filter. The frequency resolution was 12.6 GHz. Transmission over 40 km was demonstrated at 10 Gbit/s using 810 fs pulses.

A group at Southampton University demonstrated both BPSK and QPSK (quaternary phase-shift keying) encoding in the time domain, using super-structure fiber Bragg gratings [25, 26]. A super-structure fiber Bragg grating has a rapidly varying refractive modulation of uniform amplitude and pitch, onto which an additional slowly varying amplitude/phase CDMA code has been imposed along its length. The shape of the impulse response directly follows the shape of the special super structure. Short pulses reflected from gratings are reshaped into a coded pulse sequence. Pattern recognition can be obtained by match-filtering the coded signal, using a decoder grating with the conjugate impulse response. They have demonstrated up to 255-chip QPSK optical coding and 2 WDM [wavelength division multiplexing], 2OCDM at 1.25 Gbit/s transmission.

Another approach is that in which optical transversal filters are used as encoders and decoders [11-20]. The detailed principle of operation will be explained in a later section.

2. The Application of OCDM to High-Spectral-Efficiency Transport Systems

The rapid increase in demand for bandwidth from end users forces the network infrastructure to a capacity of peta-bit/s, and to be agile. Due to their low transmission loss, optical fibers are ideal for high-capacity signal-transmission media. However, the gain bandwidths of the present optical amplifiers are limited. Over 10 Tbit/s WDM [wavelength-division multiplexing] transmission has been reported by fully utilizing the present amplifier wavelength bands, that is, the S-, C-, and L-band wavelength regions [27, 28]. To meet the peta-bit/s capacity requirement, the spectral efficiency is becoming a key issue for the full utilization of limited wavelength resources. From this point of view, some approaches for increasing spectral efficiency have been demonstrated, such as duo-binary encoding with 0.6 bit/s/Hz spectral efficiency [29], and vestigial sideband filtering with polarization multiplexing, with 1.28 bit/s/Hz [28]. OCDM is another candidate for the ultimate spectral efficiency.

We have demonstrated the feasibility of an over-Tbit/s BPSK-OCDM/WDM link, with 0.4 bit/s/Hz spectral efficiency, by simultaneous multi-wavelength optical encoding of a single supercontinuum (SC) source [13]. In order to upgrade the spectral efficiency, in addition to polarization multiplexing, we applied quaternary phase-shift keying (QPSK) optical encoding/decoding at 40 Gbit/s, accompanied by ultra-fast optical time gating and optical hard thresholding for interference noise suppression. As a result, 6.4 Tbit/s OCDM/WDM (4 OCDM × 40 WDM × 40 Gbit/s) transmission, using only the C-band wavelength region, was experimentally demonstrated, with 1.6 bit/s/Hz spectral efficiency [14].

Compared to BPSK optical coding, QPSK optical coding is known to provide a larger number of codes with more-desirable cross-correlation characteristics [14]. As shown in Figure 2, time-spread QPSK pulse codes are used as the optical codes, and optical transversal filters are used as the optical encoders and decoders. An optical code of a three-chip QPSK pulse-code sequence with a chip interval of 5 ps is generated. The impulse response of the optical encoding has a frequency periodicity of 200 GHz, because

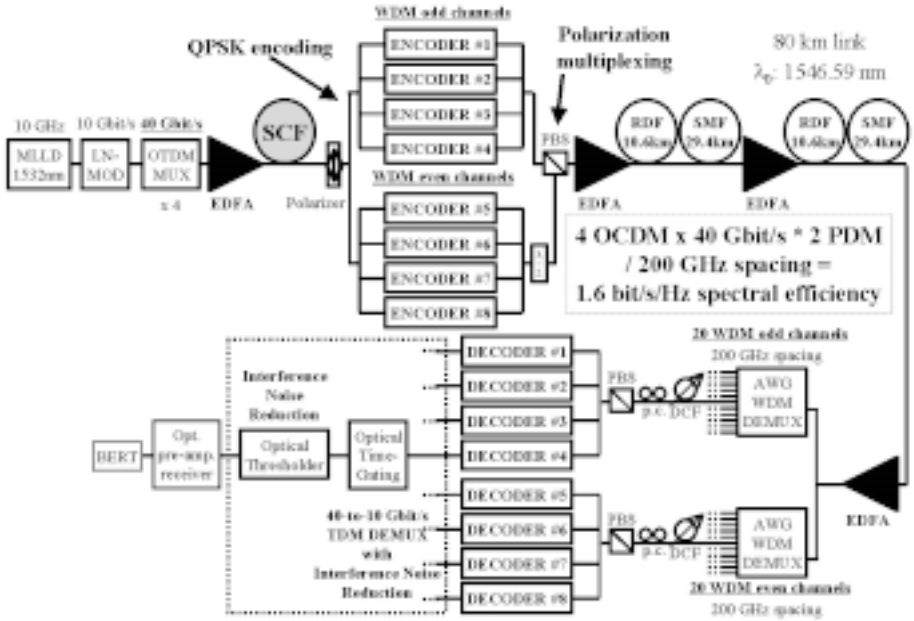

Figure 3. The experimental setup for 6.4 Tbit/s (4 OCDM × 40 WDM × 40 Gbit/s) transmission with 1.6 bit/s/Hz spectral efficiency.

the chip interval of the optical encoder is 5 ps [30]. As a result, simultaneous multi-wavelength encoding, having a WDM channel spacing of 200 GHz, can be achieved using a single optical encoder, when a broadband coherent optical pulse, such as a supercontinuum pulse, is used as a chip pulse [13].

Besides QPSK optical encoding/decoding, ultra-fast optical hard thresholding, along with optical time-gating, is applied for high spectral efficiency. In order to achieve the strict sense of high processing gain, optical time gating must be introduced to extract only the main lobe of the autocorrelation. As a result, the interference noise arising from interference codes existing outside the time frame of the main lobe are rejected [11]. In addition, the interference noise existing inside the time frame of the main lobe is also greatly reduced by the introduction of hard thresholding in the optical domain, [14]. As a consequence, by applying QPSK-codes accompanied by optical time-gating and optical hard thresholding, both the number of optical codes in the same WDM channel and the data rate can be greatly increased, resulting in a high spectral efficiency.

Figure 3 shows the experimental setup of a 6.4 Tbit/s OCDM/WDM (4 OCDM × 40 WDM × 40 Gbit/s) transmission [14]. A 10 GHz, 1.5 ps pulse train of the mode-locked laser diode (MLLD), at 1532 nm, was modulated with a 10 Gbit/s PRBS (pseudo-random bit sequence) of $2^{23}-1$, and optically multiplexed to 40 Gbit/s. After being amplified to an average power of 0.48 W, it was launched into a supercontinuum fiber (SCF) [31]. The 40 Gbit/s SC signal so generated was linearly polarized and split into eight signals, and each served as the light source for simultaneous multi-wavelength optical encoding, using a QPSK optical encoder. Two groups of four different optically encoded signals were generated. One group was changed to the orthogonal polarization, and both groups of four OCDM signals were multiplexed to orthogonally polarized multi-wavelength 2 × 4 OCDM × 40 Gbit/s signals, using a polarization beam splitter (PBS). Each group had a WDM channel spacing of 200 GHz, which corresponded to 1.6 bit/s/Hz spectral efficiency. The transmission line was composed of two spans of a reversed-dispersion fiber (RDF) and a single-mode-dispersion fiber (SMF) pair. Each span was 40 km long, and the total length was 80 km. The average zero-dispersion wavelength was 1546.59 nm. After 80 km transmission, it was split into two, and each was WDM DEMUX (wavelength-division demultiplexed) by a 20-channel arrayed wavelength grating (AWG), having a channel spacing of 200 GHz. The pass-band wavelengths of the two AWGs were separated by 100 GHz (WDM Channel 1: 1532.68 nm; Channel 40: 1563.86 nm). After WDM DEMUX, the frequency chirping was compensated for, and the polarization was demultiplexed. Then, it was decoded by an optical decoder. Optical time gating was performed at a 10 GHz repetition rate: this acted to both reject the interference noise outside the time-gating window, and did 40 Gbit/s to 10 Gbit/s OTDM demultiplexing. Optical time-gating was performed at a 10 GHz repetition rate by using a nonlinear optical-loop mirror (NOLM) based on a 100 m high-nonlinear-dispersion-shifted fiber (HNLF) [32]. Optical time-gating rejected the interference noise outside the main lobe of the autocorrelation. For ultra-fast operation, a short length of HNLF was used. The control pulse used for 10 GHz optical time gating was a 1.5 ps pulse train from the mode-locked laser diode at 1562.5 nm for the gating of WDM Channel 1 to Channel 22 (1533-1549 nm), and at 1542.2 nm for the gating of WDM Channel 23 to Channel 40 (1550-1564 nm). The walk-off between signal and control pulses was less than 300 fs, resulting in ultra-high-speed operation. The optical time-gating window ranged from 1.5 ps to 1.8 ps for all WDM channels. Optical hard thresholding was achieved by using the second nonlinear optical-loop mirror. Optical hard thresholding was achieved by the utilization of the nonlinear transmission response of the second nonlinear

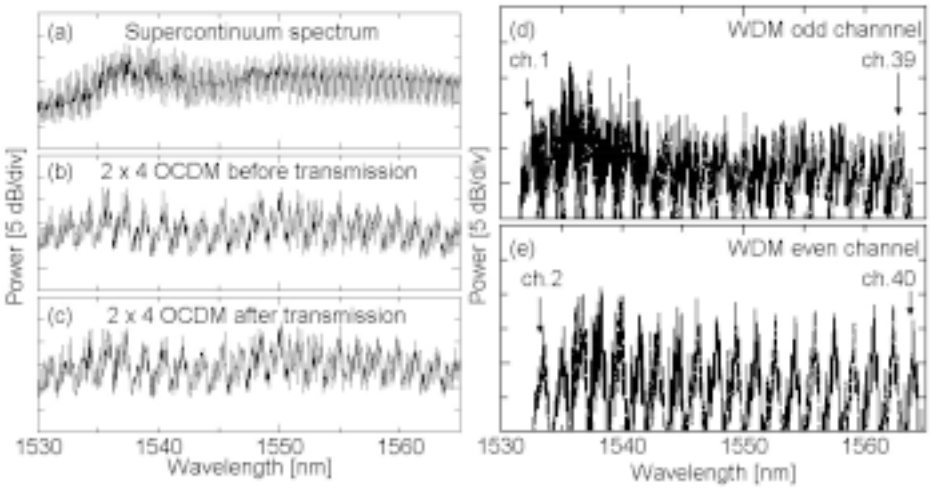

Figure 4. (a) The 40 Gbit/s SC spectrum. The spectra of 2 × 4 OCDM (b) before and (c) after transmission. The spectra of (d) odd and (e) even WDM channelsafter WDM and polarization DEMUX.

optical-loop mirror. The nonlinear optical-loop mirror acted as a pulse shaper by setting the proper threshold level, in the sense that it reflected lower-intensity signals, but only transmitted the higher-intensity signal by limiting its intensity to an appropriate level. By adjusting the input signal power, interference noise inside the autocorrelation main lobe after optical time gating was suppressed, and both signal "0" and "1" level power variations were greatly reduced. For ultra-high-speed operation, the device length and group delay had to be shortened. By the use of a short length of 50 m high-nonlinear-dispersion-shifted fiber as a hard-thresholding nonlinear optical-loop mirror, the group delay in all the wavelength ranges (1533-1564 nm) of the WDM channels was less than 200 fs, resulting in ultra-high-speed operation. Bit-error rates (BERs) were measured using an optically pre-amplified receiver.

Figures 4a-4e show the optical spectrum of (a) the supercontinuum at the output of the supercontinuum fiber, (b) the multi-wavelength 2 × 4 OCDM signals before transmission, (c) the signals after transmission, and (d) the odd WDM channels, and (e) the even WDM channels, after WDM and polarization DEMUX. Figure 5a shows the eye diagrams of WDM Channels 1,2,39, and 40 after optical decoding. The interference noise of other three unmatched codes severely distorted the signal-to-noise ratio. As shown in Figure 5b, by optical time gating of the main lobe of the matched correlation waveforms, interference noise outside the time-gate window was greatly reduced. In addition to this, as shown in Figure 5c, by introducing optical hard thresholding, interference noise inside the time-gate window was greatly reduced in both the signal "0" and "1" level, resulting in a clear eye opening. The measured BERs of the 4 OCDM × 40 WDM data signals were less than 1×10^{-9} .

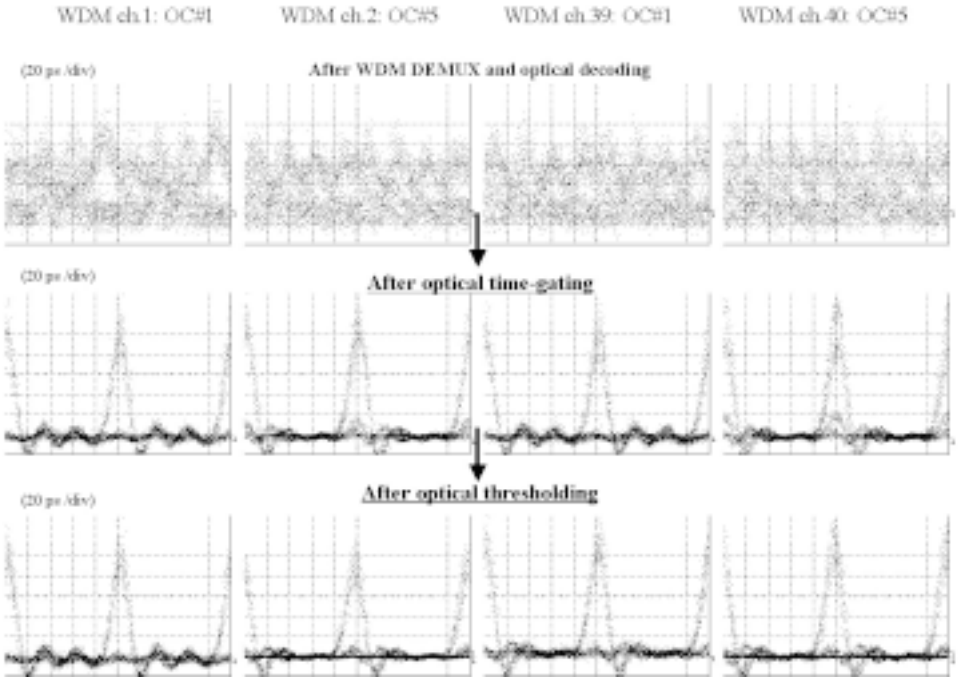

Figure 5. Eye diagrams of optically decoded signals of WDM Channels 1, 2, 39, and 40 (a) after optical decoding, (b) after optical time gating, and (c) after optical hard thresholding.

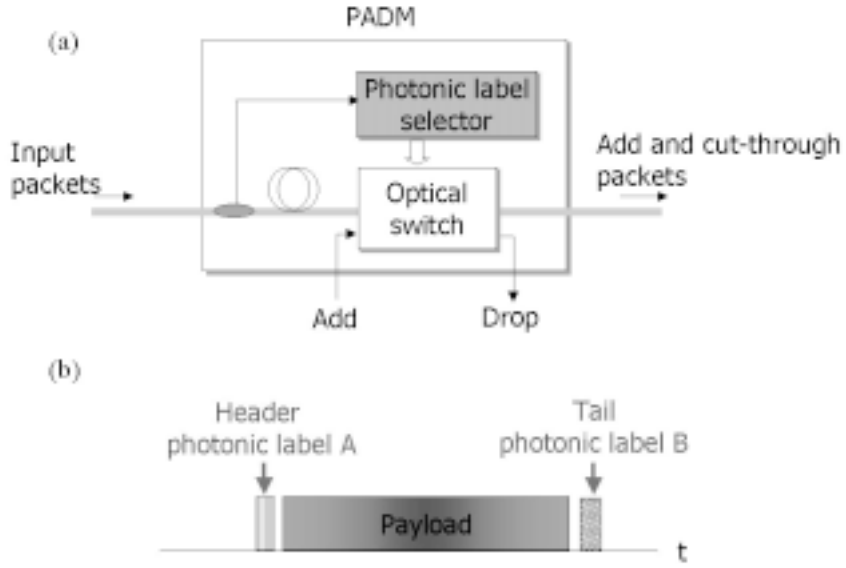

Figure 6. (a) The basic architecture of a photonic label-based add/drop multiplexer (PADM), and (b) the optical packet structure.

3. The Application of OCDM to a Photonic Access Node

In this section, the application of OCDM to a photonic access node and the experimental demonstration of 10 Gbit/s packet add/drop multiplexing, based on optical code correlation, will be explained [16, 33].

Wavelength add/drop multiplexers (ADM) enable each wavelength to be either added or dropped, and electronically processed, at the node, or to optically bypass the node's electronics. However, wavelength add/drop multiplexing is of the granularity of the wavelength. It is limited, in that it can only handle traffic on an optical channel, and cannot handle traffic on a packet-by-packet basis. This may waste the wavelength resources, and limit the usage of optical channels. On the other hand, conventional synchronous optical network add/drop multiplexing has a finer granularity for handling traffic. It picks out low-speed streams from a high-speed stream and, likewise, adds low-speed streams to a high-speed stream. However, the speed of electrical processing will eventually become a bottleneck, due to the overall processing capability. Therefore, there will be a growing demand for a high-speed multifunctional add/drop multiplexer that can handle traffic at a finer granularity. Photonic add/drop multiplexing (ADM) is

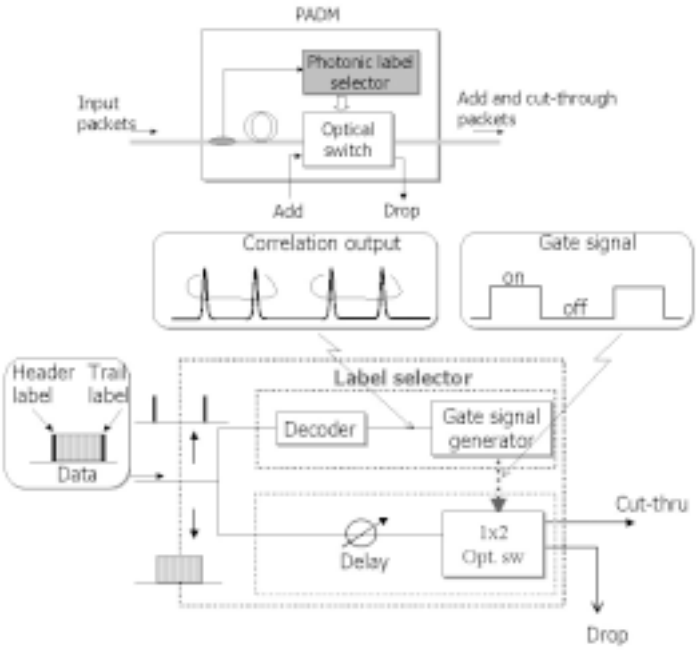

Figure 7. A photonic label-based add/drop multiplexer.

located at a node, and drops the arriving packets to the node, bypasses the node, or adds the generated packets from the node. It handles traffic on a single wavelength on a packet-by-packet basis. Figure 6a shows the basic architecture of a photonic ADM (PADM). The fundamental functions of the PADM include photonic label processing and optical switching. The input and output ports are connected to WDM links of a single wavelength. The photonic label of the arriving packet is processed and, according to the label, the optical switch is driven by the control signal to direct the packet to the outgoing port, either for dropping or bypassing. Figure 6b shows the optical packet structure. The label is simply a relatively short fixed-length identifier, which bears the information of the destination and source. A flag that indicates the end must be attached at the end of the packet. Therefore, two photonic labels are attached: the header label and the tail label. By using two labels, a variable-length packet can be handled. Optical codes are used as the photonic label. Eight-chip BPSK codes are used as optical codes, and optical transversal filters are used as optical encoders and decoders. The decoding is based upon matched filtering in the time domain.

As shown in Figure 7, the photonic label of the arriving packet is compared with a local label in the photonic label selector by performing optical correlation between the optical code of the arriving packet and the assigned code of the node. When the incoming label matches the local label, a control signal is generated to drive the optical switch to drop the packet data. The switch is reset to the bar-state again by the second label at the tail. On the other hand, when the incoming label does not match the local label, the switch remains in the bar-state to bypass the packet. Add multiplexing is accomplished in the same manner.

Figure 8 shows the experimental setup for photonic ADM. Two kinds of optical packet were generated at 10 Gbit/s, using two different optical codes. A label was attached at the top and tail of the packet data. After 50 km of transmission, the label was detected using an optical decoder, and the correlation waveform controlled the optical switch. The measured waveforms of a dropped packet at Port 1 and bypass packets at Port 2 are shown in Figure 9. Both the dropping and bypassing functions were confirmed at BERs less than 10^{-9}, based on optical correlation [16, 33].

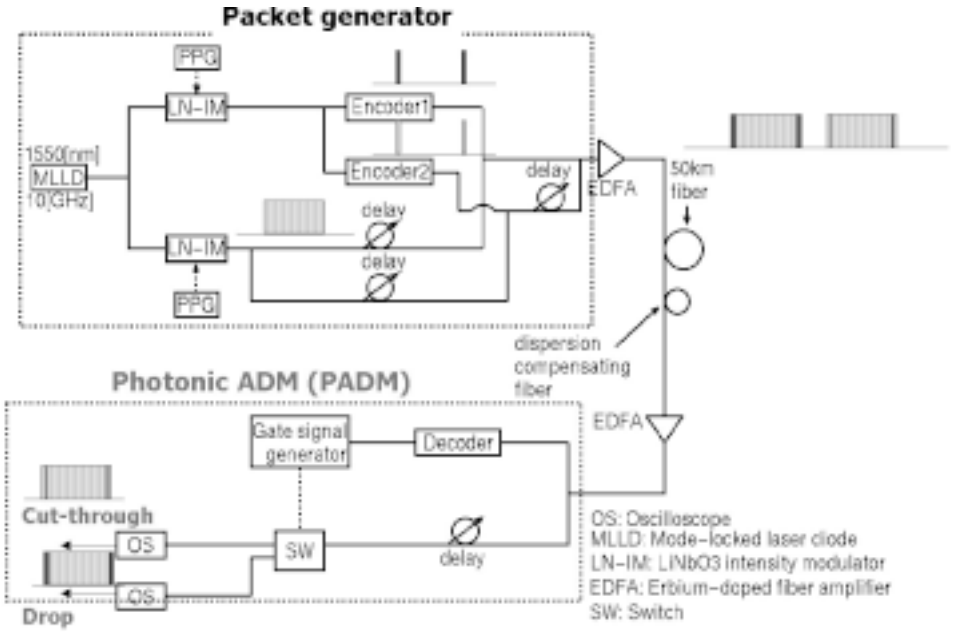

Figure 8. The experimental setup for a PADM.

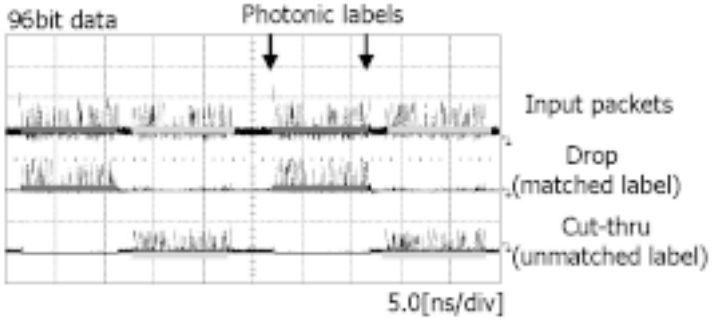

Figure 9. The experimental results of the dropping and bypassing functions of a PADM.

4. The Application of OCDM to an Optical Path Network

In this section, the application of OCDM to an optical path network is introduced. OCDM could be favorably applied not only to multiple-access networks, but also to path networks. The optical code path (OCP), defined as the logical path determined by the optical code (OC), has been proposed within the concept of OCDM networks [17, 18]. OCDM can be effectively overlaid onto existing WDM path networks. The introduction of optical codes provides a soft capacity for networks, and saves network resources. In future hybrid OCDM/WDM networks, flexible optical codes and wavelength conversions will be key technologies for establishing the optical path. As a node technology, simultaneous optical code and wavelength conversion in an operational bandwidth of 8.05 THz was experimentally demonstrated by supercontinuum generation [18]. Furthermore, all-optical 3R [re-amplification, re-timing, and re-shaping] was applied for a transparent network. Finally, an optical code and wavelength convertible virtual optical code/wavelength path (VOCP/VWP) network with a total link length of 180 km, with four network nodes, was also experimentally demonstrated.

Figure 10 shows the experimental setup of the VOCP/VWP path network. For simplicity, the data transport of Node A to Node C in Optical Path 1, and of Node A to Node E in Optical Paths 2 and 3, in the bottom figure, are demonstrated. Three types of optical codes and wavelength conversions must be done at Node B: λ1-OC1 to λ1-OC2 (optical code, OC, conversion); λ1-OC2 to λ2-OC2 (wavelength conversion); and λ2-OC2 to λ1-OC1 (OC and wavelength conversions) in Optical Paths 1, 2, and 3, respectively. Each network node was linked with several tens of km of transmission fibers.

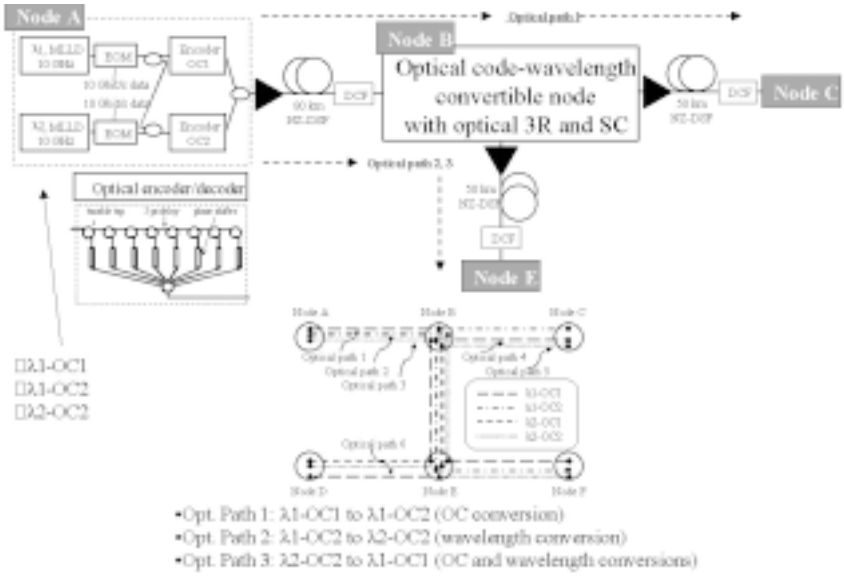

Figure 10. The experimental setup of a VOCP/VWP network.

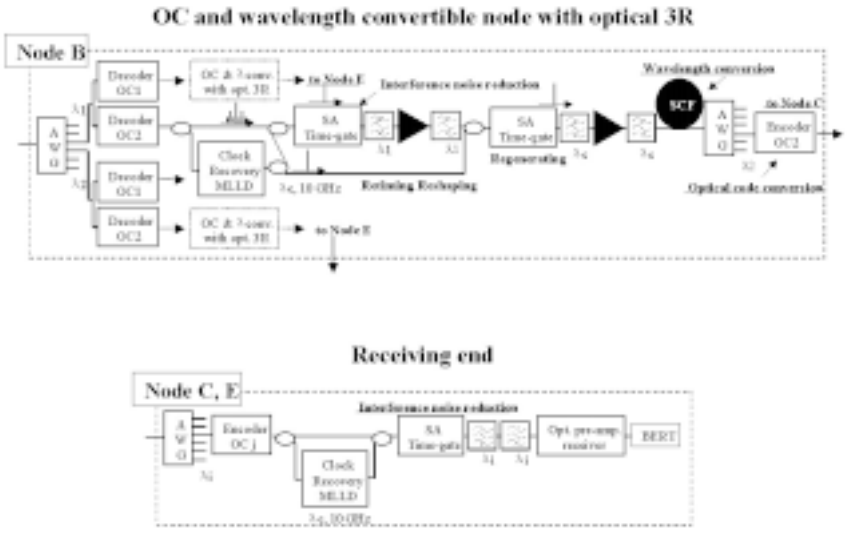

Figure 11. (a) The architecture of Node B, and (b) the architecture of Nodes C, E.

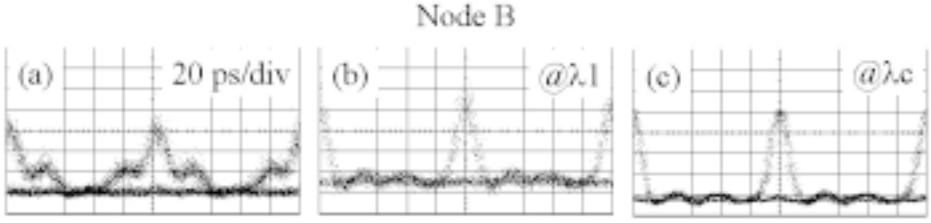

Figure 12. The eye diagrams (a) of the decoded λ1-OC2 with interference codes, (b) after optical time gating for interference noise reduction at λ1, and (c) the decoded signal at lc after optical 3R.

At Node A, λ1-OC1, λ1-OC2, and λ2-OC2 were generated and multiplexed. 10 GHz, 1.5 ps pulse trains from the mode-locked laser diodes at λ1 and λ2 were modulated at 10 Gbit/s. Optical transversal filters were used as eight-chip BPSK optical encoders/decoders. As shown in Figure 11a, at Node B, received signals were decoded, 3R regenerated, wavelength converted by SC generation, and OC converted. First, they were wavelength demultiplexed and decoded by optical decoders. The decoded signals were divided into two. One of these lead to an injection-locked mode-locked laser diode (MLLD) for 10 GHz clock recovery. The recovered clock pulses were divided, and one of these was used for the pump pulses of a semiconductor saturable absorber time gate. After time gating, the decoded signals were, in turn, used for the pump pulses of the second saturable absorber (SA) time gate to gate the clock pulse train. By controlling the optical time gate ON/OFF state using decoded signals, the data coding could be transferred to newly generated clear optical pulses. Thus, all-optical 3R was obtained. For wavelength conversion, a supercontinuum (SC) was produced with pumping by 3R-regenerated signals. After spectrum-slicing using an arrayed wavelength grating (AWG) at the wavelength to be converted, they were optically encoded with the optical code (OC) to be converted. Consequently, simultaneous optical coding and wavelength conversion with optical 3R was obtained. As shown in Figure 11b, after subsequent transmission over 50 km, optically coded and wavelength converted signals were detected at Node C or Node E. As was done in Node B, after being wavelength demultiplexed and decoded, optical time-gating was done with the recovered 10 GHz optical clock to reduce interference noise.

The eye diagram measured at Node B of the decoded λ1-OC2 after 80 km of transmission is shown in Figure 12a. The measured eye diagram of the recovered clock induced optically time-gated signals is shown in Figure 12b. Compared to Figure 12a, the sidelobe noise and interference noise are greatly reduced. Figure 12c shows the optically 3R regenerated decoded signal at λc. As is obviously shown by comparison with Figure 12b, the SNR is increased and the timing jitter is reduced by optical 3R. Figure 13 shows the optical spectrum of 24-channel WDM spectrum-sliced supercontinuum pumped by an optically 3R decoded signal that ranges from 1524.9 nm to 1590.0 nm, which corresponds to an 8.05 THz bandwidth. Figure 14 shows the measured BERs back-to-back, after 80 km transmission, after optical coding and wavelength conversion with optical 3R at Node B, and after subsequent 50 km transmission at Node C or Node E. In the comparison of the BERs after 80 km transmission and the BERs after optical coding and wavelength conversion, almost power-penalty-free optical coding and wavelength conversion were successfully demonstrated by introducing optical time-gating detection followed by optical 3R. From the viewpoint of a VOCP/VWP path network, optical coding and wavelength conversion signal transport on a total link length of 180 km with four network nodes were also successfully demonstrated.

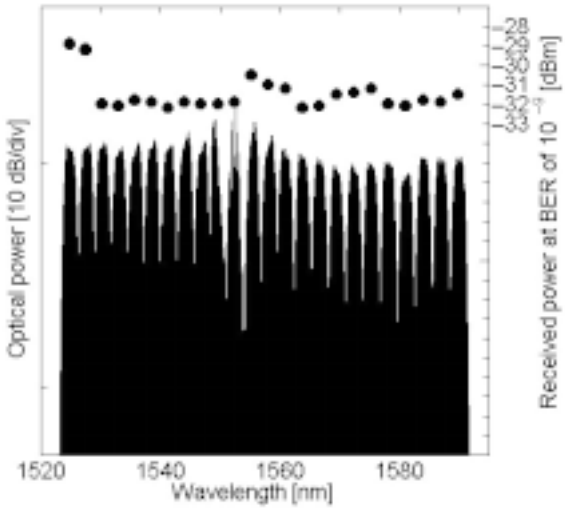

Figure 13. The optical spectrum after the spectrum-sliced SC is pumped by the optical 3R decoded signal, and the received power at a BER of 10^{-9}, for each wavelength.

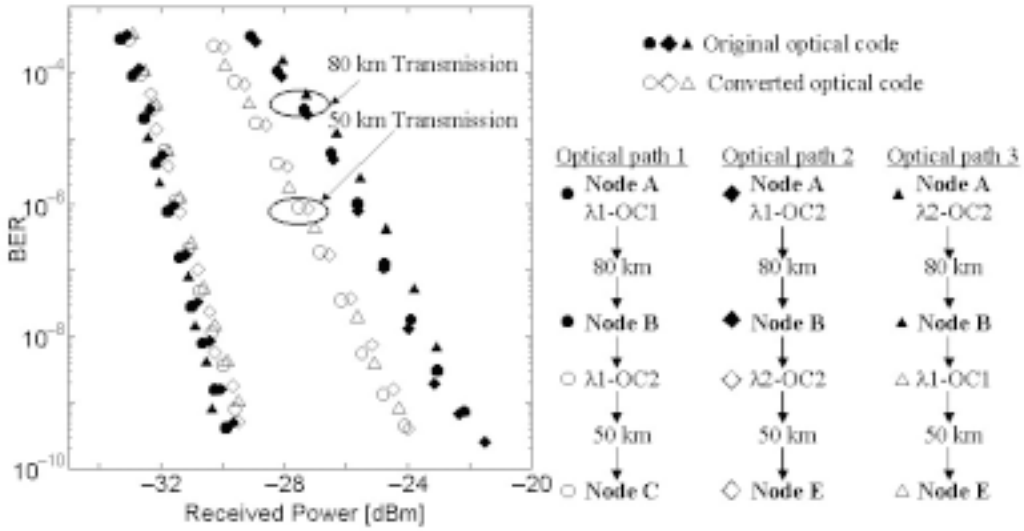

Figure 14. The measured BERs: back-to-back, after 80 km of transmission, after OC and wavelength conversion with optical 3R, and after subsequent 50 km transmission.

5. The Application of OCDM to Photonic Routing

A photonic label-switching router has been proposed in [19, 20]. Photonic label processing is based upon optical code correlation. The proposed scheme is a potential solution for resolving the electronic-router bottleneck in current Internet protocol over WDM networks. The architecture of a photonic label-switching router, including the photonic label processing, the photonic label swapping, and the optical switching and their optical implementations, were studied. The results of proof-of-concept experiments for photonic label processing and photonic label swapping will confirm their feasibility. Figure 15a shows IP over a photonic network in which photonic IP routers were employed at the node. Electronic routers were totally replaced with the photonic IP routers in the core network. Label switching was adopted for the algorithm for forwarding of IP packets. A packet can be forwarded to the destination via designated intermediate nodes. The node configuration in IP over a photonic network is shown in Figure 15b. It consists of the photonic label-switching routers and the wavelength demultiplexer/multiplexer. The photonic label-switching router (PLSR) is distinct from its electronic counterparts, in

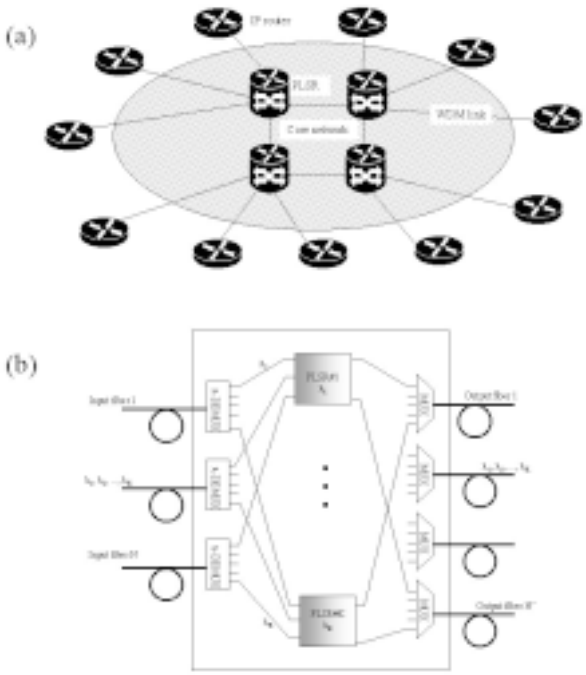

Figure 15: (a) IP over a photonic network employing label-switching routers (PLSRs), (b) The node configuration of IP over a photonic network.

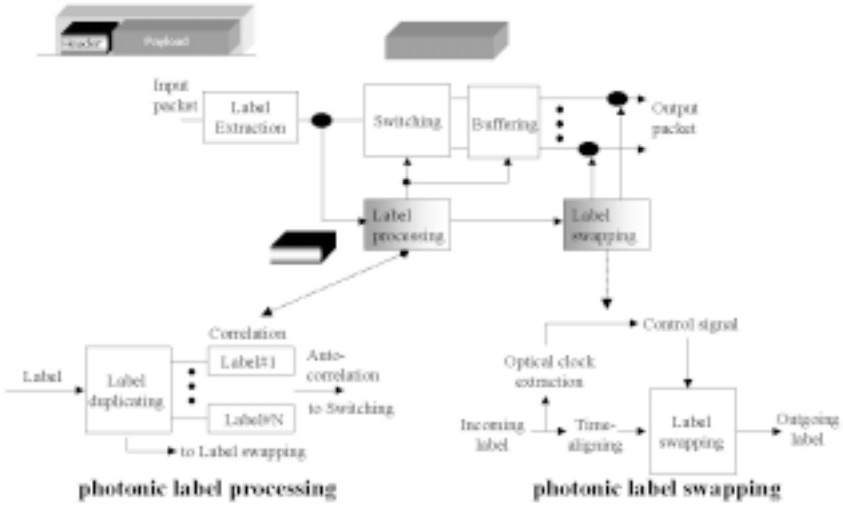

Figure 16. The architecture of the PLSR.

that the processing of IP packets is mainly performed in the optical domain, without optical-to-electrical conversion. Figure 16 shows an architecture for the photonic label-switching router. Each label is mapped onto a single optical code, and the IP packet is encapsulated in an optical frame. The main building blocks are the photonic label processor, the photonic label swapper, and an optical switch. Exact matching for the table lookup is adopted due to the property of optical correlation, because the optical correlation identifies a photonic label only when all the bits of the label coincide with those of the label entry in the lookup table. The optical payload is gated for routing to the desired port in the switch fabric. Also, the label has to be swapped at the output of the label-switching router according to the address bank.

Figure 17 shows the principle operation of the label processing. An in-coming photonic label is optically duplicated by optical amplification and power-splitting into as many copies as there are label entries in the table. Thus, all the optical correlations between the copies and the label entries can be performed in parallel. An autocorrelation peak emerges in the bit time duration only where the codes match. That no optical logic operation is involved is unique to the photonic label processing; only optical correlation is used. The processing is performed by using simple passive optical devices.

Figure 18 shows the experimental setup for photonic label processing. In the optical transmitter, a photonic label of an eight-chip BPSK optical code is generated, and a 64-bit long burst payload data signal is attached. The optical packet is directed to the photonic label processor. The output signal of the autocorrelation peak is detected when the input label matches the label of the correlator. As a result, only the autocorrelation output signal can drive the opening the optical gate switch, and can guide the packet to the desired output port. Otherwise, the gate switch remains closed. Figure 19a shows the 64-bit long packet with photonic Label #1, and Figures 19b and 19c show the auto- and cross-correlation outputs of the packet, which are decoded with Label #1 and Label #2. The observed payload data at Port 1 and Port 2 of the two different input packets, having labels matched with Correlator #1 and matched with Correlator #2, are shown in Figures 19d and 19e. These clearly show that the address processor alternatively switches

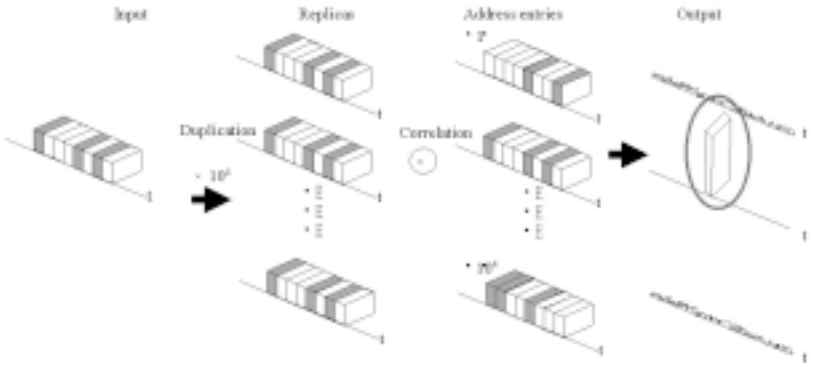

Figure 17. Parallel optical correlation for photonic label processing.

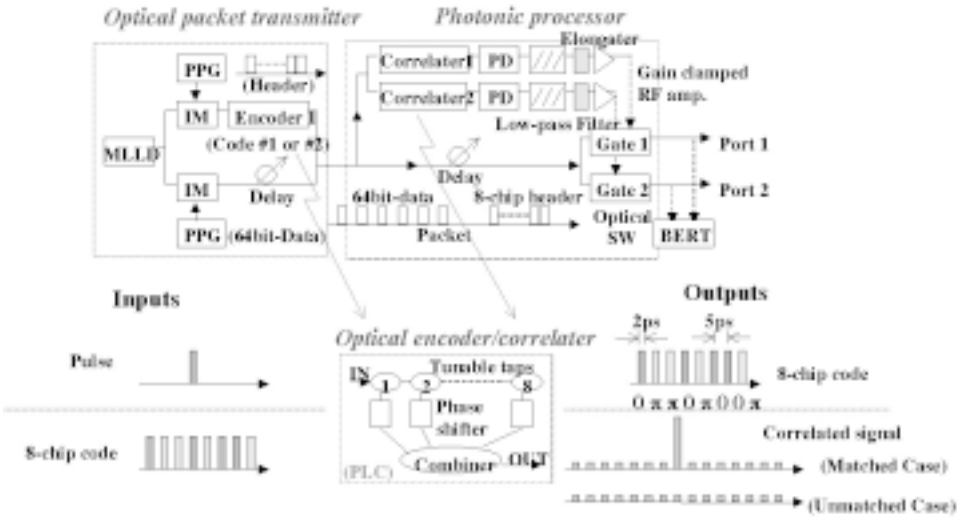

Figure 18. The experimental setup for 1 × 2 photonic label processing.

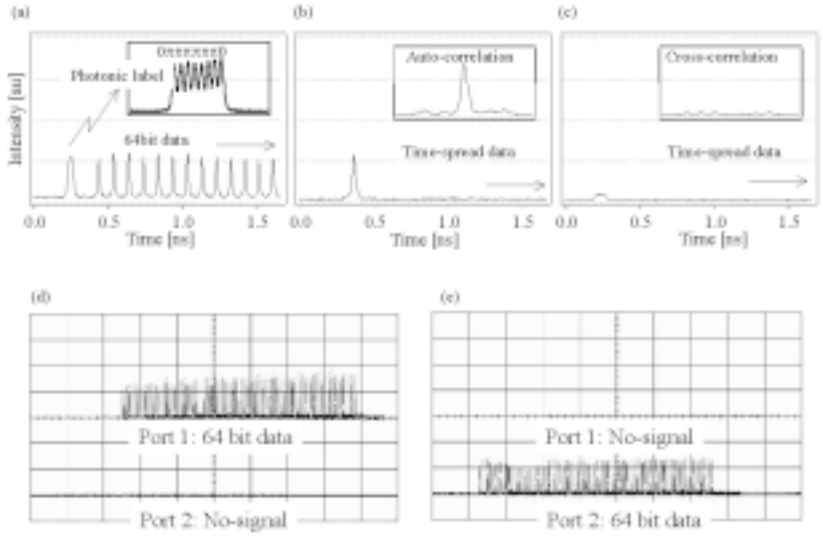

Figure 19. Streak camera traces of (a) a generated 64-bit-long packet with photonic Label #1, (b) the autocorrelation output of the packet decoded with Label #1 (matched label), (c) the cross-correlation output decoded with Label #2 (unmatched label), (d) the observed payload data at Port 1 and Port 2 for two different input labels, matched with Correlator #1 and (e) matched with Correlator #2.

two optical gates as the input optical code changes between Label #1 and #2. This means that the label processor can distinguish the eight-chip-long optical codes at the label of packets, and can control the optical switch.

The operating principle for photonic label swapping is shown in the upper part of Figure 20a. This enables converting the incoming photonic label to a desired label in the optical domain. Suppose that the label to swapped propagates, along with the control optical pulses, in an optical fiber. By use of cross phase modulation, the induced phase shift can be π. As a result, label swapping can be obtained by photonic processing. Figure 20b shows the experimental setup for photonic label swapping. Optical Encoders #2 and #3 generated a four-chip-long BPSK optical code and the control pulse, respectively. Label swapping was performed by cross phase modulation in a dispersion-shifted fiber. The output-swapped label was inspected by Correlator #3. Figure 21a shows the output of Correlator #3 without the control pulse. The signal code of [0000] and the setup of Correlator #3 are both the same, resulting in the autocorrelation trace. Figures 21b and 21c show the outputs with the control pulse for the Correlator #3 setups of [0000] and [00$\pi\pi$], respectively. The resultant cross- and auto-correlation waveforms confirm that the label was swapped by optical means. A photonic label-switching router, in which the photonic label processing is based upon optical code correlation, has been investigated. The architectures of the PLSR, including the photonic label processing, the photonic label swapping, and the optical switching, and the optical implementations of these, have been experimentally demonstrated.

The target performance of the photonic label-switching router is estimated to be multi-tera-bit/s. If we use a 32-chip-long optical code for IP routing, the processing speed of the optical correlation is 155 ps. Therefore, the processing speed of the photonic routing is 6.5 G packet per second. For a 1000-bit-long packet, the transmission capacity per wavelength can be 6.5 Tbit/s.

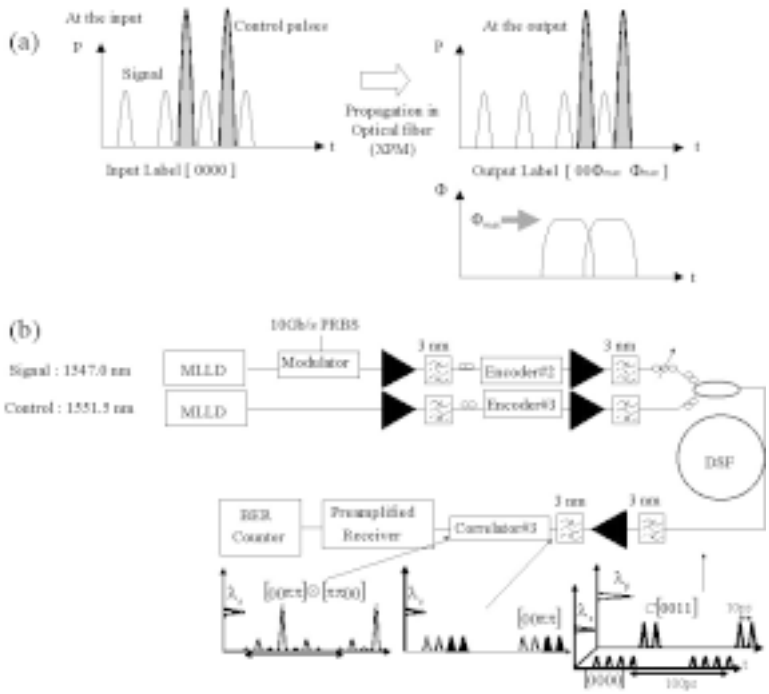

Figure 20. (a) The principle of photonic label swapping using XPM, and (b) the experimental setup for photonic label swapping.

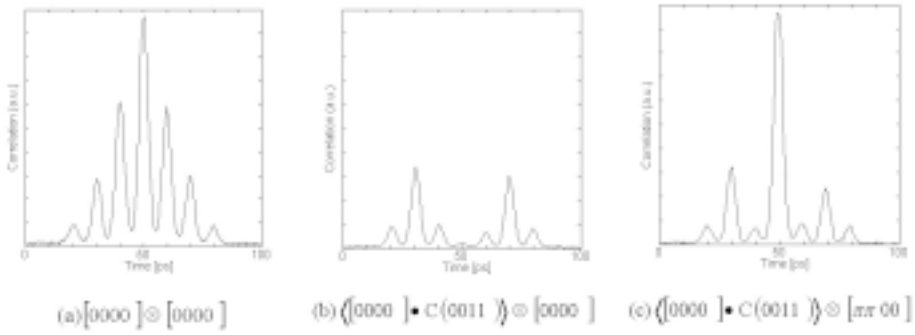

Figure 21. The output of Correlator #3 (a) without the control pulse, (b) the swapped output with the control pulse [0011], representing the cross-correlation decoded with the code sequence [0000], and (c) the swapped output with the control pulse [0011], representing the cross-correlation decoded with the code sequence [00ππ].

6. Conclusion

In this paper, ultra-fast photonic networks, based on optical code-division multiplexing, have been reviewed. The demonstrated applications of OCDM include a high-spectral-efficiency transport system, a photonic access node, optical path networks, and photonic routing. OCDM is a promising technique for future photonic networks.

7. Acknowledgement

The author wishes to thank K. Kitayama, of Osaka University, for collaborations and valuable discussions. The author also thanks T. Iida, T. Shiomi, K. Hasuike, T. Itabe, H. Fukuchi, W. Chujo, and F. Kubota of the Communications Research Laboratory for their encouragement.

8. References

1. R. C. Dixon, “Spread Spectrum Systems with Commercial Applications,” New York, Wiley-Interscience, 1994.

2. R. Dixon, “Why Spread Spectrum,” *IEEE Communications Society Magazine*, **13**, 4, 1975, pp. 21-25.

3. R. Scholtz, “The Spread Spectrum Concept,” *IEEE Transactions on Communications*, **COM-25**, 8, 1977, pp. 748-755.

4. R. Pickholtz, D. Schilling, and L. Milstein, “Theory of Spread Spectrum Communications – A Tutorial,” *IEEE Transactions on Communications*, **COM-30**, 5, 1982, pp. 855-884.

5. W. Utlaut, “Spread Spectrum: Principles and Possible Applications to Spectrum Utilization and Allocation,” *IEEE Communications Society Magazine*, **16**, 5, 1978, pp. 21-31.

6. M. Sust, “Code Division Multiple Access for Commercial Communications,” in W. Ross Stone (ed.), *Review of Radio Science 1992-1994*, Ghent, Belgium, International Union of Radio Science, 1994, pp. 155-179.

7. E. Marom, "Optical Delay Line Matched Filter," *IEEE Transactions on Circuits and Systems*, **25**, 6, 1978, pp. 360-364.

8. G. Vannucci, "Combining Frequency Division Multiplexing and Code Division Multiplexing for High Capacity Optical Network," *IEEE Network*, **3**, 2, 1989, pp. 21-30.

9. J. A. Salehi, "Code Division Multiple Access Techniques in Optical Fiber Networks I. Fundamental Principles," *IEEE Transactions on Communications*, **COM-37**, 8, 1989, pp. 824-833.

10. N. Karafolas, D. Uttamchandani, "Optical CDMA System Using Bipolar Codes and Based on Narrow Passband Optical Filtering and Direct Detection," *IEEE Photon. Technol. Lett.*, **7**, 9, 1995, pp. 1072-1074.

11. K. Kitayama, H. Sotobayashi and N. Wada, "Optical Code Division Multiplexing (OCDM) and its Application to Photonic Networks," *IEICE Transactions on Fundamentals of Electronics, Communications and Computer Sciences*, **E82-A**, 12, 1999, pp. 2616-2626.

12. H. Sotobayashi, W. Chujo, and K. Kitayama, "Optical Code Division Multiplexing (OCDM) and Its Application for Petabit/s Photonic Network," *Information Sciences*, **149**, 2003, pp. 171-182.

13. H. Sotobayashi, W. Chujo, and K. Kitayama, "1.52 Tbit/s OCDM/WDM (4 OCDM × 19 WDM × 20 Gbit/s) Transmission Experiment," *IEE Electron. Lett.*, **37**, 11, 2001, pp. 700-701.

14. H. Sotobayashi, W. Chujo and K. Kitayama, "1.6-b/s/Hz 6.4-Tb/s QPSK-OCDM/WDM (4 OCDM × 40 WDM × 40 Gb/s) Transmission Experiment Using Optical Hard Thresholding," *IEE Photon. Technol. Lett.*, **14**, 4, 2002, pp. 555-557.

15. H. Sotobayashi and K. Kitayama, "10 Gb/s OCDM/WDM Multiple Access Using Spectrum-Sliced Supercontinuum BPSK Pulse Code Sequences," Optical Amplifiers and their Applications (OAA '99), PD7, Nara, June 1999, pp. Pdp7-1-Pdp7-3.

16. K. Kitayama and M. Murata, "Photonic Access Node Using Optical Code-Based Label Processing and Its Applications to Optical Data Networking," *IEEE/OSA J. Lightwave Technol.*, **19**, 10, 2001, pp. 1401-1415.

17. K. Kitayama, "Code Division Multiplexing Lightwave Networks Based Upon Optical Code Conversion," *IEEE J. Select. Areas Commun.*, **16**, 9, 1998, pp. 1309-1319.

18. H. Sotobayashi, W. Chujo, and K. Kitayama, "Transparent Virtual Optical Code/Wavelength Path Network," *IEEE Journal of Selected Topics in Quantum Electronics*, **8**, 3, 2002, pp. 699-704.

19. H. Sotobayashi and K. Kitayama, "Optical Code Based Label Swapping for Photonic Routing," *IEICE Trans. Commun.*, **E83-B**, 10, 2000, pp. 2341-2347.

20. K. Kitayama, N. Wada, and H. Sotobayashi, "Architectural Considerations for Photonic IP Router Based Upon Optical Code Correlation," *IEEE/OSA J. Lightwave Technol.*, **18**, 12, 2000, pp. 1834-1844.

21. J. A. Salehi, A. M. Weiner, J. P. Heritage, "Coherent Ultrashort Light Pulse Code-Division Multiple Access Communication Systems," *IEEE/OSA J. Lightwave Technol.*, **8**, 3, 1990, pp. 478-491.

22. H. P. Sardesai, C. C. Chang, A. M. Weiner, "A Femtosecond Code-Division Multiple-Access Communication System Test Bed," *IEEE/OSA J. Lightwave Technol.*, **16**, 11, 1998, pp. 1953-1964.

23. H. Tsuda, H. Takemouchi, T. Ishii, K. Okamamoto, T. Goh, K. Sato, A. Hirono, T. Kutrokawa, C. Amoto, "Photonic Spectral Encoder/Decoder Using an Arrayed-Waveguide Grating for Coherent Optical Code Division Multiplexing," Optical Fiber Communication Conference Technical Digest, 1999, pp. PD32/1-PD32/3.

24. H. Tsuda, H. Takemouchi, T. Ishii, K. Okamamoto, T. Goh, K. Sato, A. Hirono, T. Kutrokawa, C. Amoto, "Spectral Encoding and Decoding of 10 Gbit/s Femtosecond Pulses Using High Resolution Arrayed-Waveguide Grating," *IEE Electron. Lett.*, **35**, 14, 1999, pp. 1186-1188.

25. P.C. Teh, P. Petropoulos, M. Ibsen, and D. J. Richardson, "Phase Encoding and Decoding of Short Pulses at 10 Gb/s Using Superstructured Fiber Bragg Gratings," *IEEE Photon. Technol. Lett.*, **13**, 2, 2001, pp. 154-156.

26. P. C. Teh, M. Ibsen, J. H. Lee, P. Petropoulos, and D. J. Richardson, "Demonstration of a Four-Channel WDM/OCDMA System using 255-chip 320-Gchip/s Quaternary Phase Coding Gratings," *IEEE Photon. Technol. Lett.*, **14**, 2, 2002, pp. 227-229.

27. K. Fukuchi, T. Kasamatsu, M. Morie, R. Ohhira, T. Ito, K. Sekiya, D. Ogasawara, and T. Ono, "10.92-Tb/s (273 × 40-Gb/s) Triple-Band/Ultra-Dense WDM Optical Repeater Transmission Experiment," *Proceedings of the Optical Fiber Communications Conference 2001 (OFC2001)*, 2002, Post-deadline paper PD24, pp. PD24-1-PD-24-3.

28. S. Bigo, Y. Frignac, G. Charlet, W. Idler, S. Borne, H. Gross, R. Dischler, W. Poehlmann, P. Tran, C. Simonneau, D. Bayart, G. Veith, A. Jourdan, and J. Hamaide, "10.2 Tbit/s (256 × 42.7 Gbit/s PDM/WDM) Transmission over 100 km TeraLight Fiber with 1.28 bit/s/Hz Spectrum Efficiency," *Proceedings of the Optical Fiber Communications Conference 2001 (OFC 2001)*, 2002, Post-deadline paper PD25, pp. PD25-1-PD-25-3.

29. T. Ono, Y. Yano, K. Fukuchi, T. Ito, H. Yamazaki, M. Yamaguchi, and K. Emura, "Characteristics of Optical Duobinary Signals in Terabit/s Capacity, High-Spectrum Efficiency WDM System," *IEEE/OSA J. Lightwave Technol.*, **16**, 1998, pp. 788-797.

30. H. Sotobayashi and K. Kitayama, "Transfer Response Measurements of a Programmable Bipolar Optical Transversal Filter by Using the ASE Noise of an EDFA," *IEEE Photon. Technol. Lett.*, **11**, 7, 1999, pp. 871-873.

31. H. Sotobayashi and K. Kitayama, "325 nm Bandwidth Supercontinuum Generation at 10 Gbit/s Using Dispersion-Flattened and Non-Decreasing Normal Dispersion Fibre with Pulse Compression Technique," *IEE Electron. Lett.*, **34**, 13, 1998, pp. 1336-1337.

32. H. Sotobayashi, C. Sawaguchi, Y. Koyamada, and W. Chujo, "Ultrafast Walk-Off Free Nonlinear Optical Loop Mirror by a Simplified Configuration for 320 Gbit/s TDM Signal Demultiplexing," *OSA Opt. Lett.*, **27**, 17, 2002, pp. 1555-1557.

33. K. Kitayama, N. Kataoka, N. Wada, and W. Chujo, "10 Gbit/s Packet-Selective Photonic Label-Based ADM Experiment, *Proceedings of the 27th European Conference on Optical Communications*, Th.L.1.6, 2001, pp. 548-549.

Recent Development of Data Processing in Polarimetric and Interferometric SAR

E. Pottier
S.R. Cloude
W.M. Boerner

Abstract

There currently is widespread interest in the development of radar sensors for the detection of surface and buried targets, and for the remote sensing of land, sea, and ice surfaces. An important feature of electromagnetic radiation is its state of polarization, and a wide range of classification algorithms and inversion techniques has recently been developed, based on the transformation of polarization state by scattering objects. There are three primary ways in which multi-parameter radar measurements can be made: multi-frequency, single or multi-baseline interferometry, and multi-polarization. While several airborne systems can now provide diversity over all three of these, it is the combination of polarimetry with interferometry at a single wavelength that forms the central focus of future challenges in developing new and original data processing. The main reason for this is the imminent launch of a series of advanced satellite radar systems, such as PALSAR, an L-band SAR sensor on board the NASDA ALOS satellite; and Radarsat II, a C-band polarimetric sensor. These are typical of a new generation of radars with the potential for providing data from various combinations of polarimetry and interferometry. This paper seeks to review recent progress in polarimetric and interferometric SAR [synthetic-aperture radar] data processing, covering advances in classification of polarimetric SAR data, and addressing the important topic of quantitative data inversion of radar data by considering applications in forest-height mapping, using polarimetric interferometry SAR data processing.

1. Introduction

SAR remote sensing allows all-weather, global-scale imaging and estimation of important biological and geophysical parameters of the Earth's surface. This is achieved by sensing scattered electromagnetic fields reflected from the Earth's surface, when emitted by an electromagnetic energy source situated on an aircraft, spacecraft, or satellite outside of the Earth's atmosphere. The development of multi-parameter SAR techniques, such as polarimetric SAR (POLSAR) and interferometric SAR (InSAR), is advancing rapidly, and these novel radar technologies are constantly extending the range of applications of radar in remote sensing.

Radar polarimetry ("polar:" polarization; "metry:" measure) is the science of acquiring, processing, and analyzing the polarization state of an electromagnetic field. The polarization information contained in the waves backscattered from a given medium is highly related to its geometrical structure and orientation, as well as to its geophysical properties, such as humidity, roughness and conductivity of soils, etc.

Radar polarimetry deals with the full vector nature of polarized electromagnetic waves, and when the wave passes through a medium of changing index of refraction, or when it strikes an object or a scattering surface and it is reflected; then, characteristic information about the reflectivity, shape, and orientation of the reflecting body can be obtained by

Eric Pottier is with the Institut d'Electronique et de Télécommunications de Rennes (IETR – UMR CNRS 6164), Université de Rennes 1, Campus de Beaulieu, Bat 11D, 263 Avenue Général Leclerc, CS30452, 35042 Rennes cedex, FRANCE;
Tel: and Fax: + (33) (0) 223 23 57 63/69 63;
E-mail: eric.pottier@univ-rennes1.fr.

Shane R. Cloude is with AEL Consultants, Granary Business Centre, CUPAR, Fife, KY15 5YQ, Scotland, UK;
Tel: and Fax: + (44) (1334) 652919/654192;
E-mail: scloude@aelc.demon.co.uk;

Wolfgang-Martin Boerner is with the University of Illinois, Chicago, ECE/CSN, m/c 154
900 W. Taylor Street, SEL-W (607) - 4210, Chicago, IL 60607-7018 USA;
Tel: and Fax: + 1 (312) 996-5480;
E-mail: wolfgang.m.boerner@uic.edu.

[Editor's note: This invited paper is the Commission F Tutorial Lecture, presented at the XXVII General Assembly of URSI in Maastricht, The Netherlands, 17-24 August, 2002.]

implementing polarization processing [1]. With radar polarimetry, the textural fine structure, target orientation and shape, symmetries, and material constituents of the Earth's surface can be recovered with considerable improvements over standard "amplitude-only radar." With radar interferometry, the spatial structure can be explored. More recently, radar interferometry has matured as an important sensing technology for topographic mapping and land classification [2]. It has been shown that important structural information relating to vegetation height and density can be obtained by combining interferograms in different polarization states [3]. It is today possible to recover such co-registered textural plus spatial properties simultaneously by combining polarimetric and interferometric SAR techniques (POL-IN-SAR). This has important consequences for the design of future space and airborne sensors for carbon sequestration and climate-change studies.

Thanks to the new polarimetric radar sensors (ENVISAT ASAR, and the future RADARSAT-2 and ALOS-PALSAR), it has now been shown that the accelerated advancement of POLSAR techniques is of direct relevance and of priority to local-to-global environmental ground-truth measurement and validation, stress assessment, and stress-change monitoring of the terrestrial and planetary covers. POLSAR remote sensing offers an efficient and reliable means of collecting the information required in order to extract the biophysical and geophysical parameters of the Earth's surface. It has found successful application in crop monitoring and damage assessment; in forestry clear-cut mapping, deforestation and burn mapping; in land-surface structure (geology), land cover (biomass), and land use; in hydrology (soil moisture, flood delineation); in sea-ice monitoring; in ocean and coastal monitoring (oil-spill detection), etc.

Today, it can be said that more and more there is a rapidly increasing interest in the use of radar polarimetry and interferometry for radar remote sensing. Wave polarization is today of fundamental importance in the information-retrieval problem of microwave imaging and inverse scattering.

2. Polarimetric SAR Data Processing

2.1 Introduction

There currently is a great deal of interest in the use of polarimetry for radar remote sensing, and for the classification of Earth terrain components. Using a fully polarimetric SAR (POLSAR) image is one of the many important qualitative applications of radar polarimetry. In this context, an essential objective is to extract physical information from the observed scattering of microwaves by surface and volume structures. A most ground-braking development in our understanding of how to best extract physical information from the classical 2×2 coherent backscattering matrix $[S]$ has been achieved through the construction of the 3×3 coherency matrix $[T]$. $[T]$ accounts for local variations in the scattering matrix, and is the lowest-order operator suitable for extracting polarimetric parameters for distributed scatterers in the presence of additive (system) and/or multiplicative (speckle) noise [4]. Very remarkable improvements above classical "*non-polarimetric*" radar target detection, recognition, discrimination, and identification were made, especially with the introduction of the full polarimetric optimization procedures of Tragl, Novak et al., Lüneburg, Cloude, and of Cloude and Pottier [1, 4, 5]. Special attention must be placed on the "Cloude-Pottier Polarimetric Entropy (H), Anisotropy (A), Feature-Angle ($\underline{\alpha}$) parametric decomposition," because it allows for unsupervised target-feature interpretation [4]. Using the various fully polarimetric (scattering-matrix) target-feature syntheses, polarization contrast optimization, and polarimetric entropy/anisotropy classifiers, very considerable progress was made in interpreting and analyzing POLSAR image features. This includes the reconstruction of "*Digital Elevation Maps (DEMs)*" directly from POLSAR covariance-matrix image data takes, next to the familiar method of DEM reconstruction from IN-SAR image data takes [6-9]. Implementation of the "J. S. Lee Filter" for speckle reduction in polarimetric SAR image reconstruction [10-12], and of the polarimetric Wishart distribution for improving image-feature characterization [13-16], have fur-

Figure 1. The optical image (left), polarimetric color-coded image (center), and interferometric coherence (right) over Oberpfaffenhofen (Germany).

ther contributed toward enhancing the interpretation and display of high-quality SAR imagery, again requiring fully calibrated SLC-formatted POL-IN-SAR image data takes. Polarimetric SAR data classification has been widely addressed in the last decade [13, 17-20]. The tight relationship between natural-media physical properties and their polarimetric features leads to highly descriptive classification results, which can be interpreted by analyzing underlying scattering mechanisms [21, 22]. Interferometric data provide information concerning the coherence of the scattering mechanisms, and can be used to retrieve observed media structures and complexity [3, 23]. An example of the complementary aspect of polarimetric and interferometric information is given with polarimetric interferometric data acquired by the DLR E-SAR sensor at L band in repeat-pass mode, with a baseline of 10 m (see Figure 1).

The Oberpfaffenhofen scene (Germany, Figure 1) is composed of various agricultural areas, forests, and urban zones. The polarimetric color-coded image and a coherence image give different descriptions of the observed scene. It can be observed from a careful study of [24] that, in general, forests have a uniform polarimetric behavior, while the interferometric coherence shows large variations. On the other hand, some surfaces have similarly high interferometric coherence, while the polarimetric image depicts different scattering mechanisms. This part of the paper proposes a review of the most recent developments concerning statistical segmentation of POLSAR data, and introduces the different unsupervised classification procedures, based on the *Cloude and Pottier* decomposition theorem [21], and on the multivariate Wishart density function.

2.2 Unsupervised Classification of Polarimetric SAR Data

Many targets of interest in radar remote sensing require a multivariate statistical description, due to the combination of coherent speckle noise and random vector scattering effects from surface and volume. For such targets, it is of interest to generate the concept of an average or dominant scattering mechanism, for the purposes of classification or inversion of scattering data.

In 1997, S. R. Cloude and E. Pottier [4, 21] proposed a method for extracting average parameters from experimental data, using a smoothing algorithm based on second-order statistics. This original method, based on an eigenvalue analysis of the coherency matrix, employs a three-level Bernoulli statistical model to generate estimates of the average target-scattering-matrix parameters. This method does not rely on the assumption of a particular underlying statistical distribution, and so is free of the physical constraints imposed by such multivariate models.

An unsupervised classification scheme has been introduced [4, 21], based on the use of the two-dimensional $H/\underline{\alpha}$ classification plane, where all random-scattering mechanisms can be represented. This $H-\underline{\alpha}$ plane is subdivided into eight basic zones, characteristic of different scattering behaviors. The different class boundaries have been determined so as to discriminate surface scattering (ODD), volume diffusion (VOL), and double-bounce scattering (DBL) along the $\underline{\alpha}$ axis, and low, medium, and high degrees of randomness along the entropy axis. Detailed explanations, examples, and comments concerning the different classes can be found in [21]. This unsupervised estimation of the type of scattering mechanisms may reach some limitations, due to the arbitrarily fixed linear decision boundaries in the $H-\underline{\alpha}$ plane, which may not fit the data distribution, leading to noisy classification results. The use of other indicators, such as the span or specific correlation coefficients, may improve the classification results in a significant way.

In 1994, *J.S. Lee et al.* [13] developed a supervised algorithm based on the complex Wishart distribution for the polarimetric covariance or coherency matrix. This is given by

$$P\left(\langle[T]\rangle/[T_m]\right)=\frac{L^{Lp}\left|\langle[T]\rangle\right|^{L-p}e^{-L\,Tr\left([T_m]^{-1}\langle[T]\rangle\right)}}{\pi^{\frac{p(p-1)}{2}}\Gamma(L)\ldots\Gamma(L-p+1)\left|[T_m]\right|^{L}} \quad (1)$$

where L is the number of looks and p is the dimension of the target vector, $\underline{k}$, with $p=3$ for the reciprocal case ($S_{HV}=S_{VH}$), and $p=4$ for the non-reciprocal case. $[T_m]$ is the feature coherency matrix of the mth class.

This supervised algorithm is a maximum-likelihood classifier, based on the complex Wishart distribution for the polarimetric coherency matrix. Each class is characterized by its own feature coherency matrix, $[T_m]$, which is estimated using training samples from the mth class: ω_m. According to the Bayes maximum-likelihood classification procedure, an averaged coherency matrix, $\langle[T]\rangle$, is assigned to the class ω_m, if

$$\langle[T]\rangle\in[T_m] \text{ if } d_m\left(\langle[T]\rangle\right)<d_j\left(\langle[T]\rangle\right),\ \forall j\neq m,$$

with

$$d_m\left(\langle[T]\rangle\right)=Tr\left([T_m]^{-1}[T]\right)+\ln\left(\left|[T_m]\right|\right)\cdot \quad (2)$$

This relation shows that if the number of looks (L) increases, the a priori probability, $P\left([T_m]\right)$, of the class ω_m plays less of a role for the classification. It is generally assumed that without a priori knowledge, the different $P\left([T_m]\right)$ are equal, in which case the distance measure is not a function of the number of looks, (L).

Usually, to implement the classification, the coherency matrix, $[T_m]$, is estimated using pixels within differ-

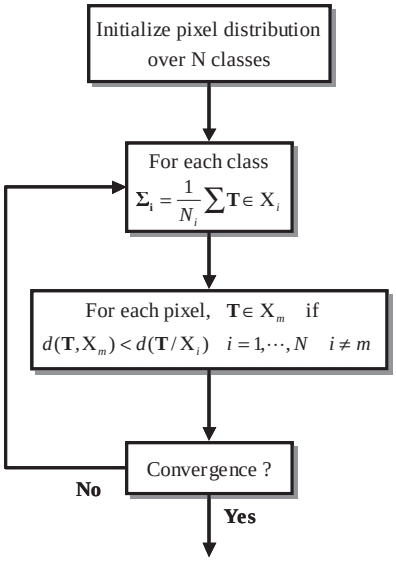

Figure 2. The unsupervised maximum-likelihood segmentation scheme.

ent selected areas of the *m*th class, and data are then classified pixel by pixel. These different training sets have to be selected in advance. For each pixel, represented by the averaged coherency matrix, $\langle [T] \rangle$, the distance $d_m(\langle [T] \rangle)$ is computed for each class, and the class associated to the minimum distance is assigned to the pixel. During the procedure, each feature coherency matrix $[T_m]$ is iteratively updated from the initial estimate. This iterative procedure, based on a distance measure, similar to the *k*-mean method, is simple and easy to apply. In addition, this algorithm, based on the Wishart distribution, uses the full polarimetric information. Figure 2 depicts the unsupervised segmentation process.

In 1998, J. S. Lee et al. [14] proposed an unsupervised classification method that uses the $H/\underline{\alpha}$ classification plane to initially classify the polarimetric SAR image. As mentioned previously, the supervised algorithm based on the complex Wishart distribution needs different training sets to initialize the procedure. These training sets, selected in advance, require from the user an a priori knowledge of the different significant Earth terrain components, which can be found in the POLSAR image. The most important development was to propose a combined unsupervised classification that uses the polarimetric $H/\underline{\alpha}$ decomposition and the supervised Wishart classifier.

Cluster centers are then initialized with the results of the unsupervised polarimetric $H/\underline{\alpha}$ decomposition of a scattering mechanism. This initialization provides eight classes relating to the underlying physical scattering mechanism, giving a stable initial approximation of the segmentation. Each pixel in the whole image is then reclassified by applying the distance-measure procedure, and the classification procedure stops when a termination criterion, defined by the user, is met. The termination criterion used is the number of iterations, and is here equal to four. In this case, the ratio of pixels switching class with respect to the total pixel number is smaller than 10%. Results obtained using Wishart $H-\underline{\alpha}$ segmentation are displayed in Figure 3. The main kinds of natural media are clearly discriminated by the Wishart $H-\underline{\alpha}$ segmentation scheme. This unsupervised classification algorithm modifies the decision boundaries in an adaptive way to better fit the data distribution, and takes into account information related to the back-scattered power. The entire original unsupervised Wishart classification procedure, proposed by J. S. Lee et al., and a discussion about the improvement in classification, can be found in [14]. The identification of the terrain type directly from the analysis of the classified image may cause some confusion, due to the color scheme. Indeed, during the classification, the cluster centers in the two-dimensional $H/\underline{\alpha}$ plane can move out of their zones, or several clusters may end in the same zone. This is due to the fact that the zone boundaries were set somewhat arbitrarily, as mentioned previously.

In order to improve the capability to distinguish between different classes that have cluster centers ending in the same zone, in 2000, E. Pottier and J. S. Lee proposed to extend and complement the combined Wishart classifier with the introduction of the anisotropy (A) information [15]. This polarimetric indicator is particularly useful for discriminating scattering mechanisms with different eigenvalue distributions but with similar intermediate entropy values. In such cases, a high anisotropy value indicates two dominant scattering mechanisms with equal probability and a less significant third mechanism, while a low anisotropy value corresponds to a dominant first scattering mechanism and two non-negligible secondary mechanisms with equal importance. Polarimetric data are first segmented according to the algorithm presented previously. Once this procedure has converged, the eight resulting clusters are

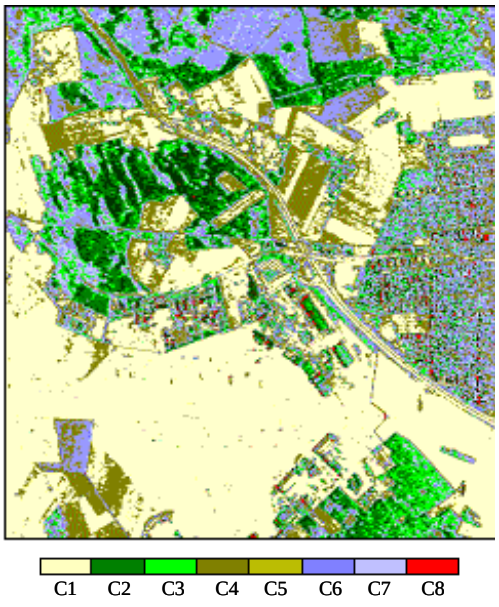

Figure 3. Wishart $H-\underline{\alpha}$ segmentation results.

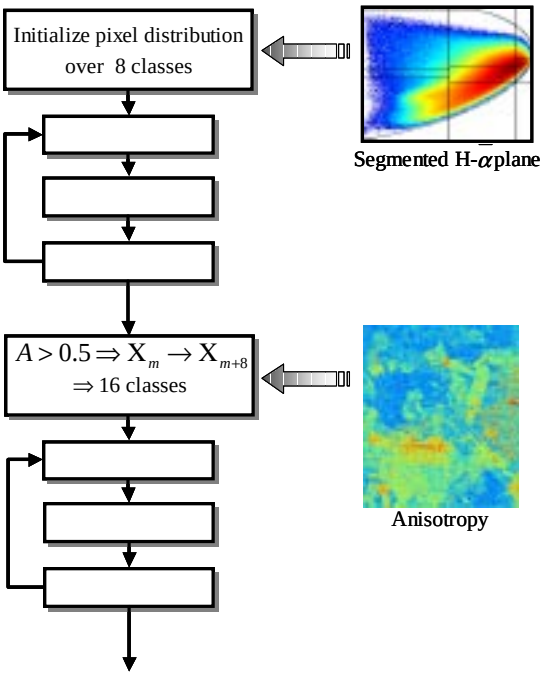

Figure 4. A synopsis of the Wishart $H-A-\underline{\alpha}$ segmentation procedure.

Figure 5. Wishart $H-A-\underline{\alpha}$ segmentation results.

split into 16 clusters by comparing the anisotropy of each pixel to a threshold fixed to 0.5. The 16 segments are then used to initialize a second Wishart ML segmentation procedure. Figure 4 depicts the synopsis of the Wishart $H-A-\underline{\alpha}$ segmentation procedure. The segmentation results presented in Figure 5 show improvements in classification, and an enhanced description of the Oberpfaffenhofen scene. The introduction of the anisotropy in the clustering process permits splitting large segments into smaller clusters, discriminating small disparities in a refined way, and more details can then be observed. Some classes, indistinguishable in the classification based on entropy (H) and alpha angle ($\underline{\alpha}$) are now clearly visible with the introduction of the anisotropy information [15]. This classification scheme does not provide any information concerning the nature of the scattering mechanism associated with each cluster, and the analysis of the final cluster centers in the three-dimensional $H/A/\underline{\alpha}$ classification space may provide a more precise interpretation of the different classes of terrain types.

2.3 Basic Identification of Canonical Scattering Mechanisms

An efficient estimation of the nature of scattering mechanisms over natural scenes can be achieved by gathering results obtained from the polarimetric decomposition and segmentation procedures presented previously. By analyzing groups of scatterers, the identification of the polarimetric properties of compactly segmented clusters permits reducing the influence of the variability of polarimetric indicators encountered over natural media. The estimation of global properties provides an accurate interpretation of the observed scene's nature and structure. Volume diffusion and double-bounce scattering were found to be over-estimated during the identification of scattering mechanisms using the $H-\underline{\alpha}$ segmented plane. One of the reasons for this over-estimation resides in the calculation of

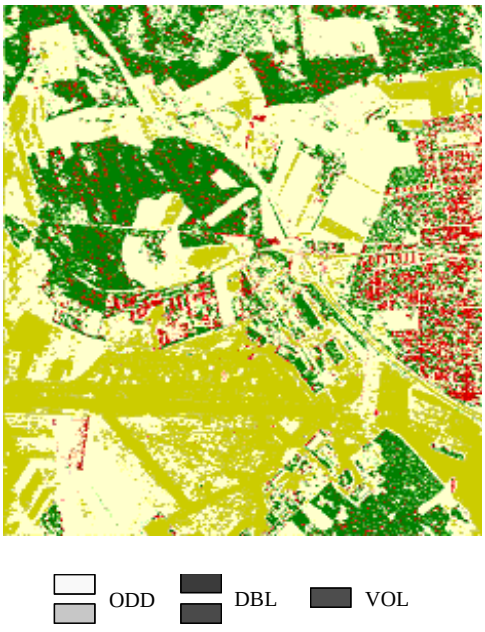

Figure 6. The selection of significant mechanisms and identification with canonical scattering mechanisms (ODD: single-bounce scattering; DBL: double-bounce scattering; VOL: volume diffusion).

the average parameters of the polarimetric decomposition. In some cases, the expansion of a coherency results in a dominant scattering mechanism and secondary mechanism showing very different polarimetric properties. The calculation of average indicators as the weighted sum of the indicators of each element of the expansion may then lead to an erroneous interpretation of the nature of the scattering mechanism. Recently, a new identification approach was proposed [16], based on the discrimination from the $H-\underline{\alpha}$ plane of the number of significant mechanisms occurring in each pixel of the POLSAR image. The selection of the relevant mechanisms and identification with canonical-scattering-mechanism results are shown in Figure 6.

This simple and basic identification procedure shows a good discrimination of the three basic scattering mechanisms over the scene under consideration. Forested areas are well separated from the rest of the scene. Buildings, characterized by double-bounce scattering, can be distinguished over the urban area and the DLR Institute. It may be noted that the identification assigns some buildings to the volume-diffusion class. The polarimetric properties, as well as the power-related information, do not permit separating these targets from forests. Such buildings, with particularly rough roofs, present specific orientations with respect to the radar line of sight that may cause a random backscattering effect. This limitation can be solved when applying an unsupervised classification process to each canonical scattering mechanism, gathering polarimetric and interferometric results [16]. This new approach shows significant improvements, compared to the strictly polarimetric case. Clear-cuts, sparse, and dense forests are separated according to their coherent properties, and, in particular, buildings having a polarimetric behavior similar to forest are then discriminated.

3. Polarimetric SAR Interferometry Data Processing

3.1 Introduction

One of the very latest developments has addressed polarimetric radar interferometry. This is now a mature technology for remote sensing, since airborne sensors are now capable of reliable repeat-pass interferometric measurements.

Radar interferometry was initially developed initially as a technique for measuring surface topography. Here, the interferometric phase is the key radar observable, and this phase can be simply related to the local elevation of a scattering point above a reference plane, through the geometry of the sensor. To a first approximation, it can be assumed that the speckle phase for the two signals at either end of the baseline is strongly correlated. A deterministic phase signal, related to the topography, can then be extracted from the phase difference. In these early studies, any residual phase variance was perceived primarily as a nuisance, acting to reduce the accuracy of the terrain-elevation model [2]. However, it was quickly realized that the local phase variance – or a closely related parameter, the interferometric coherence – contains information about the scattering mechanisms on the surface. This realization arose following a decomposition of the complex coherence into a product of terms. Most of these terms are related to system bandwidth and geometry effects. However, one of them, the volume decorrelation, contains important information on penetration depth in vegetation, ice, and ground applications. This had two important consequences for the development of interferometric methods in remote sensing. First, the change of coherence over vegetated areas provides a means for scene classification based on vegetation cover. It was also noted that as the vegetation height increases, the coherence generally decreases. Hence, this provided a means of classifying vegetation on the basis of its height. Second, unlike other sources of decorrelation, the volume coherence is complex, i.e., it has an associated phase. This phase adds to that of the underlying ground topography to provide what is called vegetation bias [23, 25, 26]. This bias is a nuisance if ground mapping is the desired aim of the processing. However, this phase offset itself contains important information about the density and height of the vegetation. This, when combined with the coherence, provides two parameters that are directly related to the vertical structure of the vegetation cover on the surface [3, 23, 26, 27].

In this part, we review recent developments in the use of polarimetric radar interferometry for tree-height estimation, which is today a key point in the remote sensing of global vegetation cover and biomass.

The structure of vegetation is a key ecosystem factor, which reflects biomass stock successions and growth dynamics. Parameters such as tree height, crown width, stand and canopy density, and the underlying ground topography are direct inputs into biomass-determination models, and enable ecological process modeling, forest inventory, and predictive modeling in hydrology. It should also be pointed out that global forest inventory and forest (above-ground) biomass are currently critical missing parts in the global climate-change debate. Hence, there is a need for a reliable remote-sensing technique to provide such information, and for developing alternate POLInSAR feature-extraction algorithms, such as that of [27].

By operating at longer wavelengths, such as L and P bands, polarimetric radar interferometry [3, 23] is well suited to this problem. It provides penetration into vegetation cover and the ground and, hence, is inherently sensitive to volume effects. It provides vertical-structure information on a scale not easily available from optical or laser sensors. This technology promises to provide the basis for important new radar remote-sensing instruments for global biomass and vegetation mapping [28].

3.2 Polarimetric Interferometric Coherence Optimization Procedure

Polarimetric radar interferometry is a sensor technology measuring the full scattering matrix at either end of the baseline [2, 3, 26, 27]. The polarimetric interferometric behavior of a target is then fully described by the two scattering matrices, $[S_1]$ and $[S_2]$. A six-element complex target vector, $\underline{\mathbf{k}}_{\mathbf{6}}$, can be obtained by stacking target vectors from each polarimetric image, gathering the polarimetric interferometric information into a compact representation [3, 23]. The corresponding 6 × 6 interferometric coherency matrix is given by

$$[\mathbf{T_6}] = \frac{1}{n}\sum_{n} \underline{\mathbf{k}}_{\mathbf{6}} \underline{\mathbf{k}}_{\mathbf{6}}^{\dagger}, \tag{3a}$$

with

$$\underline{\mathbf{k}}_{\mathbf{6}} = \begin{bmatrix} \underline{\mathbf{k}}_{\mathbf{1}} \\ \underline{\mathbf{k}}_{\mathbf{2}} \end{bmatrix} \tag{3b}$$

and

$$\underline{\mathbf{k}}_{\mathbf{i}} = [k_{i1}, k_{i2}, k_{i3}]^T . \tag{3c}$$

This coherency matrix has the following structure:

$$[\mathbf{T_6}] = \begin{bmatrix} [\mathbf{T_{11}}] & [\Omega_{\mathbf{12}}] \\ [\Omega_{\mathbf{12}}^{\dagger}] & [\mathbf{T_{22}}] \end{bmatrix}, \tag{4a}$$

with

$$[\Omega_{\mathbf{12}}] = \frac{1}{n}\sum_{n} \underline{\mathbf{k}}_{\mathbf{1}} \underline{\mathbf{k}}_{\mathbf{2}}^{\dagger} . \tag{4b}$$

The leading diagonal blocks are the conventional Hermitian coherency matrices. In applications, interest centers on exploitation of the off-diagonal block $[\Omega_{\mathbf{12}}]$, which is the 3 × 3 complex polarimetric cross-correlation matrix. As the target vector $\underline{\mathbf{k}}_{\mathbf{6}}$ follows a complex normal zero-mean distribution, $N_C(\mathbf{0}, [\Sigma_{\mathbf{6}}])$, with $[\Sigma_{\mathbf{6}}]$ its 6 × 6 covariance matrix, the 6 × 6 coherency matrix $[\mathbf{T_6}]$ then has a complex Wishart distribution, $W_C(n, [\Sigma_{\mathbf{6}}])$, characterized by n degrees of freedom [29, 30]. The interferometric cross-correlation matrix, $[\Omega_{\mathbf{12}}]$, has complex diagonal elements, from which are computed the three polarimetric complex coherences, as follows:

$$(\gamma_1, \gamma_2, \gamma_3), \tag{5a}$$

with

$$\tilde{\gamma}_i = \gamma_i e^{j\phi_i} = \frac{\left\langle k_{1i} k_{2i}^{*} \right\rangle}{\sqrt{\left\langle k_{1i} k_{1i}^{*} \right\rangle \left\langle k_{2i} k_{2i}^{*} \right\rangle}}, \tag{5b}$$

where the operator $\langle\ \rangle$ stands for averaging over the n samples represented in Equation (4). Standard real coherence values are obtained from γ_i, while the arguments correspond to the interferometric phase difference. It may be noted that the coherence defined in Equation (5) is not invariant under a change of polarimetric basis. In general, coherence may be decomposed into multiplicative contributions as follows [3, 23]:

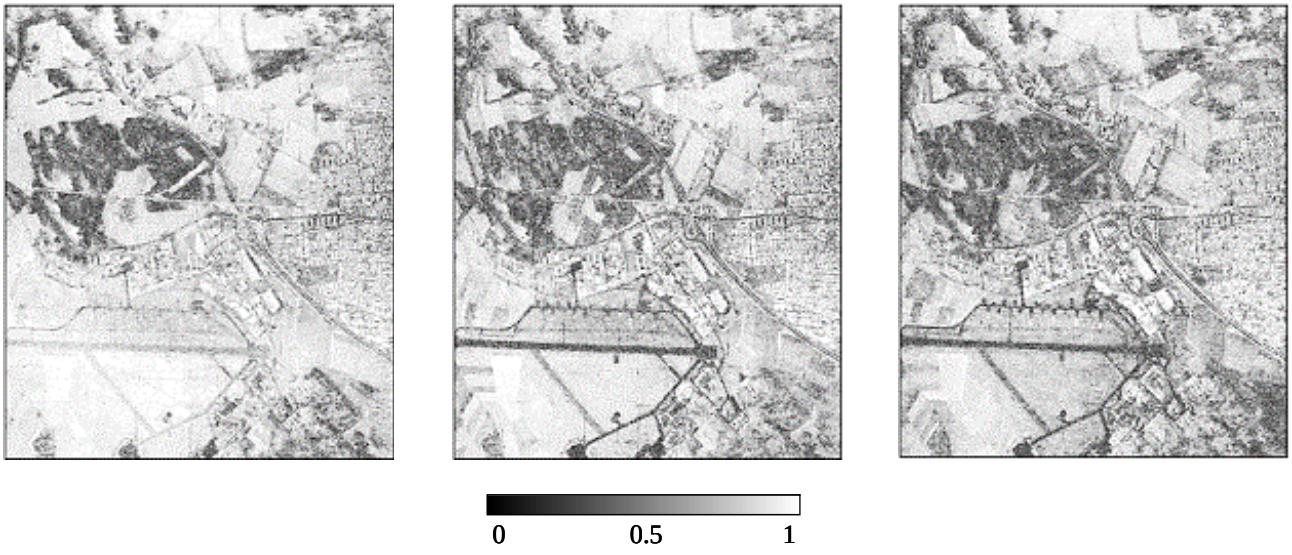

Figure 7. Interferometric coherences for the different polarimetric channels in the Pauli basis.

$$\tilde{\gamma} = \tilde{\gamma}_{SNR} \cdot \tilde{\gamma}_{spatial} \cdot \tilde{\gamma}_{temporal} \cdot \tilde{\gamma}_{polar} , \qquad (6)$$

where the different terms indicate decorrelations related, respectively, to the back-scattered wave signal-to-noise ratio (SNR), the spatial distribution of the illuminated scatterers, temporal variations between the acquisitions, and, finally, the polarization state. Coherence images for the different polarization channels are displayed in Figure 7.

Range-filtering and topographic phase-removal procedures are applied to the interferometric data sets, prior to the computation of the polarimetric interferometric coherences. The range-filtering procedures correct wavenumber shifts inherent in interferometric measurements. High coherence values are observed for surface areas in the co-polarized channels. Smooth surfaces, like the runway, scatter waves in the radar direction with a low signal-to-noise ratio, involving a low coherence in every polarization channel. In a general way, the maximum of the three-coherence set corresponds to the first or second channel, according to the dominant scattering mechanism, i.e., single- or double-bounce reflection, respectively. Over forested areas, all three coherencies have low values.

The off-diagonal complex polarimetric cross-correlation matrix $[\Omega_{12}]$ contains low-variance differential phase information, related to the height separation of scattering centers. Rather than fusing the two data sets, Cloude and Papathanassiou [3, 23] have introduced polarization filters that minimize the variance of this phase information, to locate as accurately as possible the position of the scattering center. With full polarimetric interferometry, it is then possible to select in the post processing the $\underline{w}$ vectors that maximize the coherence or minimize this phase variance, as eigenvectors of a matrix formed from sub-matrices of $[\mathbf{T_6}]$, and defined from Equation (4):

$$\tilde{\gamma} = \gamma e^{i\phi} = \frac{\underline{w}_1^{*T} [\Omega_{12}] \underline{w}_2}{\sqrt{\underline{w}_1^{*T} [T_{11}] \underline{w}_1 \underline{w}_2^{*T} [T_{22}] \underline{w}_2}} , \qquad (8)$$

with

$$\left.\begin{aligned} [T_{22}]^{-1} [\Omega_{12}]^{*T} [T_{11}]^{-1} [\Omega_{12}] \ \underline{w}_2 = \lambda \underline{w}_2 \\ [T_{11}]^{-1} [\Omega_{12}] [T_{22}]^{-1} [\Omega_{12}]^{*T} \ \underline{w}_1 = \lambda \underline{w}_1 \end{aligned}\right\}$$

$$\Rightarrow 0 \le \lambda = \gamma_{opt}^2 \le 1 , \qquad (9)$$

where the corresponding eigenvalues are the three solutions to this optimization problem, and, also, the squared value of the optimum coherences. The vector corresponding to the maximum eigenvalue is the lowest-phase-variance solution. However, there is also important information in the remaining channels, concerning the height and density of vegetation cover on the ground [24, 31].

The results of the optimization procedure presented in Figure 8 show an enhanced contrast between the different optimal coherences. The first optimal coherence has values close to one over the major part of the scene considered, and intermediate values over forested areas and low SNR targets. The third optimal coherence shows minimum values over decorrelating media, such as forest and smooth surfaces, and reaches high values for a limited amount of very coherent point scatterers. The complete optimized coherence set represents a highly descriptive indicator of the polarimetric interferometric properties of each natural medium. It provides the basis for efficient height estimation, and great potential in biomass applications [32].

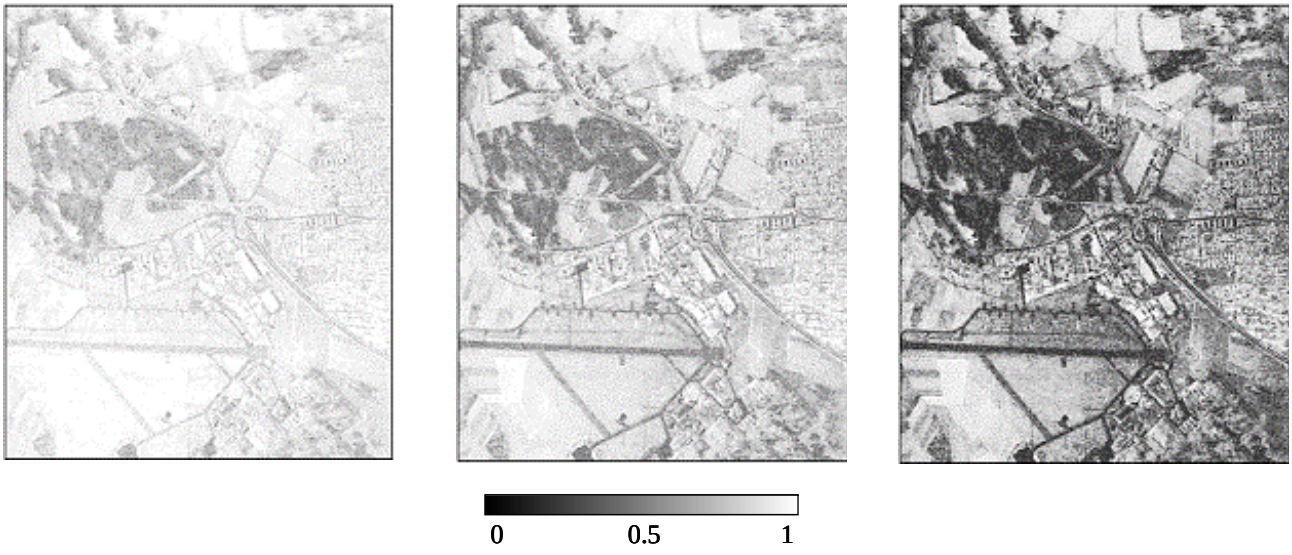

Figure 8. Optimal interferometric coherences.

3.3 A Quantitative Data-Inversion Application: The Tree-Height Estimation

To extract the tree-height information, we have to consider how to model the physical structure of scattering problems in the coherency matrix. Different algorithms have been proposed and based on a two-layer coherence model, accounting for the effects of ground scattering on the observed coherence [23, 26, 32]. To obtain an accurate and efficient height estimation, it is important to take into account different physical and complicated factors in the model. These are the effect of wave extinction due to propagation through the volume; the effect of ground scattering due to the penetrating properties of microwaves through the volume; and, at last, the effect of the Earth's topography, the variations of which modulate the phase of the interferogram, and are combined with the vegetation-bias offset to provide a mixed-phase signal. These three effects mean that we face at least a four-parameter estimation problem in the inversion scheme. Not surprisingly, this inversion is non-unique for a single-channel interferometer, and so a multi-parameter interferometer approach is required. Various solutions have been suggested to this problem, including dual-frequency, multi-baseline, and tomographic processing. Cloude and Papathanassiou, who have shown that the only single-baseline, single-wavelength proposal has been through polarimetric radar interferometry, have proposed the most important recent development in this topic [23, 31]. The physical model proposed is based on the analysis of the observed interferometric coherences, which are, for vegetated terrain, a mixture of volume and surface contributions. Cloude et al. [33-36] have shown that the optimum coherence values, obtained from Equation (9), can be written in terms of the underlying ground topographic phase (ϕ), the coherence of the random volume (γ_v) in the absence of the ground, and the three solutions (μ_1, μ_2, μ_3) of the contrast-optimization problem between the random volume component and the reflection-symmetric ground component of the volume coherency model. From the three optimum coherence values – which lie along a line inside the unit circle of the complex coherence plane [31, 36] – Cloude and Papathanassiou have then proposed a simple quantitative data inversion, which provides an efficient physical estimation of the different vegetation parameters. The relative simplicity of this model follows from the assumption of azimuthal symmetry in the volume-scattering component. This assumption has already been validated for L-band data

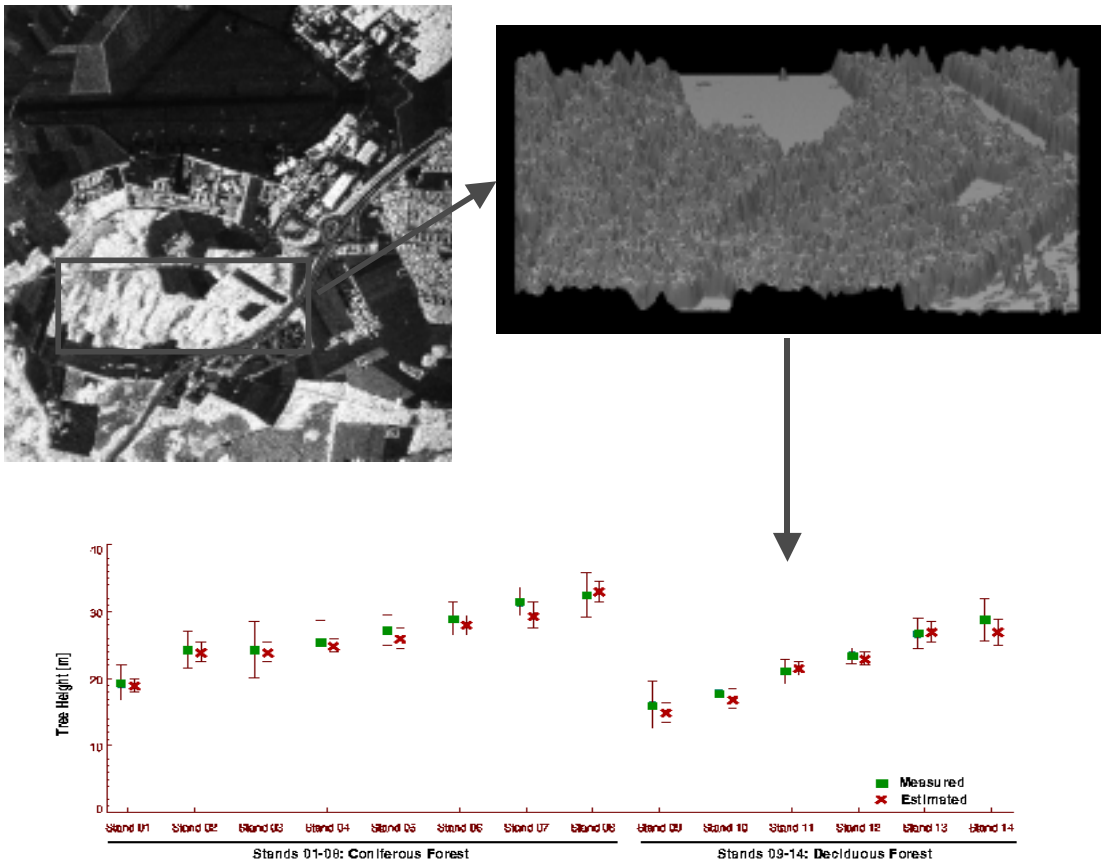

Figure 9. Tree-height estimation using L-band repeat-pass POLInSAR data from the DLR E-SAR system.

over different forest sites in Germany and Scotland [37], using the DLR E-SAR airborne radar system. The validation was carried out versus ground-truth measurements of tree heights, and also through vector SAR tomography [25, 38].

Figure 9 shows an example for mixed pine/ deciduous forest in the Oberpfaffenhofen scene (taken from reference [23]). On the left, we show an L-band SAR image, with the forest stand highlighted. On the right, we show a three-dimensional tree-height map, derived directly from the POLInSAR radar data. In the lower part of the figure, we show a quantitative comparison between the radar-estimated tree height and in-situ measurements across 14 different stands. We see good general agreement, demonstrating that single-baseline POLInSAR is capable of large-area mapping of tree height with accuracies around 10%. Recently, more-robust simplified algorithms have been developed for estimating tree height from POLInSAR data [27, 39], and studies have commenced on the design of space-based sensors suitable for global-scale mapping [40]. Future work is now centered on the use of multi-baseline and dual-wavelength POLInSAR sensors for the estimation of vertical structure in forestry applications, as well as on the application of single-baseline techniques to new applications in agriculture and ice-thickness monitoring.

4. Conclusion

In this paper, we have reviewed the most recent progress in polarimetric and interferometric SAR data processing. We have covered advances in the classification of polarimetric SAR data. We addressed the important topic of quantitative data inversion of radar data, by considering applications in forest-height mapping using polarimetric interferometry SAR data processing.

Recent developments of wave-polarization effects in radar remote sensing were summarized in historical sequence, resulting in radar polarimetry, radar interferometry, and polarimetric SAR interferometry, which represent the current culmination in airborne and space-borne "microwave remote sensing" technology.

There have been several significant developments in radar polarimetry and interferometry during the last decade, and these are continuing as we move into the new millennium. These novel technologies are making decisive and definitive changes to our understanding of "synthetic aperture radar imaging," and its applications in remote sensing.

Whereas with radar polarimetry, the textural fine-structure, target orientation, symmetries, and material constituents can be recovered with considerable improvement above that of standard "*amplitude-only*" radar, by implementing "*radar interferometry*," the spatial structure can be explored. With polarimetric interferometric SAR (POLINSAR) imaging, it is possible to simultaneously recover such co-registered textural and spatial information from POL-IN-SAR digital-image data sets.

Today, there exists a great deal of interest in the use of the potential of radar technology to provide day/night, all-weather quantitative height estimates for use in important forestry applications, such as biomass estimation and ecology studies. This is achieved by using radar interferometry with polarization diversity, a combination that is well suited to single-pass airborne as well as satellite-based global-mapping applications.

With the advent of fully operational polarimetric satellite radars (ALOS-PALSAR, Radarsat II, TerraSar-X, and ENVISAT) over the next few years, we expect future innovative and original data-processing approaches to provide the basis for many new products and services of interest to the scientific and application communities.

5. References

1. W. M. Boerner et al., "Polarimetry in Remote Sensing: Basic and Applied Concepts," in F. M. Henderson and A. J. Lewis (eds.), *Manual of Remote Sensing, Volume 8, Third Edition*, New York, Wiley, 1998, Chapter 5.

2. R. Bamler and P. Hartl, "Synthetic Aperture Radar Interferometry," *Inverse Problems*, **14**, 1998, R1-R54.

3. S. R. Cloude and K. P. Papathanassiou, "Polarimetric SAR Interferometry," *IEEE Transactions on Geoscience and Remote Sensing*, **GRS-36**, 5, September 1998, pp. 1551-1565.

4. S. R. Cloude and E. Pottier, "A Review of Target Decomposition Theorems in Radar Polarimetry," *IEEE Transactions on Geoscience and Remote Sensing*, **GRS-34**, 2, March 1996, pp. 498-518.

5. W. M. Boerner and Y. Yamaguchi, "Extra Wideband Polarimetry, Interferometry and Polarimetric Interferometry in Synthetic Aperture Remote Sensing," *IEICE Trans. Commun.*, **E83-B**, 9, September 2000, pp. 1906-1915.

6. D. L. Schuler, J. S. Lee, and G. De Grandi, "Measurement of Topography using Polarimetric SAR Images," *IEEE Transactions on Geoscience and Remote Sensing*, **GRS-34**, 5, 1996, pp. 1266-1277.

7. E. Pottier, "Unsupervised Classification Scheme and Topography Derivation from POLSAR Data Based on the H/A/a Polarimetric Decomposition," *Proceedings of 4th International Workshop on Radar Polarimetry (JIPR '98)*, IRESTE, University of Nantes, France, July 1998, pp. 535-548.

8. E. Pottier, D. L. Schuler, J. S. Lee, and T. Ainsworth, "Estimation of Terrain Surface Azimuthal/Range Slopes using Polarimetric Decomposition of POLSAR Data," IEEE International Geoscience and Remote Sensing Symposium, Hamburg, 28 June - 2 July, 1999.

9. J. S. Lee, D. L. Schuler, and T. L. Ainsworth, "Polarimetric SAR Data Compensation for Terrain Azimuth Slope Variation," *IEEE Transactions on Geoscience and Remote Sensing*, **GRS-38**, September 2000, pp. 2153-2163.

10. L. Novak and M. C. Burl, "Optimal Speckle Reduction in Polarimetric SAR Imagery," *IEEE Transactions on Aerospace and Electronic Systems*, **26**, March 1990, pp. 293-305.

11. J. S. Lee, K. W. Hoppel, S. A. Mango, and A. Miller, "Intensity and Phase Statistics of Multi-Look Polarimetric and Interferometric SAR Imagery," *IEEE Transactions on Geoscience and Remote Sensing*, **GRS-32**, 1994, pp. 1017-1028.

12. J. S. Lee, M. R. Grunes, and G. De Grandi, "Polarimetric SAR Speckle Filtering and its Implications for Classification," *IEEE Transactions on Geoscience and Remote Sensing*, **GRS-37**, 5, September 1999, pp. 2363-2373.

13. J. S. Lee, M. R. Grunes, and R. Kwok, "Classification of Multi-Look Polarimetric SAR Imagery Based on the Complex Wishart Distribution," *International Journal of Remote Sensing*, **15**, 11, 1994, pp. 2299-2311.

14. J. S. Lee, M. R. Grunes, T. L. Ainsworth, L. J. Du, D. L. Schuler, and S. R. Cloude, "Unsupervised Classification using Polarimetric Decomposition and the Complex Wishart Distribution," *IEEE Transactions on Geoscience and Remote Sensing*, **GRS-37/1**, 5, September 1999, pp. 2249-2259.

15. E. Pottier and J. S. Lee, "Unsupervised Classification Scheme of POLSAR Images Based on the Complex Wishart Distribution and the H/A/a Polarimetric Decomposition Theorem," Third European Conference on Synthetic Aperture Radar, EUSAR 2000, Munich, 23-25 May 2000.

16. L. Ferro-Famil, E. Pottier, and J. S. Lee, "Classification and Interpretation of Polarimetric SAR Data," IEEE International Geoscience and Remote Sensing Symposium, June 2002, Toronto, Canada.

17. J. A. Kong, S. H. Yueh, R. T. Shin, and J. J. van Zyl, "Classification of Earth Terrain using Polarimetric Synthetic Aperture Radar Images," in J. A. Kong (ed.), *PIERS Volume 3*, New York, Elsevier, 1990, Chapter 6.

18. E. Rignot, R. Chellappa, and P. Dubois, "Unsupervised Segmentation of Polarimetric SAR Data Using the Covariance Matrix," *IEEE Transactions on Geoscience and Remote Sensing*, **GRS-30**, 4, July 1992, pp. 697-705.

19. J. J. van Zyl "Unsupervised Classification of Scattering Behavior Using Radar Polarimetry Data," *IEEE Transactions on Geoscience and Remote Sensing*, **GRS-27**, 1, July 1989, pp. 36-45.

20. K. S. Chen, W. P Huang, D. H. Tsay, and F. Amar, "Classification of Multifrequency Polarimetric SAR Image Using a Dynamic Learning Neural Network," *IEEE Transactions on Geoscience and Remote Sensing*, **GRS-34**, 3, 1996, pp. 814-820.

21. S. R. Cloude and E. Pottier, "An Entropy Based Classification Scheme for Land Applications of Polarimetric SAR," *IEEE Transactions on Geoscience and Remote Sensing*, **GRS-35**, 1, January 1997, pp. 68-78.

22. A. Freeman and S. Durden "A Three Component Scattering Model for Polarimetric SAR Data ," *IEEE Transactions on Geoscience and Remote Sensing*, **GRS-36**, 3, May 1998, pp. 963-973.

23. K. P. Papathanassiou and S. Cloude, "Single-Baseline Polarimetric SAR Interferometry," *IEEE Transactions on Geoscience and Remote Sensing*, **GRS-39**, 6, November 2001, pp. 2352-2363.

24. K. P. Papathanassiou, *Polarimetric SAR Interferometry*, Dissertation, February 25, 1999, TU Graz; ISRN DLR-FB-99-07, ISSN 1434-8454, DLR-HR, Oberpfaffenhofen, Obb., Germany, May 1999.

25. A. Reigber and A. Moreira, "First Demonstration of Airborne SAR Tomography Using Multi-Baseline L Band Data," *IEEE Transactions on Geoscience and Remote Sensing*, **GRS-38**, 5, September 2000, pp. 2142-2152.

26. R. N. Treuhaft and P. Siqueria, "Vertical Structure of Vegetated Land Surfaces from Interferometric and Polarimetric Radar," *Radio Science*, **35**, 1, January 2000, pp. 141-177.

27. H-Y. Yamada, Y. Yamaguchi, E. Rodríguez, Y-J. Kim, and W-M. Boerner, "Polarimetric SAR Interferometry For Forest Canopy Analysis by Using the Super Resolution," *IEEE International Geoscience and Remote Sensing Symposium*, Sydney, June 2001, pp. 1101-1103.

28. T. Mette, K. P. Papathanassiou, I. Hajnsek, and R. Zimmermann, "Forest Biomass Estimation using Polarimetric SAR Interferometry," *Proceedings IGARSS'02* (CD-ROM), Toronto, Canada, 22-26 June 2002.

29. L. Ferro-Famil, E. Pottier, and J. S. Lee, "Unsupervised Classification of Multifrequency and Fully Polarimetric SAR Images Based on the H/A/Alpha-Wishart Classifier," *IEEE Transactions on Geoscience and Remote Sensing*, **GRS-39**, 11, November 2001, pp. 2332-2342.

30. L. Ferro Famil and E. Pottier, "Dual Frequency Polarimetric SAR Data Classification and Analysis," in J. A. Kong (ed.), *Progress in Electromagnetics Research, Volume 24*, New York, Elsevier, 2001, pp. 251-276.

31. K. P. Papathanassiou, S. R. Cloude, and A. Reigber, "Single and Multi-Baseline Polarimetric SAR Interferometry over Forested Terrain," *Proceedings of 3rd European SAR Conference EUSAR 2000*, Munich, Germany, May 2000, pp. 123-126.

32. I. Hajnsek, E. Pottier, and S. R. Cloude, "Slope Correction For Soil Moisture and Surface Roughness Retrieval," *Proceedings of 3rd European SAR Conference EUSAR 2000*, Munich, Germany, May 2000, pp. 273-276.

33. S. R. Cloude, J. Fortuny, J. M. Lopez, and A. J. Sieber, "Wide Band Polarimetric Radar Inversion Studies for Vegetation Layers," *IEEE Transactions on Geoscience and Remote Sensing*, **GRS-37/2**, 5, September 1999, pp. 2430-2442.

34. R. N. Treuhaft and S. R. Cloude, "The Structure of Oriented Vegetation from Polarimetric Interferometry," *IEEE Transactions on Geoscience and Remote Sensing*, **GRS-37/2**, 5, September 1999, p. 2620.

35. S. R. Cloude, K. P. Papathanassiou, and W. M. Boerner, "The Remote Sensing of Oriented Volume Scattering Using Polarimetric Radar Interferometry," *Proceedings of International Symposium on Antennas and Propagation, ISAP 2000*, Fukuoka, Japan, August 2000, pp. 549-552.

36. S. R. Cloude, K. P. Papathanssiou, and W. M. Boerner, "A Fast Method for Vegetation Correction in Topographic Mapping Using Polarimetric Radar Interferometry," *Proceedings of 3rd European SAR Conference EUSAR 2000*, Munich, Germany, May 2000, pp. 261-264.

37. S. R. Cloude, I. H. Woodhouse, J. Hope, J. C. Suarez Minguez, P. Osborne, and G. Wright, "The Glen Affric Radar Project: Forest Mapping using Dual Baseline Polarimetric Radar Interferometry," ESA Symposium on Retrieval of Bio and Geophysical Parameters from SAR for Land Applications, University of Sheffield, England, September 11-14, 2001.

38. A. Reigber, K. Papathanassiou, S. Cloude, and A. Moreira, "SAR Tomography and Interferometry for the Remote Sensing of Forested Terrain," *Frequenz*, **55**, March/April 2001, pp. 119-123.

39. S. R. Cloude and K. P. Papathanassiou, "A 3-Stage Inversion Process for Polarimetric SAR Interferometry," *Proceedings of European Conference on Synthetic Aperture Radar, EUSAR'02*, Cologne, Germany, 4-6 June 2002, pp. 279-282.

40. K. P. Papathanassiou, I. Hajnsek, A. Moreira, and S. R. Cloude, "Forest Parameter Estimation using a Passive Polarimetric Microsatellite Concept," *Proceedings of European Conference on Synthetic Aperture Radar, EUSAR'02*, Cologne, Germany, 4-6 June 2002, pp. 357-360.

Radio-Frequency Radiation Safety and Health

James C. Lin

Mobile-Phone Radiation Effects on Cancers in Mice

An upbeat television interview, given by authors of a paper reporting the results of an Australian study, on the occasion of its publication [1] in the September, 2002, issue of the journal *Radiation Research*, proclaimed that long-term exposure to the microwave radiation (900 MHz) from Global System for Mobile Communication (GSM) phones is safe. Moreover, the paper's authors asserted their findings as countering a previous Australian study [2], which reported an increased incidence of lymphomas in mice of the same transgenic strain and from the same supplier as those used in their experiment.

The study has been widely reported by the popular media, with headlines like "Cell Phones Don't Cause Cancer." A closer reading of the scientific paper reveals that it is fraught with inconsistencies, which make it very difficult to accept its results and conclusions as published with confidence, without further clarification and/or candid answers to some compelling questions. It appears that the study was conducted with care, but there was a lapse somewhere in the execution of the experiment, or in the sourcing of animals, or in the analysis of data, or in the environmental conditions under which the investigation was conducted. Thus, instead of shedding light on whether cell-phone radiation is safe, the latest report has abetted the controversy.

An increased risk of cancer from exposure to microwave radiation has been a major source of concern for many cell-phone users. Cancers – in particular, brain tumors – have snared the attention of scientific investigators, the general public, and the legal profession for nearly a decade. It is noteworthy that a US District Court in Baltimore, Maryland, in October, 2002, dismissed an $800 million law suit, brought by a 43-year-old Baltimore neurologist against several leading cell-phone companies, alleging that his brain tumor was caused by the use of an analog cell phone.

Lymphomas are a type of cancer that affects the lymphatic system, which is part of the body's immune system. Specifically, the lymphatic system is the body's blood-filtering tissue, which helps to fight infection and disease. Like other cancers, lymphomas occur when cells divide too much and too fast. Symptoms of lymphomas include swelling in one or more groups of lymph nodes, fever, weakness, weight loss, and an enlarged liver and spleen [3]. There are two major types of lymphomas: Hodgkin's disease and non-Hodgkin's lymphoma. Moreover, a lymphoblastic lymphoma – medium-sized lymphoid cells with a high nucleo-cytoplasmic ratio – is the most common type of non-Hodgkin's lymphoma, especially in children. Lymphoblastic lymphomas are the less-predictable type, and they are more likely to spread to areas beyond the lymph nodes. Because lymphomas impair the immune system, there is the risk of death from infection. An estimated 60,000 people per year in the US are diagnosed with lymphomas: 53,000 with non-Hodgkin's lymphoma, and 7,000 with Hodgkin's disease, according to the Lymphoma Research Foundation of America. In most cases, the cause is not known.

The clinical course for non-lymphoblastic lymphomas is less rapid than for lymphoblastic lymphomas. In mice, lymphoblastic lymphomas are usually seen in animals < 10 months of age, as a mediastinal mass with attendant respiratory distress, and rapid clinical decline when the enlarging mass compresses the thorax. Non-lymphoblastic lymphomas occur predominantly in mice > 10 months old, generally cause progressively increasing abdominal distension, and are readily palpable.

A variety of factors, including congenital status, as well as infectious, chemical, and physical agents, have been associated with an increased risk of developing lymphomas. Specifically, infectious agents, such as viral and bacterial

James C. Lin is with the University of Illinois at Chicago
851 South Morgan Street (M/C 154)
Chicago, Illinois 60607-7053 USA
Tel: +1 (312) 413-1052 (direct);
+1 (312) 996-3423 (main office)
Fax: +1 (312) 996-6465;
E-mail: lin@uic.edu

[Editor's note: This is an updated version of J. C. Lin, "Cellular-Phone Radiation Effects on Cancer in Genetically Modified Mice," *IEEE Antennas and Propagation Magazine*, **44**, 6, 2002, pp. 165-168.]

infections, have been associated with its development. In addition, chemical and physical agents – such as pesticides, solvents, arsenate, paint thinners, and lead, as well as hair dyes and high-dose ionizing radiation exposure – have all been shown to increase the incidence of lymphomas.

The protocol of both reported investigations involved the incidence of lymphomas in mice of the same transgenic strain (E-mu-Pim1), following long-term (18 to 24 months) exposure to pulse-modulated microwave fields similar to those used in digital cellular mobile telephones. The E-mu-Pim1 transgenic mice are predisposed to developing lymphomas spontaneously, and allegedly were obtained from the same source in both experiments.

As stated in the paper, the latest study was designed to "test the same central hypothesis" as that of the earlier study, but "refinements were included to overcome perceived shortcomings." Indeed, the more recent study seems to have been well designed and conducted, and many of the flaws of the earlier study were corrected. However, it is open to debate whether the latest report represents a scientific refinement. It has become apparent that it is contributing to the controversy surrounding research reports on cell-phone radiation safety. The manner and statements with which the results of the latest study were released to the press didn't help.

Controversy seems par for this particular line of cell-phone health-effect research. The first study was published in 1997. It reported a significant increase in lymphomas (2.4 times more, compared to unexposed controls) in the transgenic mice exposed to GSM-phone radiation. In brief, 100 female transgenic mice were sham-exposed, and 101 were exposed for two 30-min periods per day for up to 18 months to plane-wave fields of 900 MHz, with a pulse-repetition frequency of 217 Hz and a pulse width of 0.6 ms. Incident power densities were 2.6-13 W/m2, and specific absorption rates (SARs) were 0.008-4.2 W/kg, averaging 0.13-1.4 W/kg. At the end of the experiment, 53% of the exposed mice had lymphomas, as compared to 22% of the unexposed controls (Odds Ratio = 2.4, P = 0.006, 95% CI = 1.3-4.5). The exposed mice also recorded a faster onset of lymphomas. However, it took about two years for the results to be made public, and to be published in a scientific journal. The press release that attended the publication appeared to have been designed to minimize its impact.

There were concerns that the finding was kept secret for too long: two years. The researcher who led the study, Michael Repacholi, then at Australia's Royal Adelaide Hospital, and at present, the director of the International EMF Project at the World Health Organization (WHO) based in Geneva, Switzerland, argued that the secrecy was essential to secure a deliberate, thorough analysis of their findings. Apparently, an advance report was given to the company that sponsored the research (the Australian telecom giant, Telstra). But the scientific community and the public were kept in the dark for two more years, between the end of the experiment and the public announcement of its results and their publication in the journal, *Radiation Research* [2]. Media reports at the time suggested that Telstra had denied any attempt to interfere or of a cover-up.

Nevertheless, the 1997 study has been considered to be a prominent investigation that suggests a cancer risk from long-term exposure to cell-phone radiation. Of course, one study cannot be the basis for a definitive judgment about any health effect. Moreover, since the study suffered from some deficiencies, it was more urgent for other investigators to reproduce or confirm the study, in order to appraise the acceptability and reliability of the reported results.

There are two general types of deficiencies that were identified, which had caused the earlier publication to be criticized by research scientists and others. One type was dosimetric in nature. For example, mice were allowed to roam and huddle freely during exposure to incident power densities of 2.6-13 W/m2. Consequently, there was a wide variation of SARs (0.008-4.2 W/kg, averaging 0.13-1.4 W/kg). Only an average response could be inferred from an average SAR, not an individual SAR. Moreover, mice selected for necropsy during the experiment were not replaced with either other mice or tissue-equivalent phantoms, ergo altering dosimetry in the remaining animals. The biological type of criticism included a lack of standardized assessment criteria for deciding which mice would be selected for necropsy, and disposal of surviving mice without performing necropsy to ascertain whether there were infection and/or other relevant diseases, such as kidney failure, in those animals.

As previously mentioned in these columns [4], the value of a science-based approach is that it allows the accumulation and attainment of knowledge about the interaction of various forces in natural or under artificial environments in a systematic manner. Fundamental to the scientific approach is repeatability and confirmation.

Human and mammalian systems are complex. Their responses can be variable and are often uncertain, even under similar circumstances of exposure. It is important that investigators replicate a given observation. Moreover, most working scientists are unwilling to accept or reject scientific claims on the basis of experimental evidence that cannot be replicated or that is poorly replicated. Because a single study – however well conducted – seldom provides the definitive evidence for or against a biological response, several independently repeated or confirmed studies are needed to arrive at a statistically significant association, or at a convincing answer to the health-effect question. Thus, a number of independent experiments would normally be required to establish a reliable cause and effect relationship between mobile-phone microwave exposure and biological response.

The latest study set out to "test the same central hypothesis" as that of the earlier study, with refinements to overcome some of the perceived shortcomings. Specifically,

the variation in SAR was reduced by restraining the mice, and by using tissue-equivalent phantoms to replace autopsied mice. The new exposure system, supplied by Motorola, consisted of 15 lossy, radial, parallel-plate electromagnetic cavities ("Farris Wheel"), configured for far-field operation. Each cavity had 40 mice restrained individually in clear Perplex tubes, cylindrically arranged around a dipole antenna. The tubes were constructed to prevent each mouse from changing its orientation relative to the field, to facilitate SAR determination. The exposed groups were divided into four SAR levels: 0.25, 1.0, 2.0, and 4.0 W/kg. A standardized set of criteria (10% reduction in body mass over a week) was used for selecting mice for necropsy, and all surviving animals were necropsied.

A total of 120 lymphoma-prone, E-mu-Pim1 mice and 120 wild-type mice were exposed for 1 h/day, 5 days/week, at each of the four SAR levels, for up to 24 months. In addition, 120 E-mu-Pim1 and 120 wild-type mice were sham-exposed; there was also an unrestrained negative control group. The paper concluded that the results did not show an increase in lymphomas, following a two-year exposure to GSM-cell-phone radiation [1]. Furthermore, there was no significant difference in the incidence of lymphomas between exposed and sham-exposed groups at any of the exposure levels (with one exception). A dose-response effect was not detected. The findings showed that long-term exposures of lymphoma-prone mice to 898.4 MHz GSM radiofrequency (RF) radiation at SARs of 0.25, 1.0, 2.0, and 4.0 W/kg had no significant effects when compared to sham-irradiated animals. This was in contrast to the previous study [2], which reported that long-term (18 months) exposure of lymphoma-prone mice significantly increased the incidence of non-lymphoblastic lymphomas when compared to sham-irradiated animals.

The results of the new, double-blind mice study may or may not show an increase in lymphomas, as the paper concluded. To be sure, the latest study was not a replication of the earlier one. A replication, as a standard practice of the scientific approach, requires that the same methods and materials are followed as in the earlier study. Given that there are major differences in materials and methods (beyond refinements), the design of the latest study is more appropriately characterized as *an attempt to confirm, or refute, rather than replicate* (see "General Principles for Evaluation of Scientific Literature" in [5]).

More significantly, further consideration of the source of mice, exposure regime, animal restraint, and the omission of data from analysis in the latest study may possibly lead to a different conclusion than the paper's.

It was stated in the paper [1] that the mice were supplied from the same source used in the earlier study, and listed Taconic Farms, New York, as the source. However, mice for the earlier study [2] came from GenPharm International of Mountain View, California. Thus, the E-mu-Pim1 mice appear to not be the same, after all. Even the same strain of mice, from different suppliers, may have different characteristics, and may respond differently: a factor to be considered further.

Mice in the latest study were exposed to daily one-hour sessions, while those in the earlier study were exposed for two 30-min periods per day. The biological effect of fragmenting exposure duration is not well known. However, diurnal variations and the temporal dependence of cellular and molecular processes are well established.

The use of free-roaming verses restrained animals by themselves is not a problem, so long as the effects on these mice are characterized, with appropriate cage controls. Unfortunately, data for the cage-control mice were missing from the publication [1]. Restraining the animal in a tight tube during the exposure session constitutes a continuing stress to the animal, which may lead to significant stress responses that potentially could obscure any effect from the exposure to cell-phone radiation.

There also are some rather glaring inconsistencies in the published data [1]. For example, some or all of the mice were dead after 18 or 20 months, according to one figure (Figure 1), but they still had weight gains up to 26 months, according to another figure (Figure 2) on the same page ([1], p. 360). The study design included equal numbers of freely moving mice for negative controls (cage controls). However, data for the cage-control group were not given in the paper, and appears to have been excluded from the statistical analyses. By not having the free-moving mice form a part of the statistical-analysis group, the report was deprived of the pathophysiology of cage-control mice for comparison. The cage controls can and should serve as valuable background materials, which potentially might be masked by stress response induced by the restraining tube used for sham control.

It is noteworthy that the incidence of lymphomas among the sham controls (SAR = 0; mice are restrained but not exposed) was abnormally high in this study [1]. Specifically, among the transgenic mice, the incidence of lymphomas was 75% for the sham-control group (89 out of 120 mice developed lymphomas: 15 with lymphoblastic lymphomas, 74 with non-lymphoblastic lymphomas). In contrast, the incidence of lymphomas in the earlier study [2] was 22% for the sham-control mice (22 out of 100 mice developed the disease: 3 with lymphoblastic lymphomas, 19 with non-lymphoblastic lymphomas). The high degree of incidence in the sham controls (75% versus 22%) makes the experimental protocol impractical. It could have masked an effect from cell phones, or any other agent, for that matter. It is infeasible to come to any firm conclusions about lymphomas in transgenic mice exposed to cell-phone radiation.

These flaws, possibly in the sourcing or handling of mice, or in the statistical analysis of the data, or in the fundamental design of the experiment, limit the conclusions that can be drawn for the outcome of the latest study, despite the paper's claim.

There is another matter of consequence that should be emphasized: science-based research versus product testing [4]. A relatively large number of independent experiments would normally be required to establish a reliable cause-and-effect relationship between cell-phone radiation and biological response. This approach to scientific investigation argues against a few large-scale studies, each costing millions per year. Instead, it proposes a larger number of smaller projects, some of which could be designed as pilot studies. Following completion of these projects, perhaps, a large-scale study could then be conducted, if warranted. Such an approach would have picked up many of the apparent flaws, discrepancies, and uncertainties mentioned above. It could make the outcome of the study a great deal more useful.

In general, a multiplicity of projects in a given line of investigation could be designed as independent studies, aimed at a better fundamental understanding of the interaction. There could be a built-in process of repeating some of the experiments to resolve any uncertainty, as needed. It is emphasized that in all of these projects, there should be a sound regard for investigator-initiated innovations in project design and execution, within the acknowledged scope of objectives and specific aims. This would add value to and strengthen the usefulness of the outcome. Groups of fundamental research projects, with streamlined specific aims, would be more tractable. They could represent an intrinsic replication. They would also help to foster a widespread acceptance that the corresponding experimental results are reliable and replicable

References

1. T. D. Utteridge, V. Gebski, J. W. Finnie, B. Vernon-Roberts, T. R. Kuchel, "Long-Term Exposure of E-mu-Pim1 Transgenic Mice to 898.4 MHz Microwaves Does Not Increase Lymphoma Incidence," *Radiation Research*, **158**, 2002, pp. 357-364.

2. M. H. Repacholi, A. Basten, V. Gebski, D. Noonan, J. Finnie, A. W. Harris, "Lymphomas in E mu-Pim1 Transgenic Mice Exposed to Pulsed 900 MHZ Electromagnetic Fields," *Radiation Research*, **147**, 1997, pp. 631-640.

3. R. S. Cotran, V. Kumar, S. L. Robbins, *Pathologic Basis of Disease, Fifth Edition*, Philadelphia, Saunders, 1994.

4. J. C. Lin, "Radio-Frequency Radiation Safety and Health: Mobile Phone Safety Testing and Fundamental Scientific Research," *Radio Science Bulletin*, No. 300, 2002, pp. 31-33.

5. J. C. Lin, "Telecommunications Health and Safety: Scientific Literature on Biological Effects of Radio Frequency Radiation: Criteria for Evaluation," *IEEE Antennas and Propagation Magazine*, **44**, 2, 2002, pp. 140-142.

XXVIIth General Assembly

BUSINESS TRANSACTED BY COMMISSION A

I. Meeting of August 19, 2002

Chairman Prof. Bava called the meeting to order at 6 PM. He circulated an attendance sheet, requesting the name, the country, the address and the voting status of those present. A total of 16 voting Members were present.

I.1 Approval of the Agenda

Prof. Bava proposed an agenda for the business meeting. After a short discussion the agenda was unanimously approved.

I.2 Election of the 2002 Vice-Chair

Prof. Bava reminded the audience that the curricula of the candidates had been mailed to the voters. He then briefly summarized the candidates' scientific activities; all have experience in organizing meetings and symposia. The names of the candidates are: Boisrobert (FR), Chou (USA) and Pollitt (UK)

Chairman Bava informed those present that they had the opportunity to change their vote.

No representative elected to do so. There was the tallying of the votes by mail plus those of the attending voting members Leschiutta (IT) and de Vreede (ND). The candidates collected the following preferences:

1. Pollitt
2. Boisrobert
3. Chou

There was a brief procedural discussion and a new round of votes was collected to establish a possible new level of preference between the two candidates Boisrobert and Pollit. The outcome of the second round of voting was: Pollitt (26), Boisrobert (22)

I.3 Transition from Review of Radio Science to Radio Science Bulletin.

Chairman Bava invited the audience to discuss the proposal to eliminate the Review of Radio Science and publish instead its articles on the Radio Science Bulletin. There is also a proposal to post the R. S. Bulletin on the Web. If the proposal is accepted then an editor for Commission A must be selected and charged with the article editing process.

There was a discussion following these proposals. The final unanimous sense of the members was to accept the transition provided that the content and the acceptance criteria of the articles are maintained. The Web posting of the R.S. Bulletin met unanimous acceptance. At this time no editor for Commission A has been nominated.

I.4 Terms of Reference for Commission A.

The current terms of reference of Commission A were presented by Chairman Bava. The discussion of possible changes was remanded to future meetings of the Commission.

I.5 Scientific Commission for Telecommunication.

Chairman Bava stated that the link between URSI and ITUR is in the charge of the S.C. of this GA, Mr. Martin P. Hall. If members of Commission A want to participate in the link activities, they can contact Chairman Bava during the next Commission A business meeting on Wednesday for the transmittal of their name. There will be a meeting chaired by Mr. Hall on Thursday, August 22nd, at lunch time. Interested parties can prepare written contributions and place them in Mr. Hall's pigeonhole.

Prof. Leschiutta (IT) will make a short presentation at the next Commission A meeting on the issues between Commission A and ITUR, in particular on the leap second problem.

I.6 Philips Award

Chairman Bava stated that the Philips Co. will present "una tantum" a Y. S. award of 1000 Euros and a plaquette for the best written paper. Commission A has three candidates that can compete for the prize. The commission Chair, supported by few advisors, will propose the best Y. S. contribution of Commission A for the final selection which will occur next Friday at lunch time after a short interview between the selected Y.S. (one per Commission) and an ad hoc committee.

I.7 Procedure for Abstract Acceptance

The procedure for abstract acceptance was discussed. Some members prefer the short 1 page abstract submission, while others wish to maintain the current four-page limit.

No resolution was found and the discussion will be continued at the next business meeting.

There was a short discussion on how to control absenteeism. The current policy of not refunding the registration fee is good, but additional measure could be added.

Prof. Leschiutta proposed a reduced URSI registration fee for retired members of the Union.

I.8 Question on the Procedures of Session Organization

Mr. Martin Hall circulated a document with the requirements for organization of the URSI scientific sessions. Suggestions for amendments to the procedures were requested by chairman Bava.

II. Business Meeting of August 21, 2002

Chairman Prof. Bava called the meeting to order promptly at 18:00 and passed an attendance sheet for those present. Chairman Bava proposed an agenda (see attachment B) for meeting, which was unanimously approved by the attending members.

II.1 Summary of Council Meeting of August 20, 2002.

Chairman Bava informed the audience of the outcome of the election of the Chairs and Vice-Chairs of the URSI Commissions. The Vice-Chair election process was completed except for Commissions D and E, whose decisions will be firmed at the council meeting of August 22, 2002.

Commissions' Propositions

a) A French resolution of refunding the registration fee to members of poor countries who cannot receive travel support was rejected after show of hands
b) Following a resolution proposed by Commission J, working group was established to resolve the leap second issue
c) A French recommendation to timely distribute information about topics to be discussed at Council meetings was approved.

Chairman Bava informed the members that there are three (3) contending sites for the 2005 URSI GA : Beijing DRC, New Delhi (India) and Denver, CO (USA). Site selection will be decided at the Council meeting of August 22, 2002.

Member for Solar Power Satellite IWG. Prof. Andrew Marvin is interested in participation.

II.2 Meeting Sponsored by Commission A

Prof. Bava presented the list of the scientific meetings sponsored by Commission A (see attachment C). Type B support entails funding; type A only a statement of support.

II.3 Participation to Scientific Meetings

The reports available from URSI representatives nominated by Commission A in International Bodies can be found in the web site www.ursi.org (reports from the commissions).

The URSI Commission A representatives concerned with the following Bodies: CPEM Executive Committee (the Chair), CIPM-CCTF(Mc Steele or Leschiutta), CIPM-CCL (Helmcke), CIPM-CCEM (Erard), CIPM-RF-WG of CCEM (Stumper), Luden(IEC and ISO). Except for the Chair, Mc Steele and Leschiutta, the other representatives were not present; the incoming Chair will check the availability of those absent or will nominate other representatives.

II.4 Responsibilities of Chair and Vice-Chair

Prof Bava showed a viewgraph with the list of duties for the Chair and V.C. Commission A needs to set up its own Web site and name an editor for Review of Radio Science. Prof. Bava invited those present to suggest changes for the duty lists, none was offered.

II.5 One vs. Four Page Abstract

Chairman Bava solicited the view of the audience. There was a lively discussion, as opinions were divided on this issue. The final, unanimous sense of the group was as follows: Authors must provide a short summary (one hundred words) for the program and one page abstract of the presentation. This is the only prerequisite for possible acceptance of the work. An author at his/her discretion can supplement the abstract with additional pages (e.g. figures and equations) up to a total of four (4) pages.

II.6 Scientific Committee for Telecommunications (SCT)

Commission A has to provide a contact name to Mr. Martin Hall. Prof.. Leschiutta offered his services until a suitable member is identified. The incoming Chairman was charged with the task.

II.7 Terms of Reference for Commission A

Prof. Bava presented a viewgraph with the current Commission A terms. He solicited comments and suggestions for change from the audience. There was no discussion because the meeting had to come to an end so members could participate at the banquet dinner.

II.8 Varia

Chairman Bava showed the audience the 35-page document of the URSI GA Standard Procedures. He invited comments from the audience. Given the length of the SP's comments are expected at a later date.

Chairman Bava closed the meeting at 18:50.

III. Business Meeting of August 23, 2002

Chairman Bava called the meeting promptly at 6 PM. He circulated an attendance sheet and proposed an agenda (see attachment A). The agenda was approved with no modification. This was the least attended business meeting with only 8 members present.

III.1 Contributions of Commission A to the Scientific Program of the GA

Chairman Bava showed viewgraphs with the titles of the general lecture, the tutorial lecture, the 5 sessions (A1-A5) and the 6 joint sessions headed by Commission A. In total there were 78 platform papers and 31 posters, with a few withdrawals. In addition there were 6 joint sections with participation from Commission A. Chairman Bava commented that a session on fundamental constants has been discouraged; he also noted that DC and low frequency standards had no session in this GA. Both topics are in the terms of reference of Commission A.

III.2 News from the Council

Prof. Bava informed the audience of the outcome of the elections held at the Council meeting during the evening of August 22, 2002. Results were as follows: President K. Schlegel (D); Vice Presidents: CM Butler (USA), F. Lefeuvre (F), A. Wernick (Poland), P. Wittke (Canada). The Commission D and E Vice-Chair were announced: Commission D, F.de Fornel (F); Commission E: F. Canavero (I). The next GA will be held in New Delhi, India during the second half of October 2005. The scientific coordinator for the XXVIII GA is Prof. G Brussard and the associated coordinator from India will be appointed in the near future.

III.3 Passage of the Chair

Prof. Bava introduced the incoming Chair, Dr. Balzano who, after a short introduction, continued with agenda items.

III.4 Topics Proposed for Next GA

Dr Balzano solicited the audience for topics for the next GA in addition to or in the place of the traditional ones that can be found in the Toronto and Maastricht list of Commission A sessions. There were several suggestions:

1) Numerical Techniques in Metrology (Marvin);
2) 50 years of atomic time keeping (McSteel);
3) Links between electric metrology and fundamental constants. Stability of fundamental constants. Time stability influence on fundamental constants (Leschiutta)
4) Intercomparison between Cs fountain clocks and limit of performance(Leschiutta).
5) Characterization of receivers for radio astronomy (joint session with Commission J); Characterization of photonic and electronic devices (joint with Com. D) (Bava).
6) Dielectric and electromagnetic field measurements in materials and living tissues; Measurements in non-linear devices RF- submillimiter frequencies; Optical frequencies measurements and standards; Antenna and Radome measurements; Time domain measurements. (Balzano)

III.5 Suggestions for the terms of Reference

There were two suggestions:

1) Drop term (e) Measurements using lasers;
2) Reincorporate in Commission A the EM measurements in the bioeffects domain. The reinstatement of the bioeffect measurements in Commission A must be approached softly to avoid a turf collision with Commission K. There were too few members present to vote on this suggestions. Chair Balzano was charged with circulating the suggestions and poll the membership of Commission A.

III.6 Summary of the Meeting with Ross Stone.

Commission A needs to supply 6 review papers for the Radio Science Bulletin, which now will publish the papers that used to appear on Radio Science Review.

Dr. Stone needs the titles or at least the topics by the end of 2002 or very beginning of 2003. Publication will start in Dec. 2003. Members of Commission A are invited to submitted titles and authors for these papers, which are expected to be about 12 pages long. Papers must be submitted and completed 6 weeks before the publication of RSB. Dr. Balzano will serve as Commission A editor

III.7 Commission A representatives in other organizations

Dr. Balzano invited the audience to communicate to him the names of members who sit in other scientific societies.

III.8 Topics from those present

Dr. Balzano invited comments from the audience on any topic. There was a complaint on a 10 minute time intrusion in the general lecture of Commission A by the convener of tutorial lecture of Commission G. Dr. Balzano was requested to convey a complaint to the Council (it was done during the New Coordinating Committee meeting of August 24).

III.9 Closing

Since there were no additional topics from the audience Dr. Balzano thanks those present and closed the meeting at 19:15.

BUSINESS TRANSACTED BY COMMISSION C

I. Business Meetings

I.1 Welcome to URSI General Assembly in Maastricht

The Commission held open business meetings on 19th, 21st, and 23rd, August, 2002. The following persons were present at least at one meeting, but mostly at several: Ernst Bonek, Austria (Chair); Masami Akaike, Japan (Vice-Chair); Paul Wittke, Canada; Maurice Bellanger, France; Witold Krzymien, Canada; Guido Tartara, Italy; Eleary Beonard, Denmark; Ernst Zollinger, Switzerland; David Thomson, Canada; Reiner Thoma, Germany; Jean-Claude Bic, France; Joseph Shapira, Israel; Jan-Olof Gustavsson, Sweden; Zhihua Wang, China; Blagovest Shishkov, Bulgaria; Said EL Khamy, Egypt; Mairtin Odroma, Ireland; Mark Cummings, USA; Kensuke Ogawa, Japan; Alfred Hero, USA; Robert Weigel, Germany, Lajos Nagy, Hungary; Andy Molisch, USA; Börje Forsell, Norway.

At the opening of the first business meeting, the Chair welcomed everyone to the meeting and attendees introduced themselves. The Chair then reported briefly the activity of Commission C in this triennium and set the scene.

I.2 Future of Review of Radio Science

The Chair proposed a slight change in the style of the Review of Radio Science (RRS), that is, the future RRS will not be a triennium publication but will be a quarterly publication, merging into the Radio Science Bulletin (RSB). All members of the meeting expressed their agreement.

I.3 Election of the next Vice-Chair

Two candidates, Peter Farkas (Slovakia) and Andreas F. Molisch (Austria), for the next Vice-Chair were nominated. Andreas F. Molisch was elected as a result of 36 points to Peter Fakas of 24 points.

I.4 Commission Editor for the new Radio Science Bulletin

A. Molisch was agreed to serve as Commission Editor for RSB (incorporating RRS).

I.5 Review of the Terms of Reference

The Terms of Reference was discussed on the business meeting on 23rd August. The existing Terms of Reference are considered to be very broad, relating not only to proper radio science technology but also infrastructural technologies to radio communication systems. Among them, Commission C is considered necessary to focus on radio communication systems and signal processing technologies. As Commission C provides enabling technologies for many other commissions' work, collaboration with other commissions is also essential. Now Commission C has concreted new Terms of Reference: **"Radio-Communication Systems and Signal Processing"**

The Commission promotes Research and Development in:
a. Radio-Communication and Telecommunication Systems;
b. Spectrum and Medium Utilization;
c. Information Theory, Coding, Modulation and Detection;
d. Signal and Image Processing in the area of radio science.

The design of effective radio-communication systems must include scientific, engineering and economic considerations. This Commission emphasizes research into the scientific aspects, and provides enabling technologies to other areas of radio science.

I.6 Role of National Representatives of "C"

Further enhancement of the national and international activity of Commission C should strongly be prompted for the next triennium. While National Representatives are desired to have close contact with Commission C, Commission C also is encouraged to try to cooperate with radio scientists in each country in parallel to National Representatives.

I.7 The program for the next General Assembly

The program of the next General Assembly will focus the sessions on mobile radio communications, including wireless access an ultra-wide-band access, and image processing. Since the field of Commission C is very broad, cooperative organization of sessions with other Commissions is necessary.

For organizing the next General Assembly held in New Delhi, a wide contact with Indian scientists in the field of Commission C will be solicited. A list of leading scientists in India based upon the international conferences held in India so far will be helpful.

I.8 Other business

Further discussions will be made on the following points:
(1) Necessity for the steering committee to assist chair,
(2) Representative of Commission C for SCT,
(3) Future Terms of Reference, as it is or the commission split and renamed,
(4) Competition, cooperation, and/or interaction with other international conferences and organizations.

II. Review of General Assembly

Commission C organized one tutorial, five C sessions (including one poster session), and twelve joint sessions. Among twelve joint sessions, five sessions were led by Commission C. Since the technical field that Commission C deals with is wide and has relating parts with other Commissions, such joint sessions show characteristic feature of Commission C. Close contact/collaboration henceforth with other Commissions will be further encouraged.

Each session room was filled to capacity and the discussions among the presenters and audience were quite active, which reflects a wide interest to technical subjects of Commission C.

The following are the sessions organized by Commission C:

Tutorial: "Modeling of directional wireless propagation channels," presented by A. Molisch,

C1: "Software reconfigurable radio systems," organized by R. Kohno,

C2: "Antenna array signal processing and multiple-input multiple-output," organized by A. Molisch and M. Viberg,

C3: "Blind signal detection," organized by V. Koivnen,

C4: "Recent advances in telecommunication systems," organized by P. Wittke,

CAF: "Broadband access systems in wireless communication," organized by H. Ogawa and T. Tanem,

CFAB: "Subsurface remote sensing and its application," organized by J. Sachs, D. Noon, G. Smith, and P. van den Berg,

CBF: "Wave propagation modeling for mobile communication systems," organized by W. Wiesbeck and H. Bertoni,

CF: "Adaption to changing radio channel," organized by R. Bultitude and Y. Karasawa,

CFA: "Channel sounding in mobile communication systems," organized by R. Thoma and S. Saunders, and Q. Balzano.

BUSINESS TRANSACTED BY COMMISSION E

Chair: Pierre Degauque (France)
Vice – Chair: Flavio Canavero (Italy)

I) Working groups during the past triennium, their involvement in the sessions of the General Assembly and comments on their activities

The Commission E activities are based on the work conducted by the working groups (WG). During the past triennium, the Chair or Co-Chairs organized a lot of sessions in EMC Symposia and, of course, they were very active in the preparation of the technical sessions of the General Assembly (GA). In the following, after recalling the names of these WG, a brief summary of the sessions they have organized is given, together with discussions within the business meetings on the opportunity or not to continue, modify or stop a WG.

- E.1: Spectrum Utilization Management and Wireless Telecommunication
  Co-Chairs: G. Hurt (USA) and R. Struzak (Poland)
  The session proposed on this subject at the Maastricht URSI GA was entitled: "Mathematical Methods in Frequency Assignment". Nevertheless, only three papers were planned and any speaker was present. Since it seems difficult to be attractive in this field, it has been decided not to maintain this working group in the next triennium.
- E.2: Intentional Electromagnetic Interference
  Co-Chairs: M. Wik (Sweden) and W. Radasky (USA)
  Four papers were presented during the GA, the title of the session being the same as the name of the WG. Two contributions reviewed the different categories of EM threats and the susceptibility aspects of the electronic equipment. The two others were focused on specific technical aspects.
  It must be recalled that this WG was created in 1999, following a recommendation introduced by Prof. Ianoz and supported by Com. E, for performing additional research pertaining to a EM Terrorism and to investigate techniques for appropriate protection.
  During the business session, M. Wik suggested that M. Bäckström replaced him as a Co-Chair. This has been approved.
- E.3: High Power Electromagnetics
  Co-chairs: C.E. Baum (USA) and R.L. Gardner (USA)
  9 papers were presented during the session organized by Baum and Gardner on this topic.
- E.4: Terrestrial and Planetary Lightning Generation of Electromagnetic Noise
  Co-Chairs: Z. Kawasaky (Japan) and V. Cooray (Sweden)
  The conveners of the related session "Lightning observation from space and global lightning activity" (6 papers) were Z. Kawasaki and A. Bondiou. V. Cooray did not wish to continue as a Co-Chair. Z. Kawasaky agreed to continue this work but proposed that the name of the WG became: "Lightning discharges and related phenomena". This has been approved for the next triennium.
- E.5: Interaction with and Protection of, Complex Electronic Systems

Co-chairs: J. Nitsch (Germany), P. Degauque (France), M. Ianoz (Switzerland) and J.P. Parmentier (France)
A full session entitled "EM interaction with complex system" took place at the GA and was organized by Parmentier and Ianoz. Related papers were also presented in two other sessions: "Radiation from and coupling to PCB" and "EM interaction with and susceptibility of analogue and digital electronics".
Michel Ianoz being retired from the Ecole Polytechnique Federale de Lausanne, he wished to stop being a Co-Chair. Since this WG had already four Co-Chairs, it was decided not to nominate a new person.

- E.6. Effects of transients on equipment
  Co-Chairs: J. ter Haseborg (Germany), V. Scuka (Sweden) and B. Demoulin (France).
  The Co-Chairs reported that it was difficult to gather information on this research area and it seems that the number of people involved in this field decreases rapidly. Any specific session dealt with this subject at the GA and it was decided during the business meeting to stop this WG.
- E.7. Extra-Terrestrial and Terrestrial Meteorologic-Electric environment
  Chair: H. Kikuchi (Japan)
  Any session was organized on this subject and, during the discussion, it appeared that this WG must be renewed at least by changing its technical content. Nevertheless, it has been kept for the next triennium but keeping in mind that a new proposal must be made at the next URSI GA. Furthermore, the interest of the Com. E community must be clearly pointed out.
- E.8. Geo-electromagnetic disturbances and their effects on technological systems
  Co-Chair: M. Hayakawa and R. Pirjola (Sweden)
  9 papers were presented in the session "Terrestrial Electromagnetic Phenomena". M. Hayakawa suggested changing both the name of the WG and the Co-Chairs. He proposed for the new WG: "Terrestrial and Planetary Electromagnetic Noise Environment" co-chaired by: M. Hayakawa (Japan), A.P. Nickolaenko (Ukraine), Y. Hobara (France) and M. Füllekrug (Germany). This has been approved during the business meeting.
- E.9 Interference and Noise at Frequencies above 30 MHz
  Chair: J. Gavan (Israel)
  Since this topic is clearly at the frontier between Com. E and Com. F, a joint session were organized. Any change has been proposed to this WG, except to add another Co-Chair having a technical background related to Com. F

A number of Working Groups also organize joint technical sessions, three of them with Com. H.

II) Discussion on the objectives of a working group

A discussion took place during a business meeting on the role of a Working Group. Indeed, it may sometimes appear that it is not easy to clearly know who is a member of a WG, how is the information disseminated between the members and what are the duties and responsibilities of a WG.

In a first step, each Chair or Co-Chairs will write a brief presentation (typically half a page) on their WG mainly describing promising research areas which must be developed during the next triennium. Furthermore, a list of WG members (Names and email addresses) would be useful.

III) Working Groups for the next triennium

The new Working Groups that were voted for the new triennium are:

- E.1: Terrestrial and Planetary Electromagnetic Noise Environment
  Co-Chairs: M. Hayakawa (Japan), A.P. Nickolaenko (Ukraine), Y. Hobara (France) and M. Füllekrug (Germany)
- E.2: Intentional Electromagnetic Interference
  Co-Chairs: M. Bäckström (Sweden) and W. Radasky (USA)
- E.3: High Power Electromagnetics
  Co-chairs: C.E. Baum (USA) and R.L. Gardner (USA)
- E.4: Lightning Discharges and Related Phenomena
  Co-chairs: Z. Kawasaki (Japan)
- E.5: Interaction with and Protection of, Complex Electronic Systems
  Co-chairs: J. Nitsch (Germany), P. Degauque (France) and J.P. Parmentier (France)
- E.6: Extra-Terrestrial and Terrestrial Meteorologic-Electric Environment
  Chair: H. Kikuchi (Japan), E.A. Mareev (Russia)
- E.7: Geo-electromagnetic Disturbances and Their Effects on Technological Systems
  Chair: A. Viljanen (Finland)
- E.8: Interference and Noise at Frequencies above 30 MHz
  Chair: J. Gavan (Israel)

Joint Working Group

EGH. Seismo Electromagnetics (Lithosphere-Atmosphere-Ionosphere Coupling)
Co-Chair for Commission E: M. Hayakawa (Japan)
Co-Chair for Commission G: S. Pulinet (Russia)
Co-Chair for Commission H: M. Parrot (France) and O.A. Molchanov (Russia)

IV) Preparation of the New Delhi GA

After discussion, few ideas on possible sessions, tutorials and General Lectures came out. It was decided to go further in the discussion during the URSI meeting which will take place during the EMC Zurich Symposium, Feb. 2003.

V) Other business

- Election of the Vice Chair. Pr. Flavio Canavero was elected as Vice-Chair. He will also serve as the Commission E Editor of the Radio Science Bulletin
- After discussion, it appears that it was not necessary to change the Terms of Reference for Commission E.
- Support for the various academic meetings. The following meetings will be supported in the coming triennium either in mode A (without financing) or in mode B(with financing)
  . EMC Zurich, Feb. 2003
  . IEEE EMC, Istanbul, May 2003
  . Telecom 2003 et Journées Franco-Marocaines, Oct. 2003
  . EMC Europe, Eindhoven, 2004
  . EMC'04, Sendai, 2004
  . EMC Wroclaw, 2004
  . Colloque CEM, Toulouse, 2004

In Europe, there is a debate and discussions between the organizers of the main EMC European events to merge or not the meetings. At the time of the URSI GA in Maastricht, there was any definitive decision. Therefore, the names of EMC meetings which will be sponsored beyond 2004 cannot be now specified.

BUSINESS TRANSACTED BY COMMISSION J

Chair: Professor Jacqueline N. Hewitt (United States)
Vice-Chair: Professor INOUE Makoto (Japan)

I. First Business Meeting: 19 August 2002

I.1 Election of Vice-Chair

Three candidates were nominated for the position of vice-chair, and Richard Schilizzi was elected by votes of Commission J national delegates.

I.2 Discussion of Commission J budget

A motion was made and seconded to allocate half of the next triennium's budget to travel support for the General Assembly, encouraging participation from many countries.

Professor Hewitt reviewed the activities and budget expenditures of the previous triennium.

I.3 Nomination of a candidate for the Philips Prize

Professor Hewitt announced the existence of the Philips Prize for the best Young Scientist paper in this triennium. A committee consisting of Makoto Inoue, Roy Booth, and Peter Napier was appointed to review the papers and to put forward to the Board Commission J's candidate.

I.4 Commission J resolutions

Resolutions on radio quiet zones and the redefinition of UTC eliminating the leap second were discussed. Concerning the former, an amendment was approved and a drafting group was appointed. The second resolution was unanimously approved with eight delegates present to vote.

I. 5. Submission of abstracts and papers, and merging of RRS and RSB

The submission procedure of abstracts and papers was discussed. Submission procedures involving fewer actions on the part of the author were supported.

It was voted that the two publications (Review of Radio Science and Radio Science Bulletin) should be combined. A suggestion was made that the review articles should be indexed in the NASA Astrophysics Data System (ADS).

II. Second Business Meeting: 21 August 2002

II.1 Report on Tuesday Council Meeting

It was reported by the Chair that in the Council Meeting on 20 August , R. Schilizzi had been approved as the Vice Chair. The resolution on the leap second was approved with the provision that "committee" be replaced by "working group," and a discussion of radio quiet zones was postponed until 22 August.

II.2 Reports of working groups and IUCAF

Activity reports of the Global VLBI Working Group (GVWG) and Leap Second were presented. A new Chair of the GVWG (J. Romney, NRAO) was proposed by R. Schilizzi (current GVWG Chair) and approved. The IUCAF

Chair (D. Emerson) reported on the status of IUCAF membership from URSI: five URSI members - W.A. Baan, P.P. Baptista, M. Davis, K. Ruf, and A. van Eyken - have completed their terms, and W.A. Baan and K. Ruf, both former chairs, were co-opted. A new member, Professor Yashwant Gupta (India), was proposed and approved.

II.3 Resolutions

A proposal for the inter-commission resolution on the Solar Power Satellite (SPS) from the host Commission H was supported, with amendments. The inter-commission working group on RFI was proposed by A. van Ardenne, and approved. Participants were skeptical about the effectiveness of the inter-commission working group, Scientific Committee for Telecommunications (SCT).

III. Third Business Meeting: 23 August 2002

III.1 Report on Thursday Council Meeting

The resolution on Radio Quiet Reserves had been approved, and New Delhi will be the site for the next GA in 2005.

III.2 Scientific program for GA 2005

Some proposals were given for the scientific sessions for GA 2005. However, it was argued that we should circulate proposals for the sessions more widely after this GA, as the number of participants in the last business meeting was limited. This was agreed.

BUSINESS TRANSACTED BY COMMISSION K

Chair : Professor S. Ueno (Japan)
Vice-Chair : Professor B. Veyret (France)

I. Open Commission Meeting: Tuesday 19 August

The Commission held one Open Commission meeting, on Tuesday 19th August 2002 at 6 p.m. It was attended by a about 50 delegates and members. The approved agenda was the following:

- Introduction
- Election of Vice Chair for 2002-2005
- GA 2002 Organization and Program
- Session proposals for GA 2005
- Report on K articles in Radio Science Bulletin
- Scientific Committee on Telecommunications (SCT) (interaction between Commission K and WHO)
- Intercommission Working Group on Solar Power Satellite lead by Commission H
- Other business

I.1 Election of a Vice-Chair

Three candidates had been nominated for the position of Vice-Chair for the next triennium : F. Prato (Canada), K. Hansson Mild (Sweden) and G. D'Inzeo (Italy). At the business meeting, any Official Member who was present and had previously voted was given the opportunity to change his vote, and any Member who had not voted was allowed to do so. In the ballot, 35 votes were cast, resulting in the submission to the Council of the following two names, in order of preference: (1) F. Prato, (2) G.D'Inzeo.

I.2 Terms of Reference

The following Terms of Reference were not modified.

The Commission is charged with promoting research and development in the following domains :

(a) physical interactions of electromagnetic fields with biological systems;
(b) biological effects of electromagnetic fields;
(c) interaction mechanisms;
(d) human exposure assessment;
(e) experimental exposure systems;
(f) medical applications.

The Commission emphasises its interdisciplinary character and fosters research co-operation among various disciplines.

I.3 Review of Radio Science

The Commission K Editor of the Review of Radio Science for the last triennium, Bernard Veyret reported on the procedure he had used to select the topics and authors of the Commission K chapters. The result was good reviews of important topics. The incoming Commission K editor is F. Prato.

I.4 Inter-Commission Working Groups

There is only one Joint Working Group KE : EMI with Medical Equipment (Co-Chair for Commission E : S. Alfas, Denmark), which was not discussed further.

I.5 2004 Symposium

A Symposium on topics to be announced will be organised by B. Veyret in Bordeaux, France, in the Spring of 2004.

I.6 Commission K Programme in Maastricht

The Chair initiated a discussion on the Commission K Programme in Maastricht. The technical contents of the sessions were considered to be well balanced between the Commission sessions and the joint sessions organised with other Commissions (see list below).

I.7 SCT

B. Veyret will be Commission K's member of SCT, as a liaison with WHO.

I.8 Vote of Thanks

There was a vote of thanks for Prof. S. Ueno who had worked hard during the last triennium.

II.Scientific programme

Commission K organised six scientific sessions, namely:

- K1: Mechanisms & modelling of electromagnetic interaction with biological systems
  F. Barnes (USA) and G. d'Inzeo (Italy)
- K2: Biological effects of electromagnetic fields
  L. Anderson (USA) and T. Shigemitsu (Japan)
- K3: Hazard assessment for wireless communication
  B. Veyret (France) and M. Taki (Japan)
- K4: Biomedical applications of electromagnetic fields and waves
  J. Lin (USA) and C. Gabriel (UK)
- K5: Epidemiology of exposure to environmental electromagnetic fields
  R. de Seze (France) and N. Yamaguchi (Japan)
- K6: Topics in biomagnetics
  S. Ueno (Japan} and B. Veyret (France)

Commission K further participated in four joint sessions.

- KA: Exposure Assessment For Cellular And Personal Telecommunications
  N. Kuster (K, Switzerland) and Q. Balzano (A, Italy)
- KB: Computation of Electromagnetic Fields in the Human Body
  O. Gandhi (K, USA) and M. Okoniewski (B, Canada)
- KC: Health Effects of Mobile Telephones
  M. Taki (K, Japan) and G. Neubauer (C, Austria)
- KE: Electromagnetic Interference with Medical Devices
  T. Nojima (K,Japan) and Michael R. Murphy (USA)

ISES Annual Report for 2002

1. Introduction

The International Space Environment Service is a permanent service of the Federation of Astronomical and Geophysical Data Analysis Services (FAGS) under the auspices of the International Union of Radio Science (URSI) in association with the International Astronomical Union (IAU) and the International Union of Geodesy and Geophysics (IUGG). The ISES was called IUWDS (International URSIgram and World Days Service) until 1996. The IUWDS was formed in 1962 as a combination of the former International World Days Service, initiated in 1959 as a part of the IGY, and the former URSI Central Committee of URSIgrams which initiated rapid international data interchange services in 1928.

The mission of the ISES is to facilitate near-real-time international monitoring and prediction of the space environment by: the rapid exchange of space environment information; the standardization of the methodology for space environment observations and data reduction; the uniform publication of observations and statistics; and the application of standardized space environment products and services to assist users reduce the impact of space weather on activities of human interest.

Three main functions accomplish the task of the ISES. Firstly, the International URSIgram Service provides standardized rapid free exchange of space weather information and forecasts. Secondly, the ISES prepares the International Geophysical Calendar each year. This calendar gives a list of 'World Days' during which scientists are encouraged to carry out their experiments. And thirdly, on behalf of COSPAR, the monthly Spacewarn Bulletins summarize the status of satellites in earth orbit and in interplanetary space.

The ISES also sponsors meetings to improve space weather services and to promote the understanding of space weather and its effects for users, researchers, the media, and the general public. Solar-Terrestrial Prediction Workshops were held thus far, in Boulder (1979), Meudon near Paris (1984), Leura near Sydney (1989), Ottawa (1992), and Hitachi near Tokyo (1996). In recent years ISES has had its business meeting in conjunction with the Space Weather Week meetings organized by NOAA Space Environment Center. Through such meetings, ISES members play an active role in the transition of scientific results into operational space weather services.

2. The International Ursigram Service in 2002

The International Ursigram Service in 2002 operates through eleven Regional Warning Centers (RWC) and one Associate Regional Warning Center (ARWC). The 11 RWCs are located in: Beijing (China), Boulder (USA), Brussels (Belgium), Lund (Sweden), Moscow (Russia), New Delhi (India), Ottawa (Canada), Prague (Czech Republic), Sydney (Australia), Tokyo (Japan) and Warsaw (Poland); the ARWC in Toulouse (France). The RWC in Boulder plays a special role as 'World Warning Agency (WWA)', acting as a hub for data exchange and forecasts.

Each RWC collects data available in its own geographic area, concerning the state of the sun-earth environment, both from its own observatories and from regional scientific institutes and universities. These data and reports are distributed daily, on request to users and to other RWCs. Information transmitted through the ISES network is analyzed by Regional Warning Centers which produce a number of "summary" reports and forecasts. The "Geoalert", a forecast of solar-geophysical conditions for the next few days, is a particularly important one of these reports. Geoalerts prepared by RWCs are sent to the WWA in Boulder each day. The WWA then issues a Geoalert which is distributed worldwide each day at 0300 UT through the ISES network.

3. Publications

The International Geophysical Calendar (IGC) is prepared and distributed by the Secretary for World Days. The IGC can be accessed on the ISES Home Page and is also printed annually in many international journals. 1800 copies of IGC 2003 were printed and distributed in December, 2002.

The World Warning Agency for Satellites issues the Spacewarn Bulletin every month on behalf of COSPAR. The Spacewarn Bulletin provides a listing of launches and brief details of each launch. The WWA for Satellites is operated by the World Data Center-A for Rockets and Satellites, NASA/GSFC.

The ISES Website contains information about ISES and its Warning Centers, copies of the ISES code book, and links to the home pages of ISES centers. The URLs for ISES activities are given below.

- **ISES Home Page**: http://www.ises-spaceweather.org/
- **International Geophysical Calendar**: http://www.ises-spaceweather.org/geo_calender/
- **Spacewarn Bulletins**: http://nssdc.gsfc.nasa.gov/spacewarn

4. The ISES Directing Board

In 2002 Dr K. Marubashi retired as Director of ISES. Elections were held by e-mail ballot for the position of

director, and subsequently for the position of deputy director. The new office holders are:

- ISES Director: Dr David Boteler, Natural Resources Canada, Geomagnetic Laboratory, 7 Observatory Crescent, Ottawa, Ontario K1A 0Y3, Canada, Tel: 1-613-837-2035, Fax: 1-613-824-9803, E-mail: dboteler@.nrcan.gc.ca
- ISES Deputy Director: Dr. Henrik Lundstedt, Swedish Institute of Space Physics, Lund Space Weather Center, Scheelev. 17, SE-223 70 Lund, Sweden, Tel: +46-46-2862120, Fax: +46-46-129879, E.mail: henrik@lund.irf.se

The 2002 Directing Board meeting was held in Boulder, Colorado, on April 14. Reports were received from the Regional Warning Centers and a re-examination was started of the data utilized and exchanged by RWCs. Other topics discussed included verification of forecasts, ESA participation in ISES, and ISO standards for space environment models. New working groups were set up concerned with satellite effects (chair: A. Hilgers), geomagnetic effects (chair: L. Trichtchenko), and radio effects (R. Dabas) and ISO Standards (chair: R. Thompson).

The next Directing Board meeting is planned to be held in Boulder on May 18, 2003.

5. ISES Directing Board Membership

The present list of ISES officers and representatives is as follows:

- ISES Director:
  D. H. Boteler,dboteler@NRCan.gc.ca
- ISES Deputy Director:
  H. Lundstedt, henrik@lund.irf.se
- ISES Secretary for Space Weather:
  J. Kunches, Joseph.Kunches@noaa.gov
- ISES Secretary for World Days:
  H. Coffey Helen.E.Coffey@noaa.gov
- RWC Australia (Sydney) delegate:
  R. Thompson, richard@ips.gov.au
- RWC Belgium (Brussels) delegate:
  P. Cugnon, pierre.cugnon@oma.be
- RWC Canada (Ottawa) delegate:
  H.-L. Lam, HLam@NRCan.gc.ca
- RWC China (Beijing) delegate:
  H. Wang, hnwang@bao.ac.cn
- RWC Czech Rep. (Prague) delegate:
  D. Buresova, buresd@ufa.cas.cz
- RWC India (New Delhi) delegate:
  R.S. Dabas, rsdabas@csnpl.ren.nic.in
- RWC Japan (Tokyo) delegate:
  T. Nagatsuma, tnagatsu@crl.go.jp
- RWC Poland (Warsaw) delegate:
  Z. Klos, marz@cbk.waw.pl
- RWC Russia (Moscow) delegate:
  V.A. Burov, hciag@sunny.aha.ru
- RWC Sweden (Lund) delegate:
  H. Lundstedt, henrik@lund.irf.se
- WWA USA (Boulder) delegate:
  J. Kunches, Joseph.Kunches@noaa.gov
- FAGS Representative:
  E.A. Tandberg-Hanssen, tandberger@cspar.uah.edu
- IAU Representative:
  H. Coffey, Helen.E.Coffey@noaa.gov
- IUGG Representative:
  H. Coffey, Helen.E.Coffey@noaa.gov
- URSI Representatives:
  P. Wilkinson, phil@ips.gov.au
  R. Pirjola, Risto.Pirjola@fmi.fi
  S. Pulinets, pulse@igeofcu.unam.mx

6. ISES Regional Warning Centres

RWC Australia: IPS Radio and Space Services, PO Box 1386, Haymarket NSW 1240, Australia, http://www.ips.gov.au/

RWC Canada: Natural Resources Canada, Geomagnetic Laboratory, 7 Observatory Crescent, Ottawa Ontario K1AOY3, Canada, http://spaceweather.ca/

RWC Czech Republic: Institute of Atmospheric Physics, Academy of Sciences, Bocni II, 141 31 Prague 4, Czech Republic, http://rwcprague.ufa.cas.cz/

RWC Japan: Communications Research Laboratory,4-2-1 Nukui-Kitamachi, Koganei, Tokyo 184-8795, Japan, http://hirweb.crl.go.jp/

RWC Russia: Institute of Applied Geophysics, Rostokinskaya str., 9, 129128 Moscow, Russia, http://www.geospace.ru

World Warning Agency: NOAA Space Environment Center, 325 Broadway, Boulder, CO, USA, http://www.sec.noaa.gov/

RWC Belgium: Solar Influences Data Analysis Center (SIDC), Royal Observatory of Belgium, Ringlaan – 3 – Avenue Circulaire, B-1180 Brussel, Belgium, http://sidc.oma.be/

RWC China: National Astronomical Observatories, Chinese Academy of Science, 20A Datun Road, Chaoyang District, Bejing, China, http://rwcc.bao.ac.cn/

RWC India: National Physical Laboratory, New Delhi – 110012, India, http://www.nplindia.org/npl/index.htm

RWC Poland: Space Research Centre, Polish Academy of Sciences, Bartycka 18A, 00-716 Warsaw, Poland, http://www.cbk.waw.pl/rwc/rwc.html

RWC Sweden: Swedish Institute of Space Physics, Scheelev. 17, SE-223 70 Lund, Sweden, http://www.lund.irf.se/rwc

ARWC France: CLS, 8-10 rue Hermes, 31526 Ramonville Saint-Agne, France, http://www.cls.fr/previsol

Dr. David Boteler, Director of ISES

IUCAF Annual Report for 2002

1. Introduction

The Scientific Committee on Frequency Allocations for Radio Astronomy and Space Science, IUCAF, was formed in 1960 by URSI, IAU, and COSPAR. Its brief is to study the requirements of radio frequency allocations for radio astronomy, space science, and remote sensing in order to make these requirements known to the national and international bodies that allocate frequencies. IUCAF operates as a standing committee under the auspices of ICSU, the International Council for Science and is strongly supported by URSI, IAU, and COSPAR. ICSU works under the umbrella of the United Nations organization UNESCO.

2. Membership

At the end of 2002 the composition of membership for IUCAF was:

URSI	W. van Driel	France
	A.J. Gasiewski	USA
	Y. Gupta	India
	A. Tzioumis	Australia
	G. Wannberg	Sweden
IAU	S. Ananthkrishnan	India
	R.J. Cohen	UK
	D.T. Emerson(Chair)	USA
	M. Ohishi	Japan
	K.F. Tapping	Canada
COSPAR	S. Gulkis	USA
	J. Romney	USA

Additional Co-opted Members:

W.A. Baan	(former Chair)	The Netherlands
K. Ruf	(former Chair)	Germany

Ex Officio Advisers:

Director ITU Radio Bureau	Robert Jones, Canada
ITU Radio Board	Ryszard Struzak, Poland
Councilor Study Group 7	Kevin Hughes, UK
Councilor Study Group 1	AlbertNalbandian, Armenia

(note: The Plenipotentiary Conference of the ITU has recently elected Mr. Valeri Timofeev from Russia as new Director of the Radio Bureau. The new councilor for both Study Groups 1 and 7 is Mr. Dusan Schuster from Slowenia.)

The URSI GA in 2002, marked the completion of terms with IUCAF of the URSI members M. Davis, A. van Eyken and P. Poiares Baptista. At the 2002 GA, the retiring members were replaced by A. Gasiewski (Commission F), Y. Gupta (Commission J) and G. Wannberg (Commission G); the new Commission F and G members bring expertise in remote sensing and ionospheric physics to the committee. In addition, during 2002 Jon Romney joined IUCAF as a representative from COSPAR; Jon brings VLBI experience to IUCAF.

At the GA, two former chairs of IUCAF, W. Baan and K. Ruf, also completed their terms as URSI representatives. However, IUCAF is fortunate that both have agreed to continue to serve with the committee as co-opted members.

IUCAF continues to maintain its network of Correspondents in more than 35 countries in order to interact with national authorities responsible for radio frequency management.

3. International Meetings

During the period of January to December 2002, IUCAF Members and Correspondents took part in the following international meetings:

February:	ITU-R Working Party 7D in Geneva, Switzerland
March:	ITU-R Task Group 1-7 in Washington DC, USA
April:	ITU-R Working Party 4A in Geneva, Switzerland
May:	ITU-R Working Party 8D in Geneva, Switzerland
June:	IUCAF Summer School on Spectrum Management in Radio Astronomy, at Green Bank, WVa, USA
August:	URSI General Assembly, Maastricht, The Netherlands
September:	ITU-R Working Party 8D in Geneva, Switzerland
October:	ITU-R Working Party 7D in Geneva, Switzerland
	SFCG-22 in Monteporzio Catone, Italy
November:	ITU-R Task Group 1-7 in Geneva, Switzerland
	ITU-R CPM in Geneva, Switzerland

Additionally, many IUCAF members and correspondents participated in national or regional meetings (including CRAF, CORF, the FCC etc.), dealing with spectrum issues in general or preparing for WRC-2003.

3.1 IUCAF Business Meetings

During the year 2002 IUCAF had a number of face-to-face meetings as a committee. These meetings took place in Geneva, Switzerland, in Washington DC, USA, in Maastricht, The Netherlands, and at Green Bank, WVa, USA. Such meetings are always held before Working Party 7D, Task Group 1-7, or ITU CPM meetings, with the

purpose of discussing and focusing on important issues on the agenda of the respective meetings in preparation for the public ITU sessions. During these ITU sessions, typically lasting a week to 10 days, a number of ad-hoc meetings of IUCAF are held to discuss further the IUCAF strategy. Other IUCAF business such as changes in the membership, action plans for future workshops or initiatives, and future contributions to international spectrum meetings were also discussed at these meetings.

Although such face-to-face meetings at the ITU venues and elsewhere have been convenient and effective, throughout the year much IUCAF business continues to be undertaken via email communications between the members and correspondents.

Open IUCAF meetings were held at the URSI General Assembly in Maastricht in August, and also at the URSI US National meeting in Boulder in January.

3.2 Summer School on Spectrum Management in Radio Astronomy

The responsibility for taking care of international and national regulatory issues involved in maintaining access to interference-free spectrum, essential to radio astronomy, has been taken by a relatively small number of individuals – notably, by the IUCAF membership. Demands on the radio spectrum are increasing dramatically, due to huge increases in the demand and available of wireless applications, communications satellites, and the marketing of new technologies such as ultra-wide band systems. The development and health of radio astronomy depend critically on astronomers' continued access to the radio spectrum, and this in turn demands that astronomers and particularly radio observatories pay closer attention to the technical and regulatory issues that arise in relation to managing the radio spectrum, particularly as they relate to radio astronomy. There is a need to make a broader section of the radio astronomy community much more aware of the issues, and there is a need for more radio astronomers to become involved in technical and regulatory activities that protect radio astronomical observations.

To this end, the first ever Summer School on "Spectrum Management and Radio Astronomy" was held, at the NRAO observatory in Green Bank, WVa from June 9th to June 14th. It was, by any criterion, a great success. Approximately 35 formal lectures were presented during the week, in addition to some hardware demonstrations by Green Bank staff. There were 45 participants from 12 countries; 23 from the US and 22 foreign. Seven of the participants were female, 38 male - a much higher female representation than is generally found in Astronomy, Engineering or in Spectrum Management. The Summer School was made possible by grants from the NSF, from URSI, and via IUCAF from ICSU (the International Council for Science.) Details of the Summer School, including most of the Power Point presentations, are available via http://www.iucaf.org/sschool/ .The lectures will be compiled into a book, to be printed by NRAO. The intention is to repeat the Summer School on a 3-year cycle.

4. Contact with the Unions

IUCAF keeps regular contact with the secretariats of the supporting unions and with the ICSU secretariat. The Unions plays a strong supporting role for IUCAF and the membership is greatly encouraged by their support.

IUCAF was strongly represented at the URSI General Assembly, held in Maastricht, The Netherlands, in August 2002. An open IUCAF meeting was held during the assembly, and new URSI members from URSI Commissions F, G and J were elected.

IUCAF members actively participated in national URSI meetings and in IAU Seminars and Symposia. An open IUCAF meeting was held during the US National URSI meeting in Boulder, Colorado in January 2002.

5. Affairs of the International Telecommunication Union

5.1 ITU-R Task Group 1-7 on the Protection of Passive Services from Unwanted Emissions

Task Group 1-7 of ITU-R continued to constitute the biggest workload on the committees; meetings were held in March and November of 2002, with the deadline of producing agreed documents in time for the CPM meeting held in Geneva in November.

As a result of the continued pressure from the active Space Services the protection of the passive services has been limited to a consideration on a "band-by-band" basis. Rather than having general limits that would benefit all spectrum users by reducing unwanted emissions as specified in Rec. 66, compromises are being discussed, limiting the degree of protection afforded to the radio science bands to what is considered practical by the interfering service in specific bands. This "band-by-band study" was continued in Task Group 1-7 of ITU-R Study Group 1.

Additionally, TG 1-7 was responsible for preparing text on agenda item 1.8.2 for the preparatory meeting of WRC-03. This agenda item asks for consideration of regulatory measures to protect the passive scientific radio services in their frequency bands from unwanted emissions, taking into account the results of the "band-by-band studies". The final version of CPM text, which forms part of the CPM Report that helps delegated at the WRC to discuss and take decisions on the agenda items, was produced at the March 2002 meeting, but the work on the "band-by-band studies" continued in the November meeting, in the week preceding the CPM. Hence the concentrated work during and between

the meetings. IUCAF had been very active in the formation of TG 1-7, continuing the work of TG 1-5 and with the appropriate mandate. Dr. Willem Baan, IUCAF member and former IUCAF chairman, had been nominated to be co-chairman of that ITU-R Task Group. Largely due to his and his co-chairman's able guidance, but also due to excellent IUCAF contributions, timely delivery of input to the Conference Preparatory Meeting occurred and a number of band-by-band studies could be concluded with reasonable results. This texts will not go as far as radio astronomers and remote sensing scientists would have liked, but should represent a reasonable compromise that leaves all options open for the World Radiocommunication Conference in 2003.

Many "band-by-band studies" are still under way, and more may be started when new satellite systems are proposed by industry. These studies may become part of the normal life of the frequency managers of the scientific services.

5.2 ITU-R Working Party 7D

Working Party 7D met in February and October this year. WP7D is devoted to Radio Astronomy.

The largest fraction of the work continued to be devoted to issues related to TG1-7 matters. A number of band-by-band studies was brought forward and liaison statements written for TG1-7. From the other work, one topic deserves special mention: one satellite company is working on wide-band communication systems, including earth-to-space, space-to-earth and satellite-to-satellite links, which will operate at optical frequencies. This early-stage study was brought to the attention of WP7D. 7D radio astronomers are now talking to their colleagues who observe at optical wavelengths, to try to convince them of the benefits of ITU-R work; the ITU will now start to consider optical frequencies to be within its scope. Optical astronomers have been fighting "light pollution" for long time and with good success in some cases. However, the use of the optical spectrum has so far not been regulated by an international agency like ITU, and protection of optical telescopes against light pollution has to be done locally, and individually for each site. At least for the use of the optical spectrum for communication purposes, this picture may change in future.

The more regular work in 7D comprises revisions of many ITU-R recommendations, which need to be updated following the very significant changes in the frequency bands above 71 GHz that occurred at WRC-2000, and also to accommodate improved technical parameters. One new recommendation, which could be completed within WP7D and handed upwards to the approval process, deals with radio frequency bands above the current limit of 275 GHz, and which are of importance to radio astronomy. Additionally, WP7D has started to revise the ITU-R Handbook on Radio Astronomy and plans to publish a second edition soon. In all cases, IUCAF members play key roles in bringing these issues forward.

5.3 Other Working Parties

It has become the rule in recent years that the specialist Radio Astronomy working party at the ITU, WP7D, is attended by representatives of other interests. At a recent WP7D meeting in Geneva there were 50 participants registered for the meeting, but only 14 of those present had actually used a radio telescope. The unavoidable impact of this is that many of the documents produced by WP7D, representing the interests of Radio Astronomy, already contain compromises to accommodate the interests of other groups. This potentially puts radio astronomers at a significant disadvantage in the ITU process.

In an attempt to compensate for this development, IUCAF has tried to have representatives at other ITU working parties. This is not always possible and puts a severe strain on our manpower resources, but during 2002 at least one IUCAF member attended meetings of WP4A (Efficient orbit & spectrum utilization) and WP8D (Mobile satellites & radio determination satellites). This has proved to be quite useful, and it is hoped that the practice can continue.

6. Publications and Reports

IUCAF has contributed a number of documents to the proceedings of Task Group 1-7 and Study Group 7. These documents have all become available on the ITU-R web pages, so have not necessarily been distributed separately by email. IUCAF now has a permanent web address, http://www.iucaf.org , where the latest updates on the organization's activities will always become available.

7. Conclusion

IUCAF interests and activities range from preserving what has been achieved through co-ordination or mitigation techniques, to looking very far into the future of highest frequency use. Current priorities, which will certainly keep us busy through the next two years, include the band-by-band studies for cases where allocations are made to satellite down-link services close in frequency to the radio astronomy bands, and the preparations for and participation at the WRC-03.

IUCAF is thankful for the moral and financial support that has been given for these continuing efforts by ICSU, URSI, IAU, and COSPAR during the recent years. IUCAF also recognizes the clear support that has been given by radio astronomy observatories and universities to individual members in order to participate in the work of IUCAF.

Darrel Emerson, Chairman IUCAF
Tucson, AZ, USA
http://www.iucaf.org

Commission B

Call for Papers
2004 URSI International Symposium on Electromagnetic Theory

Pisa, Italy May 23-27, 2004

General Information

In a long tradition, Commission B, "Fields and Waves", of the International Union of Radio Science (URSI) organizes a triennial series of international symposia on electromagnetic theory. The next symposium in this series is the 2004 International Symposium on Electromagnetic Theory, which will be held in Pisa, Italy, May 23-27, 2004. It is hosted by the Italian Member Committee of URSI and is organized by a Local Organizing Committee at the University of Pisa, in collaboration with the Italian Electromagnetic Society (SIEm). The scope of the Symposium covers all areas of electromagnetic theory and its applications. The working language of the Symposium is English. There will be a limited number of Young Scientist Awards (YSA) available for application.

Suggested Topics

Contributions concerning all aspects of electromagnetic theory and its applications are welcome. Novel and innovative contributions are particularly appreciated. Special topics will also be announced in the Final Call for Papers in addition to the following list.

- New basic theoretical developments
- Scattering and diffraction
- Inverse scattering and imaging
- Time domain methods
- High-frequency methods
- Guided waves
- Solutions to canonical problems
- Propagation and scattering in layered structures
- Random media and rough surfaces
- Metamaterials and complex media
- Beam and pulse propagation and scattering in lossy and/or dispersive media
- Non-linear phenomena
- Antennas: general aspects
- Antenna arrays, planar and conformal
- Numerical methods: general aspects
- Numerical methods for integral and differential equations
- Hybrid methods
- Interaction of EM waves with biological tissues
- EM theory and applications for radio systems
- Antennas and propagation for communication systems: smart antennas, UWB systems, etc.
- Mathematical modelling of EM problems
- Others

Session Proposals

Proposals of novel topics, special sessions as well as session organization are welcome. Send the proposal as soon as possible to mando@antenna.ee.titech.ac.jp.

Symposium Location

The Symposium will be held at the University Conference Centre, in downtown Pisa. This important University city is located near the Tyrrhenian Sea (11 Km) in north-western Tuscany, along the banks of the Arno river, and approximately 80 Km west of Florence. Worldwide known for its extraordinary Leaning Tower, Pisa is a place of artistic treasures, heritage of its millenary history whose point of highest splendor dates back to the age of Maritime Republics (12th century).

Symposium Time Table

June, 2003	Final Call for Papers
Nov. 1, 2003	Deadline for receipt of YSA papers in the 3-pages camera-ready format and YSA applications (see the conference Web site for instructions)
Nov. 15, 2003	Deadline for receipt of papers in the 3-pages camera-ready format (see Web site)
Jan. 15, 2004	Notification of authors regarding acceptance of papers, notification of YSA applicants
Mar. 15, 2004	Deadline for pre-registration of authors
May 23-27, 2004	Symposium

Conference Contacts

General questions and Symposium technical program:
Prof. Makoto Ando, Chair, Commission B of URSI
Department of Electrical and Electronics Engineering
Tokyo Institute of Technology
2-12-1, Oookayama, Meguro
Tokyo 152-8552, Japan
E-mail: mando@antenna.ee.titech.ac.jp
Phone: +81-3-57342563 Fax: +81-3-57342901

Questions regarding local arrangements:
Prof. Giuliano Manara, Chair, Local Organizing Committee
Department of Information Engineering,
University of Pisa, Via Diotisalvi 2
I-56126 Pisa, Italy
E-mail: g.manara@iet.unipi.it
Phone: +39-050-568552 Fax: +39-050-568522

Conference Secretariat
URSI-B2004 Conference Secretariat
Department of Information Engineering,
University of Pisa, Via Diotisalvi 2
I-56126 Pisa, Italy
E-mail: URSI-B2004@ing.unipi.it
Phone: +39-050-568511 Fax: +39-050-568522

Submission and Further Information

The instructions for the submission of papers and the updated information on the Symposium will be available in the Final Call for Papers and on the conference Web site:

www.ing.unipi.it/URSI-B2004

Conferences

CONFERENCE ANNOUNCEMENTS

URSI/COSPAR International Reference Ionosphere Workshop

Rhodes University, Grahamstown, South Africa, 6 - 10 October 2003

The URSI/COSPAR Working Group on the International Reference Ionosphere (IRI) will hold its next annual meeting at Rhodes University, Grahamstown, South Africa, from October 6 to 10, 2003. IRI is the reference standard for ionospheric parameters recommended for international use by the Committee on Space Research (COSPAR) and by the International Union of Radio Science (URSI). The annual meetings are the primary venue for improvements and refinements of the IRI representation of ionospheric electron density, electron temperature, ion composition, ion temperatures and electron and ion drift. The special emphasis of the 2003 Workshop will be on quantifying ionospheric variability. All papers related to IRI are welcome, particularly papers that point out shortcomings of the model, papers that introduce improvements or new parameters, and papers that report on applications of the IRI model. It is expected that selected papers from this meeting will be published in Advances in Space Research.

Organizing Committee

L. McKinnell (South Africa), A. Poole (South Africa), D. Bilitza (USA)

Programme Committee

B. Reinisch (USA), D. Bilitza (USA), L. McKinnell (South Africa), K. Oyama (Japan), K. Rawer (Germany), P. Dyson (Australia), S. Radicella (Italy/Argentina), P. Bradley (U.K.), S. Pulinets (Russia)

Abstracts

Abstracts are due by APRIL 15, 2003. Please include title, author(s), address with Fax and e-mail and send by e-mail to L.McKinnell@ru.ac.za. The length of the whole abstract should not be more than one page.

Contact

The homepage for the IRI 2003 workshop will be at http://phlinux.ru.ac.za/hoia/IRI2003/

More information about the IRI project and past IRI workshops can be found at http://nssdc.gsfc.nasa.gov/space/model/ionos/iri.html The homepage of the Hermann Ohlthaver Institute for Aeronomy (HOIA), the host institute, is at http://phlinux.ru.ac.za/hoia/

URSI CONFERENCE CALENDAR

April 2003

Supernovae
Valencia, Spain, 22-26 April 2003
Contact : Prof. Jon Marcaide, Dpto. Astronomia, Universidad de Valencia, E-46100 Burjassot, Valencia, Spain, Phone: +34-963983079, Fax: +34-963983084, E-mail: sne2003@reber.uv.es, http://www.uv.es/2003supernovae/

May 2003

EMC Istanbul 2003 - 2003 IEEE Int. Symp. on Electromagnetic Compatibility
Istanbul, Turkey, 11-16 May 2003
Contact : Elya B. Joffe, P.O. Box 264, Kfar-Sava 44102, Israel, Fax +972 9-765 7065,eb.joffe@ieee.org , http://www.ortra.com/emc2003/

STAMMS - Spatio-Temporal Analysis and Multimpoint Measurement in Space
Orleans, France, 12-16 May 2003
cf. announcement in RSB December 2002, p.63
Contact : LPCE/CNRS and Université d'Orléans, 3A av. de la Recherche Scientifique, F-45071 Orléans, France, Fax : +33 238 63 12 34, http://web.cnrs-orleans.fr/~weblpce/stamms/

MST 10 - Tenth International Workshop on Technical and Scientific Aspects of MST Radar
Piura, Peru, 20-27 May 2003
cf. announcement in RSB September 2002, p.68-69
Contact : Dr. Jürgen Röttger, Max-Planck-Institut fuer Astronomie, D-37191 Katlenburg-Lindau, Germany, Fax +49 5556-979 410, E-mail roettger@linmpi.mpg.de , http://jro.igp.gob.pe

June 2003

2003 IEEE International Symposium on Antennas and Propagation ; URSI North American Radio Science Meeting
Columbus, Ohio, USA, 23-27 June 2003
Contact : Profs. W. D. Burnside, J. D. Young, ElectroScience Laboratory, The Ohio State University, 1320 Kinnear Road, Columbus, OH 43212, USA; Tel: +1 (614) 292-7981; Fax: +1 (614) 292-7297; e-mail: wdb@ampere.eng.ohio-state.edu ; young.20@osu.edu, http://APS2003.eng.ohio-state.edu

August 2003

ISMOT 2003 - 9th Int. Symp. On Microwave and Optical Technology
Ostrava, Czech Rep., 11-15 August 2003
cf. announcement in RSB December 2002, p.64
Contact : Prof. Jaromír Pitora, Symposium Chair, Department of Physics, Technical University of Ostrava, 708 33 Ostrava - Poruba, Czech Republic, E-mail: ismot2003@vsb.cz , http://www.ismot2003.cz

ISAPE 2003 - the 6th Int. Symp. On Antennas, Propagation and EM Theory
Beijing, China, 17-21 August 2003
Contact : Mr. Dayong Liu, Secretary, ISAPE2003, P.O.Box 165, Beijing 100036, CHINA, Tel: +86-10-6828 3463, Fax:+86-10-6828 3458, Email:davidwd@btamail.net.cn , http://www.cie-china.org/isape2003/

October 2003

IRI Workshop
Grahamstown, South Africa, 6–10 October 2003
Contact : Dr. L McKinnell, Hermann Ohlthaver Institute for Aeronomy, Department of Physics and Electronics, Rhodes University, P O Box 94, Grahamstown, 6140, South Africa, Fax: +27 46 622 5049,L.McKinnell@ru.ac.za, *(the preferred method of communication is e-mail)*, http://phlinux.ru.ac.za/hoia/IRI2003

Telecom 2003 & JFMMA
Marrakech, Morocco, 15-17 October 2003
Contact : Prof. Ahmed Mamouni, IEMN, Cité Scientifique, Av. Poincaré, B.P. 69, F-59652 Villeneuve d'Ascq, France, Fax +33 3201 9 7880, E-mail : ahmed.mamouni@iemn.univ-lille1.fr

November 2003

APMC 2003
Seoul, Korea, 4-7 November 2003
cf. announcement in RSB December 2002, p.64-65
Contact : Prof. Hyo Joon Eom, Dept. of Electrical Engineering, Korea Advanced Institute of Science and Technology, 373-1, Kusong-dong, Yusong-gu, Taejon, Korea, Fax : +82 42-869 8036, hjeom@ee.kaist.ac.kr , http://www.apmc2003.org

ClimDiff'03
Fortaleza, Brazil, 17-19 November 2003
cf. announcement in RSB December 2002, p.65
Contact : Mr. Martin P.M. Hall, Climdiff'03, RCRU, Rutherford Appleton Laboratory, Chilton, Didcot, OX11 0OX, United Kingdom, Fax +44 1235-446140, E-mail : martin.hall@rl.ac.uk, http://www.climdiff.com

May 2004

EMTS'04 - 2004 International Symposium on Electromagnetic Theory
Pisa, Italy, 23-27 May 2004
Contact persons : Prof. Makoto Ando, Commission B Chair, Dept. of Electrical and Electronic Engineering, Tokyo Institute of Technology, J2-12-1, Oookayama, Meguro, Tokyo 152-8552, Japan, E-mail: mando@antenna.ee.titech.ac.jp and Prof. Lotfollah Shafai, Commission B Vice-Chair, Dept. of Electrical & Computer Eng., University of Manitoba, 15 Gillson Street, Winnipeg, MB R3T 5V6, Canada, E-mail: shafai@ee.umanitoba.ca

June 2004

EMC'04 Sendai - 2004 International Symposium on Electromagnetic Compatibilty/Sendai
Sendai, Japan, 1-4 June 2004
Contact :Prof. R. Koga, Dept. of Communications Network Engineering, Okayama University, Japan, koga@cne.okayama-u.ac.jp , www.dev.cne.okayama-u.ac.jp

August 2004

ISAP'04 - 2004 Int. Symp. on Antennas and Propagation
Sendai, Japan, 17-21 August 2004
Contact : ISAP'04, Attn. Dr. Tokio Taga, NTT DoCoMo, Inc., 3-5, Hikarino-oka, Yokosuka, 239-8536 Japan, E-mail : isap-2004@mail.ieice.org , http://www.ieice.org/cs/isap/2004

An up-to-date version of this Conference Calendar, with links to the various conference sites can be found at http://www.ursi.org/Calendar.html
Do you wish to announce your meeting in this Calendar? More information about URSI-sponsored meetings can be found on our web site at http://www.ursi.org/Rules.html
URSI cannot be held responsible for any errors contained in this list of meetings.

News from the URSI Community

NEWS FROM THE MEMBER COMMITTEES

EGYPT

Twentieth National Radio Science Conference (NRSC'03)

Cairo, Egypt, 18-20 March 2003

The 20th National Radio Science Conference (NRSC 2003) will be held in Cairo, Egypt. The Atomic Energy Authority will host the conference over the period 18-20 March 2003. The conference will provide a valuable opportunity to exchange and update information and stimulate discussions on current and future research activities in the fields of the committee.

Program

The technical program will consist of invited and submitted papers covered by the URSI commissions A-K: A) Electromagnetic Metrology, B) Fields and Waves, C) Signals and Systems, D) Electronics and Photonics, E) Electromagnetic Noise and Interference, F)Wave Propagation and Remote Sensing, G) Ionospheric radio and Propagation, H) Waves in Plasma, J) Radio Astronomy, K) Electromagnetics in Biology and Medicine.

Conference chairmen

- Chairman: Prof. Dr. Ibrahim Salem, Chairman of Egyptian NRS Committee, National Academy of Sciences, Tel: (202) 2580256, Fax: (202) 7921270, E-mail ia.salem@ieee.org
- Vice-Chairman: Prof. Dr. Mohamed E. Abdelaziz, Ex-chairman, Atomic Energy Authority, Tel: (202) 7350460, Fax: (202) 7380717

Contact

Prof. Dr. Said E. El-Khamy
Faculty of Engineering
Alexandria University
Tel: (203) 5464998, Fax: (202) 5921853
E-mail: elkhamy@ieee.org
Internet: http://conf.Mans.eun.eg,
http://ursi-egypt.org

UNITED KINGDOM

National URSI Symposium

Leeds, United Kingdom, 7-8 July 2003

Call for Papers

The format of the URSI meeting follows a tradition of placing emphasis on presentations by young scientists and engineers, plus keynote papers given by senior UK researchers. Young radio-science researchers are encouraged to submit one page abstracts of papers for consideration for presentation at the meeting by 2 May 2003.

Topics

Papers relevant to any of the Commissions listed below will be considered: A) Electromagnetic Metrology, B) Fields and Waves, C) Signals and Systems, D) Electronics and Photonics, E) Electromagnetic Noise and Interference, F)Wave Propagation and Remote Sensing, G) Ionospheric radio and Propagation, H) Waves in Plasma, J) Radio Astronomy, K) Electromagnetics in Biology and Medicine.

Abstract submission

The deadline for abstract submission is 2 May 2003. Important is that abstracts must be prepared and submitted as outlined below. Any abstracts not meeting these criteria will not be accepted.

1. Abstracts must be no more than one A4 page in length, and must be prepared according to this layout.
2. The file format must either be .pdf or .doc.
3. Abstracts (either .pdf or .doc) should be submitted to Margaret Quirke: m.c.quirke@ee.leeds.ac.uk

Contact

Dr Stavros Iezekiel
Institute of Microwaves and Photonics
School of Electronic and Electrical Engineering
University of Leeds
Leeds LS2 9JT, United Kingdom
Tel. +44 (0) 113 343 2088, Fax. +44 (0) 113 343 2032

USA & CANADA

2003 IEEE International Antennas and Propagation Symposium and URSI North American Radio Science Meeting

Colombus, OH, USA, 22-27 June 2003

The 2003 IEEE AP-S International Symposium, sponsored by the IEEE Antennas and Propagation Society, and the 2003 URSI (International Union of Radio Science) meeting, sponsored by all Commission of URSI will be held jointly on June 22-27 at the Hyatt Regency. The technical sessions, workshops and short courses will be coordinated between the two symposia to provide a comprehensive and well-balanced program. This meeting is intended to provide an international forum for the exchange of information on state-of-the-art research in antennas and electromagnetic engineering.

Topics

- A1. Quantum metrology and fundamental concepts
- A2. Time and frequency
- A3. Time-domain metrology
- A4. EMC and EM pollution
- A5. Noise
- A6. Materials
- A7. Bioeffects and medical applications
- A8. Antennas and EM-field metrology
- A9. Impulse Radar
- A10. Planar structures and microstrip circuits
- A11. Interconnects and packaging
- A12. Microwave to sub-mm measurements
- B1. Antennas
- B1.1. Antenna analysis and design
- B1.2. Antennas for wireless communications
- B1.3. Arrays
- B1.4. Microstrip and printed antennas
- B1.5 Mechanical distortion effects in arrays and reflectors
- B2. Novel and complex media
- B3. Guiding structures and circuits
- B4. High-frequency techniques
- B5. Inverse scattering
- B6. Numerical methods: differential-equation based
- B6.1. Frequency-domain methods
- B6.2. Time-domain methods
- B7. Numerical methods: integral-equation based
- B8. Numerical methods: hybrid and other techniques
- B9. Rough surfaces and random media
- B10. Scattering
- B11. Theoretical electromagnetics
- B12. Transient fields, effects, and systems
- B13. Propagation in complex/confined environments (e.g., mines)
- C1. Beam forming and matched field processing
- C2. Spectrum estimation
- C3. Tomographic and inverse-theory methods
- C4. Environmental problems in cellular comm. sys.
- C5. Low total energy communications and signal processing methods
- C6. System identification
- C7. Wavelets
- C8. Application
- D1. Optoelectronic techniques, devices, and materials
- D2. Cryogenic electronic devices and circuits
- D3. Optical tranmission and interconnection
- D4. Microwave, mm-wave, and sub-mm-wave devices and circuits
- D5. High-speed devices and circuits
- D6. Mesoscale devices and associated materials
- D7. Vacuum microlectronics
- D8. RF and microwave application of MEMSE1. High power electromagnetics
- E2. Effects of transients on electronic systems
- E3. Spectrum management and utilization
- E4. Communication in the presence of noise
- F1. Propagation modeling and measurement
- F2. Satellite and terrestrial propagation
- F3. Point to point propagation effects
- F4. Mobile and personal access radio propagation
- F5. Remote sensing of oceans and atmosphere
- F6. Calibration and validation of satellite measurements
- G1. Ionospheric morphology
- G2. Ionospheric modeling and data assimilation
- G3. Transionospheric radio propagation or systems effects
- G4. Radar and radio techniques for diagnostics
- G5. Space weather-radio effects
- H1. Plasma instabilities
- H2. Generation and propagation of waves in plasmas
- H3. Wave interaction and wave-particle interaction
- H4. Plasma turbulence processes and chaos
- H5. Spacecraft-plasma interaction
- H6. Applications
- J1. Radio emissions from celestial objects
- J2. Radar reflections from planetary objects
- J3. Radio wave propagation
- J4. Antennas and antenna arrays
- J5. Radio astronomy instrumentation
- J6. Signal analysis including image processing
- J7. Spectrum protection and interference mitigation
- J8. Millimeter wavelength array design
- J9. Array design with large numbers of elements
- J10. VLBI instrumentation, techniques and science
- K1. Biological effects
- K2. Biomedical applications
- K3. Dosimetry
- K4. Exposure assessment
- K5. Application of RF to medicine

Exhibits

Industrial exhibits will be open June 22-24, 2003. Special Sessions/Short Courses: Individuals desiring to organize a special session, short course or workshop, or if you have other questions, please contact the appropriate chair.

General Chair

Walter D. Burnside
Ohio State University
ElectroScience Laboratory
Phone:(614)-292-5747
Burnside.1@osu.edu

URSI Liaison

Joel Johnson
Ohio State University
ElectroScience Laboratory
Phone: (614)-292-1606
Johnson.1374@osu.edu

Special Sessions

Jin Fa Lee
Ohio State University
ElectroScience Laboratory
Phone: (614)-292-7270
Lee.1863@osu.edu

Registration

Brian Baertlein
Ohio State University
ElectroScience Laboratory
Phone: (614)-292-0076
Baertlein.1@osu.edu

Web site

http://aps2003.eng.ohio-state.edu

Miscellaneous

Tarek Habashy Named Editor of Radio Science

Tarek Habashy has been named Editor of *Radio Science*, the journal co-sponsored by URSI and published by the American Geophysical Union. He follows Robert Hunsucker, who served as the Editor for the past eight years.

Tarek Habashy received the BSc degree from Cairo University, Egypt, and the MSc and PhD degrees from the Massachusetts Institute of Technology, Cambridge, MA, USA, in 1976, 1980, and 1983, respectively, all in Electrical Engineering. He joined Schlumberger-Doll Research (SDR) in Ridgefield, Connecticut, in 1983, and he is currently a Research Director of the Mathematics and Modeling Department. He is also a Scientific Advisor at SDR, conducting research in electromagnetic waves and fields, dielectric and resistivity logging tools and techniques, inverse scattering theory, antenna theory and design, mixed boundary value problems, and numerical analysis. He served as an Associate Editor and a Guest Editor of *Radio Science*, and as a member of the advisory committee board for the book series Progress in Electromagnetic Research. He is currently a member of the editorial boards of *Inverse Problems* and the *Journal of Electromagnetic Waves and Applications*. He is a Fellow of the Institute of Physics and of the IEEE, and a member of USNC/URSI Commission B. He holds 11 US patents and has published six book chapters, over 65 scientific articles in refereed journals, and 50 conference proceedings papers. He has also presented over 30 invited talks and co-presented over 95 contributed talks in international conferences. Dr. Habashy can be reached via Tel: +1 (203) 431-5563 or +1 (203) 431-5532; e-mail: thabashy@ridgefield.oilfield.slb.com.

Aims and Scope of *Radio Science*

Radio Science welcomes original scientific contributions on all aspects of electromagnetic phenomena related to physical problems. The coverage embraces the propagation through and interaction of electromagnetic waves with geophysical media, biological media, plasmas, and man-made structures, and includes, but is not limited to, the application of electromagnetic techniques to remote sensing of the Earth and its environment, telecommunications, signals and systems, the ionosphere, and radio astronomy. All frequencies (including optical) are considered.

Manuscripts should be submitted electronically using GEMS: http://radioscience-submit.agu.org. Editor's Assistant: Kristine Pumphrey, Tel: +1 (202) 777-7378; Fax: +1 (202) 777-7385; e-mail: radioscience@agu.org.

URSI Publications

Modern Radio Science 1999

Editor: Maria Stuchly
ISBN 0-7803-6002-8
List Price : USD 49.95 Member Price : USD 45.00
IEEE Product No. PC5837

Published by Oxford University Press
in cooperation with URSI and IEEE Press
Order 24 hours a day, 7 days a week :
1-732-981 0060 (Worldwide)
1-800-678 4333 (USA & Canada)
Fax 1-732 981 9667
E-mail : customer-service@ieee.org

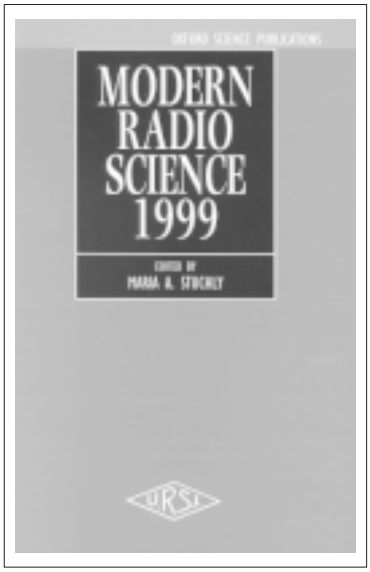

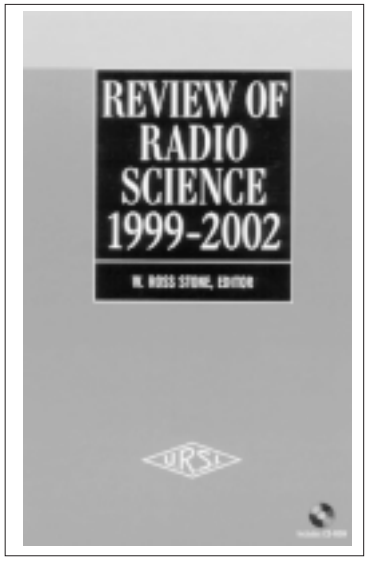

Review of Radio Science 1999-2002

Editor: W. Ross Stone
July 2002/Hardcover/977 pp
ISBN 0-471-26866-6
List Price : USD 125.00 Member Price : USD 106.25
IEEE Product No. #18493

Published by Wiley-Interscience
in cooperation with URSI and IEEE Press
Order can be sent to John Wiley & Sons, Inc.
from 8.30 a.m. to 5.30 p.m. :
1-732-469-4400 (Worldwide)
1-800-225-5945 (USA & Canada)
Fax 1-732 302-2370
E-mail : customer@wiley.com

Handbook on Radiopropagation Related to Satellite Communications in Tropical and Subtropical Countries

Editor: G.O. Ajayi
with the collaboration of :
S. Feng, S.M. Radicella, B.M. Reddy

Available from the URSI Secretariat
c/o Ghent University (INTEC)
Sint-Pietersnieuwstraat 41
B-9000 Gent, Belgium
tel. +32 9-264-33-20
fax +32 9-264-42-88
e-mail : ursi@intec.rug.ac.be

RADIO SCIENCE *Bimonthly*!

Radio Science contains original articles on all aspects of electromagnetic phenomena related to physical problems. Covers the propagation through and interaction of electromagnetic waves with geophysical media, biological media, plasmas, and man-made structures. Also included, but not limited to, are papers on the application of electromagnetic techniques to remote sensing of the Earth and its environment, telecommunications, signals and systems, the ionosphere, and radio astronomy.
ISSN 0048-6604, Volume 37

See a recent Table of Contents on the AGU Web Site: *http://www.agu.org*

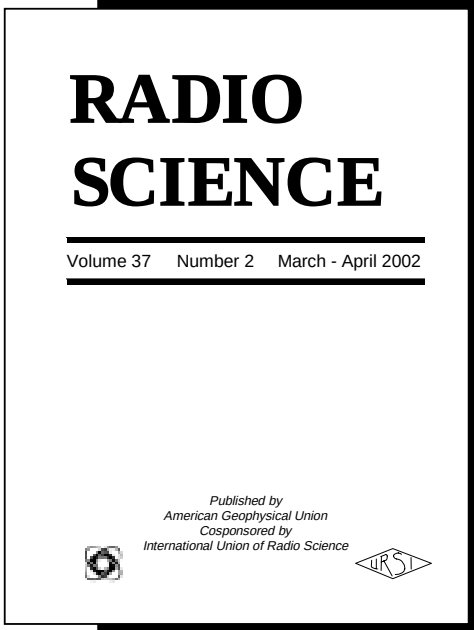

2002 Subscription Rates: On-line/ Print/On-line+Print

AGU Members & URSI Radioscientists: **$67/ $94/ $102**
Student AGU Members: **$17/ $38/ $43**
Shipping extra if outside North America for print subscriptions.

Subscribe Today!

	European Office	U.S. Office
Online:	http://www.agu.org	http://www.agu.org
E-Mail:	egs@copernicus.org	orders@.agu.org
Voice:	+49-5556-1440	+1-202-462-6900
Fax:	+49-5556-4709	+1-202-328-0566
Mail:	EGS - Orders Max-Planck Str. 13 37191 Katlenburg-Lindau GERMANY	AGU - Orders 2000 Florida Ave., NW Washington, DC 20009 USA

Cosponsored by U.R.S.I. International and published bimonthly by AGU.

Members of the Network of URSI Radioscientists may subscribe at the AGU member rate!

Submit to *Radio Science*!

Submissions to *Radio Science* are now done through the new **GEMS** electronic submissions system at **http://radioscience-submit.agu.org/**
For details on style, contact an editor's assistant listed below or consult the last pages of a recent issue of *Radio Science*.

Tarek Habashy, Editor
c/o Paul Cooper, Editor Assistant
AGU
2000 Florida Ave., NW
Washington, DC 20009

Ph: 202-777-7378
E-mail: radioscience@agu.org
Fax: 202-777-7385

AGU

Code: URSI02

Wireless Networks

The journal of mobile communication, computation and information

Aims & Scope:
The wireless communication revolution is bringing fundamental changes to data networking, telecommunication, and is making integrated networks a reality. By freeing the user from the cord, personal communications networks, wireless LAN's, mobile radio networks and cellular systems, harbor the promise of fully distributed mobile computing and communications, any time, anywhere. Numerous wireless services are also maturing and are poised to change the way and scope of communication. WINET focuses on the networking and user aspects of this field. It provides a single common and global forum for archival value contributions documenting these fast growing areas of interest. The journal publishes refereed articles dealing with research, experience and management issues of wireless networks. Its aim is to allow the reader to benefit from experience, problems and solutions described. Regularly addressed issues include: Network architectures for Personal Communications Systems, wireless LAN's, radio , tactical and other wireless networks, design and analysis of protocols, network management and network performance, network services and service integration, nomadic computing, internetworking with cable and other wireless networks, standardization and regulatory issues, specific system descriptions, applications and user interface, and enabling technologies for wireless networks.

Wireless Networks is a joint publication of the ACM and Baltzer Science Publishers. Officially sponsored by URSI

For a complete overview on what has been and will be published in Telecommunication Systems please consult our homepage:

BALTZER SCIENCE PUBLISHERSHOMEPAGE
http://www.baltzer.nl/winet

Special Discount for URSI Radioscientists

Euro 62 / US$ 65
(including mailing and handling)

Wireless Networks ISSN 1022-0038
Contact: Mrs. Inge Heleu
Fax +32 9 264 42 88 E-mail ursi@intec.rug.ac.be
Non members/Institutions: contact Baltzer Science Publishers

BALTZER SCIENCE PUBLISHERS
P.O.Box 221, 1400 AE Bussum, The Netherlands
Tel: +31 35 6954250 Fax: +31 35 6954 258 E-mail: publish@baltzer.nl

The Journal of Atmospheric and Solar-Terrestrial Physics

SPECIAL OFFER TO URSI RADIOSCIENTISTS

AIMS AND SCOPE

The *Journal of Atmospheric and Terrestrial Physics* (JASTP) first appeared in print in 1951, at the very start of what is termed the "Space Age". The first papers grappled with such novel subjects as the Earth's ionosphere and photographic studies of the aurora. Since that early, seminal work, the Journal has continuously evolved and expanded its scope in concert with - and in support of - the exciting evolution of a dynamic, rapidly growing field of scientific endeavour: the Earth and Space Sciences. At its Golden Anniversary, the now re-named *Journal of Atmospheric and Solar-Terrestrial Physics* (JASTP) continues its development as the premier international journal dedicated to the physics of the Earth's atmospheric and space environment, especially the highly varied and highly variable physical phenomena that occur in this natural laboratory and the processes that couple them. The *Journal of Atmospheric and Solar-Terrestrial Physics* is an international journal concerned with the inter-disciplinary science of the Sun-Earth connection, defined very broadly. The journal referees and publishes original research papers, using rigorous standards of review, and focusing on the following: The results of experiments and their interpretations, and results of theoretical or modelling studies; Papers dealing with remote sensing carried out from the ground or space and with in situ studies made from rockets or from satellites orbiting the Earth; and, Plans for future research, often carried out within programs of international scope. The Journal also encourages papers involving: large scale collaborations, especially those with an international perspective; rapid communications; papers dealing with novel techniques or methodologies; commissioned review papers on topical subjects; and, special issues arising from chosen scientific symposia or workshops. The journal covers the physical processes operating in the troposphere, stratosphere, mesosphere, thermosphere, ionosphere, magnetosphere, the Sun, interplanetary medium, and heliosphere. Phenomena occurring in other "spheres", solar influences on climate, and supporting laboratory measurements are also considered. The journal deals especially with the coupling between the different regions. Solar flares, coronal mass ejections, and other energetic events on the Sun create interesting and important perturbations in the near-Earth space environment. The physics of this subject, now termed "space weather", is central to the Journal of Atmospheric and Solar-Terrestrial Physics and the journal welcomes papers that lead in the direction of a predictive understanding of the coupled system. Regarding the upper atmosphere, the subjects of aeronomy, geomagnetism and geoelectricity, auroral phenomena, radio wave propagation, and plasma instabilities, are examples within the broad field of solar-terrestrial physics which emphasise the energy exchange between the solar wind, the magnetospheric and ionospheric plasmas, and the neutral gas. In the lower atmosphere, topics covered range from mesoscale to global scale dynamics, to atmospheric electricity, lightning and its effects, and to anthropogenic changes. Helpful, novel schematic diagrams are encouraged. Short animations and ancillary data sets can also be accommodated. Prospective authors should review the *Instructions to Authors* at the back of each issue.

Complimentary Information about this journal: http://www.elsevier.com/locate/JASTP? http://earth.elsevier.com/geophysics

Audience:
Atmospheric physicists, geophysicists and astrophysicists.

Abstracted/indexed in:
CAM SCI Abstr
Curr Cont SCISEARCH Data
Curr Cont Sci Cit Ind
Curr Cont/Phys Chem & Sci
INSPEC Data
Meteoro & Geoastrophys Abstr
Res Alert

Editor-in-Chief:
T.L. Killeen, National Centre for Atmospheric Research, Boulder, Colorado, 80307 USA

Editorial Office:
P.O. Box 1930, 1000 BX Amsterdam, The Netherlands

Special Rate for URSI Radioscientists 2003:
Euro 149.00 (US$ 149.00)
Subscription Information
2002: Volume 65 (18 issues)
Subscription price: Euro 2659 (US$ 2975)
ISSN: 1364-6826

CONTENTS DIRECT:
The table of contents for this journal is now available pre-publication, via e-mail, as part of the free ContentsDirect service from Elsevier Science. Please send an e-mail message to cdhelp@elsevier.co.uk for further information about this service.

For ordering information please contact Elsevier Regional Sales Offices:

Asia & Australasia/ e-mail: asiainfo@elsevier.com
Europe, Middle East & Africa: e-mail: nlinfo-f@elsevier.com
Japan: Email: info@elsevier.co.jp
Latin America : e-mail: rsola.info@elsevier.com.br
United States & Canada : e-mail: usinfo-f@elsevier.com

APPLICATION FOR AN URSI RADIOSCIENTISTS

I have not attended the last URSI General Assembly, and I wish to remain/become an URSI Radioscientist in the 2003-2005 triennium. Subscription to *The Radio Science Bulletin* is included in the fee.
(please type or print in BLOCK LETTERS)

Name: Prof./Dr./Mr./Mrs./Ms. _____
Family Name *First Name* *Middle Initials*

Present job title: _____

Years of professional experience: _____

Professional affiliation: _____

I request that all information, including the bulletin, be sent to my ☐ home ☐ business address, i.e.:

Company name: _____

Department: _____

Street address: _____

City and postal / zip code: _____

Province / State: _____ Country: _____

Phone: _____ ext: _____ Fax: _____

E-mail: _____

Areas of interest (please tick)

☐ A Electromagnetic Metrology
☐ B Fields and Waves
☐ C Signals and Systems
☐ D Electronics and Photonics
☐ E Electromagnetic Noise & Interference
☐ F Wave Propagation & Remote Sensing
☐ G Ionospheric Radio and Propagation
☐ H Waves in Plasmas
☐ J Radio Astronomy
☐ K Electromagnetics in Biology & Medicine

The fee is 40 Euro.
(The URSI Board of Officers will consider waiving of the fee if the case is made to them in writing)

Method of payment: VISA / MASTERCARD (we do not accept cheques)

Credit Card No ☐☐☐☐ ☐☐☐☐ ☐☐☐☐ ☐☐☐☐ Exp. date: _____

Date: _____ Signed _____

Please return this signed form to:

The URSI Secretariat
c /o Ghent University / INTEC
Sint-Pietersnieuwstraat 41
B-9000 GENT, BELGIUM
fax (32) 9-264.42.88